CRN: 11799

MQP QW1-1301

Fabrication of a Hydrogel with Controllable Heterogeneity in Stiffness

A Major Qualifying Project Report

Submitted to the Faculty

of the

WORCESTER POLYTECHNIC INSTITUTE

In partial fulfillment of the requirements for the

Degree of Bachelor of Science

By

Andrea Rivas

Samantha Sargalski

Kelin Song

Thursday, May 1, 2014

Qi Wen, Advisor

Sakthikumar Ambady, Co-advisor

Acknowledgements

We would like to thank the following people for all of their guidance, advice, and demonstration throughout this project. Without their help, our project would not have been possible.

Professor Qi Wen

Professor Sakthikumar Ambady

Gawain Thomas

Lisa Wall

Biomedical Engineering Department

Worcester Polytechnic Institute

Authorship

The following report demonstrates an equal effort from all three members of the team. While there was a primary author for each section, each team member contributed equally to the overall construction of the report. Editing of the final product was done as a team to ensure that all sections flowed well, and presented the desired ideas effectively.

Abstract

Perturbations in cell-substrate and cell-cell interactions play a major role in tumor development and tumor metastasis. It is becoming evident that changes in tissue stiffness contribute to the development of tumor foci and concomitant changes. In order to study and validate the mechanisms involved in initiating and sustaining these changes, it is important to develop methods to assess those changes reliably and accurately. Here, we present a novel method to create a polyacrylamide hydrogel in which micron sized stiff regions were incorporated within moderately stiff hydrogels to mimic initial changes in tissue stiffness that lead to tumor development. We optimized the design and process to produce hydrogels of uniform thickness, surface smoothness, and size and shape of stiff regions to investigate cellular response to the change in stiffness both within the stiff regions and across the boundaries. Our system can be a valuable tool to study if and how cells within the tumor foci interact and influence cells in the surrounding normal tissue; as well as to test drug molecules to reverse tumor progression and metastasis.

Table of Contents

Table of Figures

Table of Tables

Chapter 1: Introduction

The extracellular matrix is a network of proteins, mainly collagen, laminin, and fibronectin, that provides structure and support to cells and tissues (Gallant, Michael, & Garcia, 2005; Goldstein, 2006). It is known that intercellular and cellular adhesions to the extracellular matrix (ECM) are critical for the maintenance and structure of healthy cells and tissues in physiological conditions (Gallant et al., 2005). Defective adhesive interactions are linked with concerning conditions such as problems with blood clotting, disruption of wound healing, stiffening of blood vessel walls, and even the formation of cancerous tumors (Sazonova et al., 2011). Cancer cells are defined by their ability to invade healthy cells and tissues through the basement membrane, which lines most organs in order to provide a barrier between the organs tissue and the inside of the body (Swaminathan et al., 2011). It has been tested and confirmed that the stiffness of tumor cells and cancer cell lines as a whole directly correlates to their migration and invasion capabilities. The cancer cells which are stiffer in nature tend to have a harder time migrating and invading healthy tissue, while cancer cells which are softer in nature, migrate and invade healthy tissue more easily. Therefore in order to avoid defect it is extremely important that cell-cell and cell-substrate adhesion be working properly within the body, and that adhesion response to stiffness be investigated.

In current research, science has investigated the cellular signaling and adhesive behavior of cells towards substrates of different elastic moduli in order to observe the cellular response to a change in stiffness. Recent publications compare protein expression and cellular adhesion between cultures on different substrates, each with a different stiffness, however not many direct special attention to the interactions across the boundaries of different elastic moduli (Gallant et al., 2005; Goldstein, 2006; Sazonova et al., 2011). In fact, little previous research has been conducted into the cells adhesive behavior on a surface of heterogeneous stiffness, and the cells communications in such an environment.

The communication between the cells in this heterogeneous environment is key to understanding what happens when cells develop adherence problems and subsequently deform, develop migration issues, or undergo apoptosis.

This project will focus on the intercellular as well as the cell-substrate adhesion as a function of substrate stiffness, and the behavior of cells in these environments. To accomplish this goal, our team first created a polyacrylamide (PAA) hydrogel with controllable heterogeneity in stiffness. In this case, soft gels of 10 kPa with a circular stiff region of 1mm in diameter and 40kPa in stiffness located in the center of the gel. The PAA hydrogels were then validated with mechanical testing using an Atomic Force Microscope (AFM) to ensure that the heterogeneous regions in stiffness matched the stiffness levels we chose to examine. Then, our team validated that the heterogeneous regions in stiffness within the gel were easily visually determined by observing the gel using fluorescence microscopy, as the stiffer regions were stained with microbeads to be fluorescent, while the softer regions were not. The hydrogel was then functionalized with an ECM protein, collagen, in order to provide the cells with a place to bind to the substrate and grow. Finally, the cell-cell interactions were observed visually using microscopy and imaging techniques to establish the cells behavior in response to the regions of varying stiffness within the gel. The cell-substrate interactions were measured quantitatively through AFM testing to determine the cell stiffness associated with the substrate stiffness that the cells settled on. The more we are able to utilize this hydrogel with controlled heterogeneity in stiffness to investigate various cellular adhesion interactions, the more we can understand about why malfunctions in cell adhesion have such dismal physiological consequences.

Chapter 2: Literature Review

Significance in Cancer Research

The main cause of death in cancer patients today is the ability of the cancer to spread from its primary site and invade other cells and tissues through migration (Swaminathan et al., 2011). In this study, the spread of cancer from its primary site to other tissue is known as the "invasion-metastasis cascade", and it is speculated that this cascade is a huge factor in why cancer patients' prognosis decreases so rapidly once the disease starts spreading. Drugs that have been created to target this metastatic cascade have not been successful thus far due to the complexity of the cascade and the cancer cells' unpredictable migratory tendencies. Recently, cell stiffness has been connected to cancer cells' ability to migrate and infect healthy cells and tissues through the basement membrane. Swaminathan *et al.* conducted an experiment using a magnetic tweezers system in order to evaluate the stiffness of cancer cells as it correlates to their invasion and migratory capabilities. The results of the study proved that a power law was present in the migration and invasion of cancer cells. In other words, as the cancer cell lines got more invasive, they showed softer mechanical properties that allowed them to change shape and make themselves more suitable for a metastatic population. The stiffer cancer cells were unable to change their shapes so easily, and therefore were less able to suit themselves for a metastatic population, which made them less successful in migration and invasion of healthy tissues. This power law was further proved true when the results remained the same for cancer cells taken from the same patient, in the same stage, and even in the same type of cancer. The results of this study are extremely novel; by looking at the mechanical properties of cancer cells and how this allows them to migrate and invade healthy tissue, novel treatment ideas are bound to follow (Swaminathan et al., 2011).

Hydrogels

Hydrogels are defined as polymeric networks which are able to absorb large amounts of water (Hennink & van Nostrum, 2012). As a hydrogel forms a network, more or less crosslinks are present depending on the specific properties of the materials chosen to create the hydrogel, as well as the processing techniques used in order to synthesize the hydrogel (Omidian et al., 2010). Furthermore, these varying degrees of cross-linking directly correlate to the different behavior of the hydrogel. Some hydrogels with lower degrees of cross-linking show Newtonian behavior, while other hydrogels with different polymer chains introduced through cross-linking show viscoelastic, and even pure elastic behavior (Hennink & van Nostrum, 2012). Also, as different polymeric chains are introduced to the hydrogel, their physical, chemical, and mechanical properties change (Omidian et al., 2010). Due to their ability to be heavily modified based on want or need of function, hydrogels are currently being investigated for use in a large number of fields, from agriculture to household items, to medical device and biomedical research. For more information on hydrogels, their classification and polymers used, refer to Appendix 2: Hydrogels.

Existing Polyacrylamide Hydrogel Patents

The prior art of polyacrylamide hydrogel fabrication and processes related to polyacrylamide hydrogels is extensive. There are many patents on functionalization of PAA hydrogels or attaching different types or molecules to the surfaces (US6686161 B2), there are also patents on the fabrication of sterile or medical grade polyacrylamide hydrogels (CN 1228447 A; CN 1116321 C). However, we could not find many results for labeling of hydrogels and creating hydrogels with regions of different stiffness.

The only method we found of labeling a PAA hydrogel that still allows microscopy, uses a polymer film that attaches chemically to the gel's surface (EP 1281070 A4). While this solves a couple of issues, namely the need of markers that do not interfere with microscopy and the need of markers that

go with the gel, it is unspecified if it affects the gel's surface stiffness. This method of tagging PAA hydrogels, intended for electrophoresis, is not particularly suited to our projects' need.

Next, we were concerned about prior art on gels with heterogeneous stiffness. The only patent that was remotely on this subject was U.S. patent 6391937 B1, "Polyacrylamide hydrogels and hydrogel arrays made from polyacrylamide reactive prepolymers", and even so, it does not mention regions of different stiffness. This patent describes a method of creating microgel arrays 50 µm thick and separated by 500µm. While a gel with an array of stiff regions could be made in a similar fashion, we would still need to fill in the regions in between the microgels. Therefore, our project would not interfere with the claims in this patent.

Chapter 3: Project Strategy

The ultimate goals of this project were to develop a method to make a heterogeneous hydrogel with specific regions of elastic modulus and to investigate cell-cell and cell-substrate interactions across regions of different stiffness. The purpose of this chapter is to define our team's objectives and constraints as well as outline a project approach.

Initial Client Statement

In order to identify the goals of the project, our team clarified the initial client statement to understand the expected final deliverables. Our initial client statement from Professor Qi Wen and Professor Sakthikumar Ambady was:

1. *Develop a method to fabricate hydrogel with controlled heterogeneity in stiffness.*
2. *The gel should be transparent so that cells can be imaged using a regular microscope.*
3. *The gel should be mounted on a transparent microscope cover glass and uniform in thickness of about 100-500 microns, preferably in the 100-200 micron range.*
4. *Ability to control the size, shape and stiffness of heterogeneous regions.*
5. *Standardize a measurement technique to consistently characterize the heterogeneity.*
6. *Develop a method to visually determine the heterogeneity (under a microscope) across the gel.*
7. *Measure area, migration, and stiffness of cells cultured on the heterogeneous gels.*

It is important to understand all aspects of the project before designing a final product; therefore our team refined the client statement and broke it down into objectives and constraints. This was accomplished through weekly advisor meetings where our team asked questions to fully understand the scope of our project.

Objectives and Constraints

It is important to define the objectives and constraints of our project so that our project remains focused on its goals. For our first goal of developing a method to create a heterogeneous gel, our team had the following objectives and constraints:

Objectives:

1. Able to form reproducible gels
2. User can control stiffness of regions and distribution in gel
3. User friendly
4. Sterile
5. Safe starting materials and gelling technique
6. Good shelf-life
7. Cheap
8. Portable
9. Biocompatible gel
10. Visually able to determine heterogeneous regions

Constraints:

1. Final cost is less than $1 per hydrogel
2. Shelf-life in the order of months
3. Must use materials available in the lab
4. Gel must fit in incubator and under microscope

For our second goal of investigating cell behavior, our team had the following objectives and constraints:

Objectives:

1. Compatible with standard cell culture techniques
2. Allow investigation of cell-cell interaction

3. Allow investigation of cell-substrate interaction

Constraints:

1. Must use materials available in the lab
2. Must not damage hydrogel

Quantitative Analysis of Objectives

Although all of the objectives are important, it is prudent to rank them because of conflicting solutions. Our team used a pairwise comparison chart to prioritize these objectives to create the best possible final method. The pairwise comparison chart for our first goal of developing a method to create a heterogeneous gel can be found in Table 1.

Table 1 Pairwise Comparison Chart for Developing a Method to Create a Heterogeneous Gel

	Reproducible gels	User control	User friendly	Sterile	Safe process	Good shelf-life	Cheap	Portable	Biocompatible	Visually determine stiff regions	Total
Reproducible gels	X	1	1	1	0	1	1	1	1	1	8
User control	0	X	0	0	0	0	0.5	0.5	0	0	1
User friendly	0	1	X	0	0	0	0.5	0.5	0	0	2
Sterile	0	1	1	X	0	1	1	1	0.5	1	6.5
Safe process	1	1	1	1	X	1	1	1	1	1	9
Good shelf-life	0	1	1	0	0	X	1	0.5	0	0	3.5
Cheap	0	0.5	0.5	0	0	0	X	0.5	0	0	1.5
Portable	0	0.5	0.5	0	0	0.5	0.5	X	0	0	2
Biocompatible	0	1	1	0.5	0	1	1	1	X	1	6.5
Visually determine stiff regions	0	1	1	0	0	1	1	1	0	x	5

The pairwise comparison chart allows us to analyze the importance of each objective. The two most important objectives were first being a safe process for the user and then being able to reproduce the hydrogels. Following these objectives, the next important objectives were being sterile and

biocompatible, being able to visually determine stiff regions, having good shelf life, being portable and user friendly, being cheap, and allowing the user to control stiffness of regions and distribution in the hydrogel. The pairwise comparison chart for our second goal of investigating cell behavior can be seen in Table 2.

Table 2 Pairwise Comparison Chart for Investigation Cell Behavior

	Compatible w/ standard cell culture	Cell-cell interactions	Cell-substrate interactions	Total
Compatible w/ standard cell culture	X	1	1	2
Cell-cell interactions	0	X	0.5	0.5
Cell-substrate interactions	0	0.5	x	0.5

The most important objective is to have the gel compatible with a standard cell culture procedure. The following objectives were tied in being able to determine cell-cell interactions and cell-substrate interactions.

Revised Client Statement

After discussing with our advisors, our team revised the initial client statement to be more concise and specific. The goal of the project is to develop a method to create a hydrogel with specific regions of heterogeneous elastic modulus. NIH-3T3 mouse fibroblasts will be used to investigate cell-cell and cell-substrate interactions across regions of different stiffness.

Project Approach

Technical Approach

The technical aspect of this project can be divided into fabrication and validation of the hydrogel as a first component, and the study of cellular behavior and signaling as a second. We used the client

statement, objectives, and constraints established in the previous section in order to plan a comprehensive design approach.

Our first concern was safety. Hydrogels can be produced using chemicals and or procedures that can be dangerous. In order to form polymer chains, monomers have to be highly reactive and, in some cases, require free radicals in order to initiate the polymerization. Acrylamide and bis-acrylamide monomers are highly corrosive, carcinogenic, and neurotoxic. Therefore our team will take the appropriate precautions and limit our options to processes in which safety can be maintained using standard laboratory equipment. We will not consider any procedure that requires safety equipment additional to an A2 safety cabinet, latex or nitrile gloves, laboratory goggles, UV face masks, and laboratory coats. By doing so, we hope to protect ourselves, other users in the laboratory, and scientists from surrounding laboratories.

Next we focused on achieving a robust method of fabricating our hydrogel, keeping all our objectives and constraints in mind. The most precise methods of making hydrogels such as emulsification and microfluidics require advanced equipment which would interfere with our objectives to make our method easy to use and practical. Therefore we will only consider chemical crosslinking, physical crosslinking, and grafting crosslinking. We used a design evaluation matrix to rank each of these methods with respect to the parameters in this project; the design evaluation matrix can be found in Table 3. From this evaluation, grafting was the most adequate. A way to achieve graft crosslinking is through exposure to UV light, as opposed to thermal or chemical stimuli. Therefore we will focus on simplifying and adapting the equipment and experimental set-up commonly used in UV crosslinking.

Table 3 Design Evaluation Matrix

Constraints & Objectives	Physical Crosslinking	Chemical Crosslinking	Grafting Crosslinking	Radiation Crosslinking
C: Final cost <$1 per hydrogel	Y	Y	Y	N
C: Weight <1lbs	Y	Y	Y	Y
C: Self-life in order of months	Y	Y	Y	Y
C: 100-200µm thick	Y	Y	Y	Y
O: Safe process (x5)	95 x5	95 x5	95 x5	N/A
O: Reproducible gels (x4.6)	70 x4.6	75 x4.6	95 x4.6	N/A
O: Sterile (x3.6)	95 x3.6	95 x3.6	95 x3.6	N/A
O: Biocompatible (x3.6)	95 x3.6	95 x3.6	95 x3.6	N/A
O: Visually determine stiff regions (x3.3)	75 x3.3	75 x3.3	95 x3.3	N/A
O: Good shelf-life (x2.6)	95 x2.6	95 x2.6	95 x2.6	N/A
O: Portable (x2.3)	95 x2.3	95 x2.3	95 x2.3	N/A
O: User friendly (x2.3)	95 x2.3	90 x2.3	95 x2.3	N/A
O: Cheap (x1.3)	95 x1.3	92 x1.3	90 x1.3	N/A
O: User control (x1)	95 x1	95 x1	95 x1	N/A
TOTAL:	2631	2638.6	2805.5	N/A

Scoring:

0-25: Design will not meet objective.

25-50: Design will meet objective with restrictions.

50-75: Design satisfies the objective, but does not optimize it.

75-100: Design fully meets the objective.

When choosing materials for the gel and for the photocrosslinking set-up, all the objectives and constraints will need to be taken into account once again. Choosing the type of gel was not an issue; polyacrylamide is well established as a biocompatible gel that can be fabricated with different elastic moduli. We were also inclined to use polyacrylamide hydrogels due to our advisors' previous experience

with it and the availability of these materials in their laboratories. When it came to designing the photocrosslinking equipment set-up however, we face challenges due to the properties these gels need to have, specifically the stiff regions and the need to visually differentiate them.

To form the stiff regions we will need a photomask; the challenges lie in that the material has to be transparent to UV light and actually making the mask. Nitrocellulose film, 4 mil transparent film, and UV blocking acrylic are three types of commercially available materials that block or are transparent to UV light. The first is more expensive yet it allows UV light of higher energy through as compared to 4 mil transparent film. However, 4 mil transparent film is easier to work with and less expensive. While these methods allow UV light to pass through, the acrylic will block the light. An important factor to take into consideration will be whether the photomask is printed with a high quality laser printer or if it needs to be laser cut, the latter being more convenient for our hydrogel system.

Differentiating the regions of different stiffness is a major design challenge: the cues have to be visible in microscopy and should not obstruct imaging of the cells. Our team will explore the use of different fluorescent particles or dyes in different concentrations in the hydrogels. Microscopy will determine whether the regions are discernible and whether cells, if seeded onto the substrate, would be visible. Once this is achieved, determining how well the fluorescence or visual cues and the stiff regions match up with the photomask will be determined. This is important to ensure the repeatability of fabricating our hydrogel and the reliability of interpreting it.

Finally, studying cellular signaling and behavior should be straightforward after a gel with marked stiffer regions has been developed. Our client statement specifies migration, area, and stiffness of cells as parameters that need to be investigated. Microscopy would let us determine cell migration and cell area however measuring cell stiffness can be more difficult. While there are different methods

of doing so, AFM yields measurements of high precision and since we have one of these instruments available, we will determine cell stiffness through AFM.

Team Management

Due to the large nature of our project, as well as the lengthy time frame, our team decided it was necessary to use management tools in order to keep our project on track. The first tool that we used was a Gantt chart (Figure 1), which broke up the work into various tasks and showed a detailed timeline of when every task needed to be completed, down to the date. For example, in our Gantt chart it specifies that we needed to complete our first draft of our hypothetical research paper for the October 11, 2013 deadline and we were able to plan and time out the workload associated with this task based on the given timeframe, as well as any conflicting tasks, as recorded on our Gantt chart.

	Task Mode	Task Name	Duration	Start	Finish	Predece
1		**A Term Objectives**	**36 days**	**Thu 8/29/13**	**Thu 10/17/1**	
4	✓	**Deliverables Week of Sept. 15th**	**11 days**	**Tue 9/3/13**	**Tue 9/17/13**	
5	✓	Revised Client Statement	11 days	Tue 9/3/13	Tue 9/17/13	
6	✓	Clear Objectives	11 days	Tue 9/3/13	Tue 9/17/13	
7	✓	Gantt Chart	11 days	Tue 9/3/13	Tue 9/17/13	
8	✓	Background & Significance	14 days	Tue 9/3/13	Fri 9/20/13	
9	✓	**Chapters 1-3 for BME 4300 (draft)**	**10 days**	**Sat 9/14/13**	**Fri 9/27/13**	**4**
10	✓	Chapter 1 (Complete Intro)	11 days	Sat 9/14/13	Fri 9/27/13	
11	✓	Chapter 2 (Detailed outline w/ references)	11 days	Sat 9/14/13	Fri 9/27/13	
12	✓	Chapter 3 (Design process, objectives, functions, constraints)	11 days	Sat 9/14/13	Fri 9/27/13	
13		**Deliverables Week of Sept. 29th**	**19 days**	**Fri 9/20/13**	**Wed 10/16/**	**9**
14	✓	Reducing design to practice	11 days	Fri 9/20/13	Fri 10/4/13	
15	✓	Experimental design & methods (1st draft)	11 days	Fri 9/20/13	Fri 10/4/13	
16		experimental design & methods (2nd draft)	9 days	Sat 10/5/13	Wed 10/16/1	
17	✓	9-10 page hypothetical paper	5 days	Mon 10/7/13	Fri 10/11/13	13
18		**B Term Objectives**	**38 days**	**Tue 10/29/1**	**Thu 12/19/1**	**1**
19		Create heterogeneous gels	38 days	Tue 10/29/1	Thu 12/19/1	
20		Test heterogeneous gels	38 days	Tue 10/29/1	Thu 12/19/1	
21		Standarize protocol for making h. gel	38 days	Tue 10/29/1	Thu 12/19/1	
22		Show repeatability of protocol	38 days	Tue 10/29/1	Thu 12/19/1	
23		**C Term Objectives**	**37 days**	**Thu 1/16/14**	**Fri 3/7/14**	**18**
24		Cell Stiffness	37 days	Thu 1/16/14	Fri 3/7/14	
25		Cell migration	37 days	Thu 1/16/14	Fri 3/7/14	
26		Immunocytochemistry	37 days	Thu 1/16/14	Fri 3/7/14	
27		Other cell behavior	37 days	Thu 1/16/14	Fri 3/7/14	
28		**End of Project!!!!**	**24 days?**	**Sun 3/30/14**	**Thu 5/1/14**	
29		End of the Project!			Sun 3/30/14	
30		Project Presentation Day			Thu 4/24/14	
31		First draft of MQP			Mon 4/7/14	
32		eCDR due			Thu 5/1/14	

Figure 1 Gantt Chart

Another chart that our team used in order to stay on track was the Work Breakdown Structure (WBS) as seen in Figure 2. This chart shows the main goals of our project, as well as all the tasks that must be completed in order to accomplish these goals. The WBS goes into more specific detail than the Gantt chart as it allows us to see all the details of a task that go into its completion rather than just the task itself. The WBS does not show a timeline of these tasks, but rather provides more detailed subtasks for the ultimate completion of our project goals.

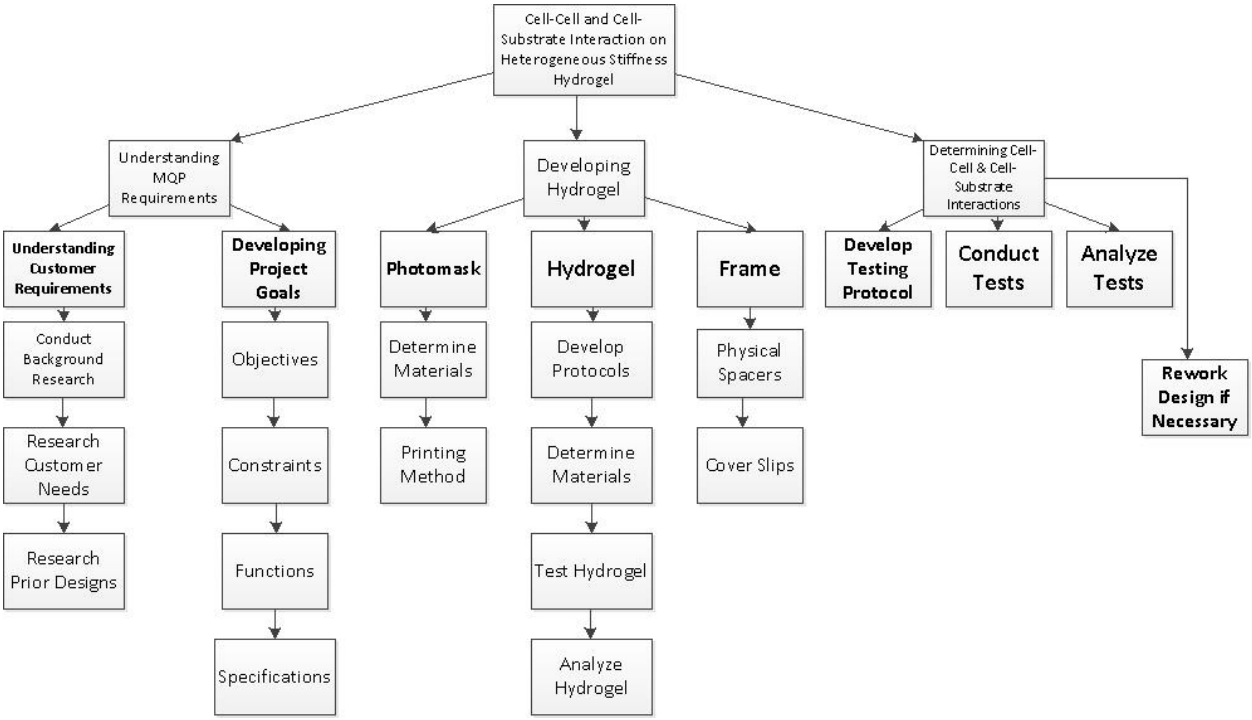

Figure 2 Work Breakdown Structure

Finally, our team used a Linear Responsibility Chart (LRC) in order to keep track of who would be responsible for completing each task according to the WBS. Basically, the LRC took each goal of the WBS, broke it down into detail and assigned a primary, secondary, and tertiary person responsible for each detail. It was extremely helpful in breaking down all of the work, and helped us to keep track of who was completing which task as well as who was responsible for writing and editing each deliverable. The LRC was also particularly useful in breaking up the work of the project equally, and to each member's specific strength so no one team member was responsible for more than another. Overall, the

Gantt chart, WBS, and LRC were essential planning tools in order to manage our time effectively, split project goals evenly, and keep track of due dates and tasks to be completed for this project.

Financial Approach

Hydrogel Synthesis and Validation

From a financial stand point, the materials for hydrogel synthesis will be the most expensive portion of our project. Fortunately, almost all the materials required to make PAA hydrogels are already available in Prof. Wen's and Prof. Ambady's laboratories such as the acrylamide, bis-acrylamide, Irgacure crosslinker, UV box, and more. The photomask was purchased from commercially available UV filtering acrylic pane (TAP Plastics, OP-3 Clear) through WPI's Biomedical Engineering Department. Laser cutting the photomask was achieved at no cost by using WPI's laser cutter available on campus. A projected bill of materials for the complete hydrogel synthesis portion of our project is found in Table 4.

Table 4 Projected Bill of Materials of Hydrogel Synthesis

Material	Cost (US Dollars)	Quantity	Total
500mL 40% acrylamide	48	1	48
500mL 2% bis-acrylamide	49	1	49
UV light	75	1	75
Glass Cover Slip, #1 thickness, 18x18mm	7.75	200	23.25
7oz RainX	4	1	4
UV filtering acrylic panes	1	10	10
Labor	$20/hour	0.5 hours	10
Total			$219.25

The total projected expense for the hydrogel synthesis portion of our project comes out to be $219.25. Due to the aid of our advisors, our team will only have to cover the cost of the UV filtering acrylic panes.

After the hydrogel synthesis, we will be using an Asylum Research MFP3D BIO Atomic Force Microscopy (AFM) to characterize the stiffness of our hydrogels. The price of AFM is $260,670. Since the

AFM is readily available to Professor Wen's lab, the main cost of AFM measurements comes from AFM cantilevers. The silicon nitride cantilevers with conical tip cost $25/each. This cost will be shared between different MQP groups, so only $100 will be deducted from our team's budget.

Cell-Cell Signaling

The cell-cell signaling and cell-substrate aspect of the project will also considerably impact the budget of the project. There are several components used in cell culture listed in Table 5. Fluorescent microscopy and phase contrast microscopy would let us determine cell migration and cell area while AFM would let us determine cell stiffness.

Table 5 Projected Bill of Materials of Cell-cell Signaling

Material	Cost (US Dollars)	Quantity	Total
Fluorescent microscope	2,000	1	2,000
Cantilever tips	100	5	100
500mL Complete media	20	3	60
100mL Trypsin-EDTA	12	1	12
Cell Culture Plates (sleeve of 10)	170.60	5	853
Total			$3,025

The total projected expense for the cell-cell signaling portion of our project comes out to be $3,025. We once again are fortunate to have the aid of Professor Wen and Professor Ambady's lab and materials where a fluorescent microscope, AFM, and cell culture materials will be provided.

Chapter 4: Methods and Alternative Designs

Functions (Specifications)

The functions for the method of polymerizing a heterogeneous hydrogel include the following:

- Provide visual cues to identify stiff regions
- Design must be compatible with standard cell culture procedures
- Design must enable cell adhesion to the gel surface
- Provide a flat and smooth surface across the entire hydrogel

Providing visual cues to identify stiff regions is vital for our project because it is important to determine where the stiff regions are without disturbing the integrity of the gel so that we can determine how cells interact on varying elastic moduli. We will be able to determine the location of our stiff region by embedding fluorescent microbeads within the hard gel so that when examined under a fluorescent microscope, the hard region will fluoresce while the soft region will not.

The ability to maintain cell culture conditions and work compatibly with standard cell culture procedures is important because the long term goal of the project is to observe cell-cell and cell-substrate interactions across varying elastic moduli. This means that our hydrogel must be in an environment that cells will adhere to and proliferate on.

Cell adhesion is important to observe cell-cell and cell-substrate interactions. Without proper adhesion, the cells will not be able to communicate to one another or with their surroundings. We enabled cell attachment to the surface by functionalizing the surface of the gel with collagen.

Finally, our hydrogel must have a flat and smooth surface across the entire system so that cell adhesion will not be affected by variances in thickness. It has been shown that topographical roughness is a profound factor in cell adhesion and proliferation (Swaminathan et al., 2011). This is an important function to consider because it has been shown that different elastic moduli have different swelling

ratios. Therefore accounting for differences in swelling ratios to create a smooth topographical surface is significant to collect useable cell data.

The specifications for the method of polymerizing a heterogeneous hydrogel include the following:

- Thickness must be 100-200µm
- Hydrogel must be transparent
- There must be a distinct stiffness change at the boundary of two regions

The first thickness specification is necessary because the thickness cannot be too thin so that cells will not respond to the stiffness of the gel. If the gel is too thin, the cells will be able to feel the stiffness of the coverslip underneath, and the data regarding cell behavior on a particular thickness will not be accurate. The thickness of the gel should also not be too thick so that it remains plausible to polymerize the hydrogel on a coverslip; therefore the optimal range is between 100-200µm.

The next specification is for the hydrogel to be transparent. This is so that visual cues of the stiff regions can be seen under a confocal microscope. The hydrogel will be determined to be transparent if light from the confocal microscope can travel through the gel and no cloudiness is perceived.

The distinct stiffness change at the boundary between the soft and hard stiffness is an important aspect of this project because it presents the novelty of our work. Creating this type of heterogeneous hydrogel is important because it will help to determine how cells react across a substrate with a distinct change in elastic moduli and not a gradient. A distinct stiffness change will be determined by having the elastic modulus change from soft to hard within 100µm.

Conceptual Design

In order to make a product that meets the desired functions and requirements, our team decided to make PAA hydrogels that would have a specified stiffer region as shown in Figure 3. The

surface of the gel would need to be smooth in order to be able to attribute changes in cellular behavior and morphology to the difference in substrate stiffness and not to a change in height or surface roughness. The stiffness should be constant within the region, in either the stiff island or the surrounding area, and there should be a distinct change in stiffness from the stiff island to the surrounding.

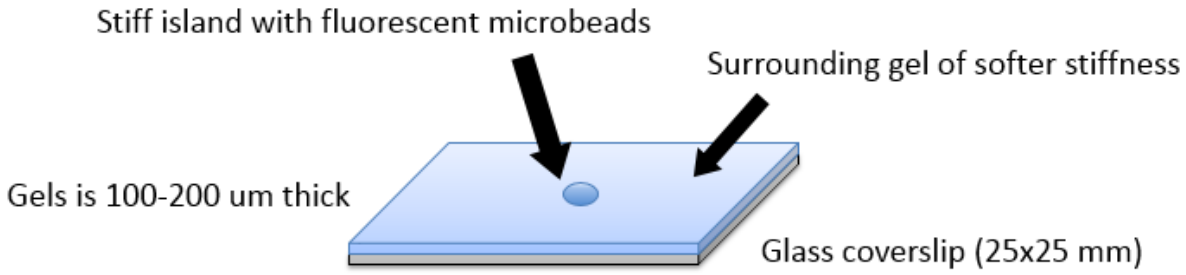

Figure 3 Schematic of the Heterogeneous Hydrogel

Preliminary Alternative Designs

There are many ways of making hydrogels; Appendix 3: Means of Fabricating Hydrogels, goes over common hydrogel fabrication techniques. To make the heterogeneous gels we had to determine which method would be most convenient. Professor Wen's laboratory usually makes PAA gels through chemical crosslinking using the initiator TEMED (N,N,N',N'-Tetramethylethylenediamine). While this method is repeatable and practical, it would be very challenging to make the regions of higher stiffness in the gel and to visually determine those regions. Therefore, after reviewing alternative methods, our team selected photocrosslinking as the most convenient way for making these heterogeneous PAA hydrogels. Conveniently, Professor Ambady had the photoinitiator, Irgacure 2959, in stock.

We conceptualized four methods that could be used to make the heterogeneous PAA hydrogels. In these designs, the crosslinking was done using the photoinitiator, and the thickness of the gel would be defined by the volume of the polymer solution added.

Spacer Photomask Method

The key aspect of the Spacer Photomask Method is using giving the photomask the additional function of determining gel thickness. The gels with regions of different stiffness could be synthesized using the experimental setups depicted in Figure 4; the components for each step are assembled from bottom to top.

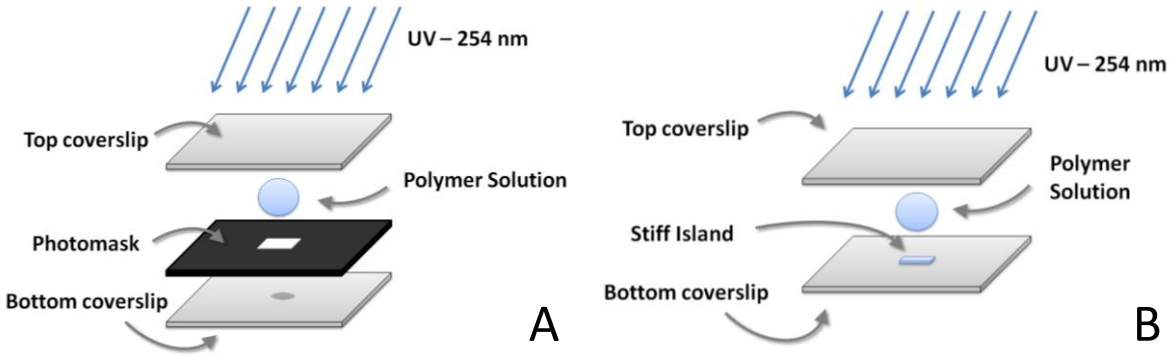

Figure 4 Spacer Photomask Method (A) First step – making the stiff islands, (B) Second Step – filling in the rest of the gel

In the first step, Figure 4A, a polymer solution is added to the spaces in the mask and exposed to ultra violet light of 254 nm wavelength, forming islands of a specific stiffness. Then the bottom coverslip can be rinsed to remove any unpolymerized precursors and a second polymer solution can be added to form the rest of the gel (Figure 4B). In this step, the gel thickness would be determined by the already made gel islands; therefore the photomask is no longer needed. Once again, UV light is shined onto the assembly to crosslink the polymer solution. In order to distinguish the regions of different stiffness, fluorescent beads can be added to either of the polymer solutions. To change the amount or size of the gel's regions of different stiffness, different photomasks can be made, and ideally, the photomask would be reusable.

Partial Polymerization Method

The partial polymerization method, similar to the other alternatives focused on polymerization of the gel through the use of UV light. In this method, 70µl of the bis-acrylamide and acrylamide solution

is micropipetted onto a 25mm glass coverslip which has been treated with APTMS and glued to a petri dish. A clean glass cover slip is placed over the top of the solution, and the petri dish is placed under UV light where it is left to polymerize for 15 minutes. After 15 minutes, a photomask with one 0.1mm radius circular patch is added to the top of the gel, and the petri dish is placed under the UV light to continue polymerization. After five more minutes under the UV light, the petri dish containing the gels is taken out from under the UV and the top photomask is removed along with the top coverslip. What results from this procedure, is a hydrogel which is heterogeneous in stiffness, because the single circle which was not covered by the photomask received the full 20 minutes of UV polymerization, making this circular island stiffer than the rest of the gel which received only 15 minutes of UV polymerization before being covered by the photomask. If hydrogels with more than one stiff region are desired, the photomask should be created with more than one 0.1mm radius circular patch.

Stamp Method

The stamp method involves designing a stamp which has protrusions that would pierce through a hydrogel as shown in Figure 5. A polymer solution for a low stiffness would be exposed to UV light to create a fully cross-linked uniform stiffness hydrogel. The stamp would then be used to pierce through the hydrogel creating little holes (Figure 5A & 5B). When the stamp is removed from the hydrogel, the little holes can be filled with a polymer solution for a high stiffness gel loaded with fluorescent microbeads (Figure 5C). The entire hydrogel is then exposed to UV light again to polymerize the little islands. If a singular region of stiffness is required or a different pattern is desired, several of stamps would be designed to fulfill these requirements and the procedure would remain the same.

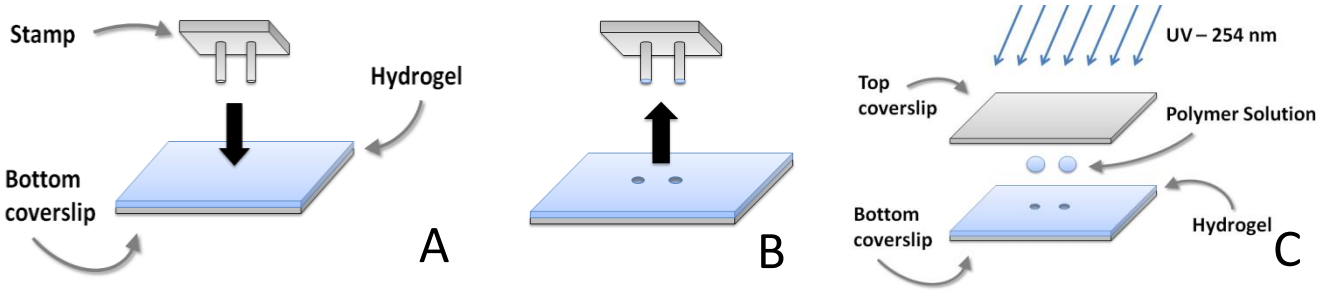

Figure 5 Stamp Method. (A-B) After the gel is made, the stamp is pressed down onto the gel and removed. (C) A new solution is added to crosslink the area

Photomask Method

This method for making the gels is very similar to the Spacer Photomask Method. In this case, the heterogeneous gel would be made as shown in

Figure 6. Cut outs in the mask will allow UV light to go through and crosslink the gel. The coverslips can be separated and rinsed, and a new polymer solution can be added to fill out the rest of the gel (

Figure 6B).

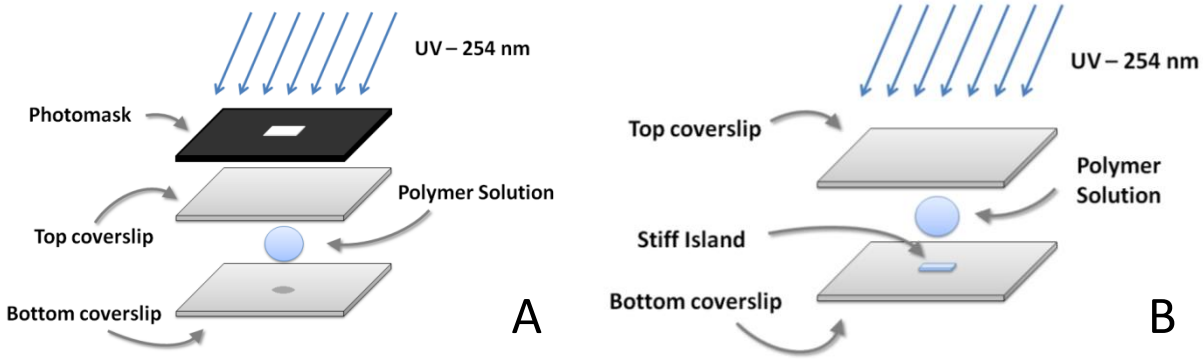

Figure 6 Assembly for the Photomask Method

Decisions

In order to make a decision for the final design, we created an evaluation matrix for our alternative designs as seen in Table 6. We included all of the constraints and objectives that were previously outlined in Chapter 3.

Table 6 Evaluation Matrix for Design Alternatives

Constraints & Objectives	Spacer Photomask Method	Partial Polymerization Method	Stamp Method	Photomask Method
C: 100-200µm thick	Y	Y	Y	Y
Safe process (x5)	95 x5	95 x5	90 x5	95 x5
Reproducible gels (x4.6)	90 x4.6	90 x4.6	90 x4.6	95 x4.6
Sterile (x3.6)	95 x3.6	95 x3.6	95 x3.6	95 x3.6
Biocompatible (x3.6)	95 x3.6	95 x3.6	95 x3.6	95 x3.6
Visually determine stiff regions (x3.3)	95 x3.3	75 x3.3	95 x3.3	95 x3.3
Good shelf-life (x2.6)	95 x2.6	95 x2.6	95 x2.6	95 x2.6
Portable (x2.3)	80 x2.3	95 x2.3	80 x2.3	80 x2.3
User friendly (x2.3)	95 x2.3	95 x2.3	95 x2.3	95 x2.3
Cheap (x1.3)	70 x1.3	92 x1.3	70 x1.3	95 x1.3
User control (x1)	95 x1	95 x1	95 x1	95 x1
TOTAL:	2722	2719	2697	**2777**

According to our evaluation matrix, the Photomask Method was ranked the highest out of the four alternative designs and met all of the constraints and objectives. It has one major set-back; the fabrication method involves multiple steps. This process is time consuming and laborious, but it is the process that best meets our purposes.

Design Calculations

One of the primary objectives for the hydrogel is that it remains at a certain thickness of between 100-200 µm. While we decided on the volume of solution used to make each individual gel based on the size of the coverslips and this desired thickness, we wanted to validate that the gels were in fact as thick as we calculated them out to be. Our team did this through measuring the height at the bottom of the gel and then at the top of the gel using the microscope in Wen's lab. For example, we measured the bottom of one gel to have a height of 5545 µm. Then, we found that the top of the gel

had a height of 5667µm. Using the optical refraction (1.33), we then calculated that the gel had a final height of 162.26 um, which lies in our desired range.

Gel Stiffness

The gel stiffness is determined by the ratio of bis-acrylamide to acrylamide and also the content of cross-linker. Three elastic moduli were selected based on a table by Tse and Engler (2010). Gels with approximate elastic moduli of 2, 10 and 40kPa were prepared in HEPES buffer, with 0.5% w/v photoinitiator, and acrylamide to bis-acrylamide ratios of 10% to 0.03% (soft), 10% to 0.1% (medium) and 8% to 0.48% (hard).

Feasibility Study and Experimental Methodology

Feasibility Study

We performed a feasibility study to make sure we could carry out the polymerization and that photocrosslinking was suitable for this process. The experiment was designed to test two major concerns:

1. That the photoinitiator, Irgacure 2959, would work and a new approach would not be needed.
2. That the rays of light from the light source would be at an angle, crosslinking an area larger than the opening in the photomask.

For this study we had all the materials to make the gel except for the photomask. In order to block the UV light from polymerizing the surrounding area of the gel we used aluminum foil to make a preliminary mask and made the opening using sharp tweezers and razor blades. The set-up is shown in Figure 7A, and the gels were fabricated as per the process described in
Figure 6.

Figure 7B shows the resulting stiff island; there is an area that is cloudy that is the shape of the opening on the mask and some of the gel around that polymerized as well. We did multiple trials and all

had similar results. From this preliminary study we determined that the Irgacure 2959 could be used for polymerization using this method and that there was something causing the gel to form in the area surrounding the mask opening. We believe this was due to the angle of the light rays and the size of the opening on the mask being too big – by using smaller mask openings, this effect could be minimized.

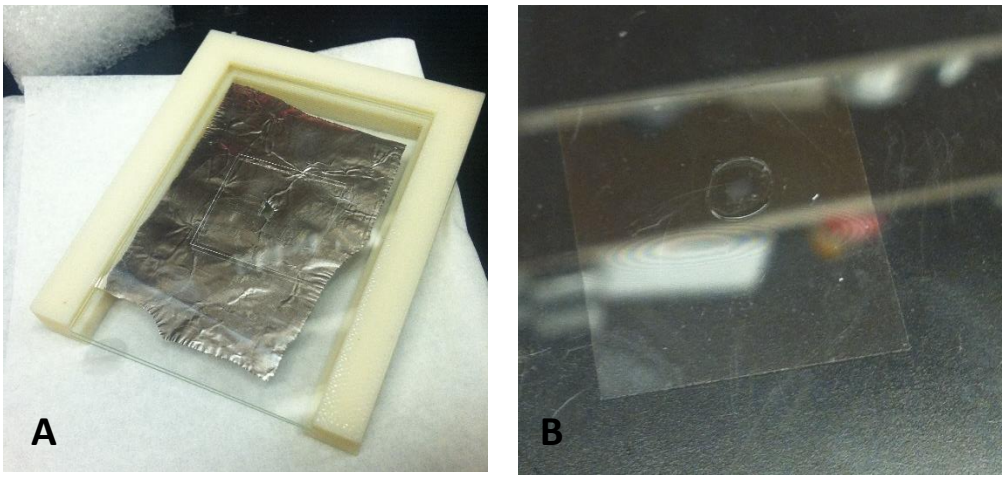

Figure 7 (A) Set-up for feasibility study and (B) the resulting stiff island

Experimental Methodology

As mentioned previously, there are two main components, (1) polyacrylamide hydrogel synthesis of varying stiffness with fluorescent beads and (2) seeding cells on the surface of the hydrogel to observe cell-cell and cell-substrate interactions. We made gels that were heterogeneous in stiffness for our experiments and also gels homogeneous in stiffness to use as controls. Detailed protocols are included in Appendix 5: Experimental Methods.

In order to simplify the fabrication process we made a plastic holder that fit six 25x25mm glass coverslips to make six gels. The holder was 3D printed on campus on the Stratysys Dimension FDM Rapid Prototyping machine using Solidworks®**.** We could use a 50x75 mm glass microscope slide on the holder to make the homogeneous gels, or we could use our photomask, which is also 50x75 mm, to make the stiff regions. We ordered acrylic panes that filter ultraviolet light (TAP Plastics, OP-3 Clear) and laser cut the pane in order to use it as our photomask. Figure 8 shows the Solidworks® file used to laser cut

(Universal Laser Systems VLS4.60 60W) six circular, 1 mm diameter, holes through the mask. Using this mask, six different gels can be made, each with a circular stiff region 1 mm in diameter.

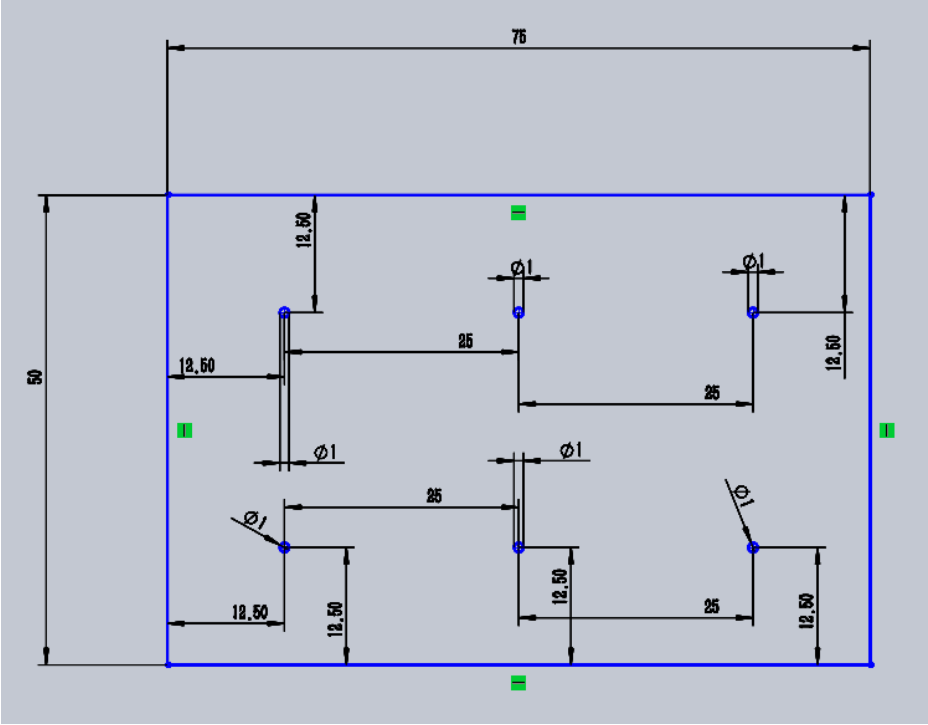

Figure 8 Solidworks drawing or the photomask.

Synthesizing Homogeneous and Heterogeneous Hydrogels

The method to fabricate the homogeneous and heterogeneous gels were developed from methods and materials used in Tse & Engler (2010) combined with methods used in Professor Wen's laboratory and modifications made throughout the project. Table 7 shows the final concentrations of the ingredients in the polymer solution, Figure 9 and Figure 10 are schematics of the set-up and process to make the gels, and Table 8 lists the additional equipment and materials needed to make the gels.

Table 7 Formulation for polymer precursor solutions (Tse & Engler, 2010).

Final Concentrations	Soft (~2 kPa)	Medium (~10 kPa)	Hard (~40 kPa)
Acrylamide (%)	4%	10%	8%
Bis-acrylamide (%)	0.1%	0.1%	0.48%
Irgacure 2959 (% w/v)	5 w/v %	5 w/v %	5 w/v %
HEPES (mM)	N/A	28 mM	28 mM
0.2 µm fluorescent beads (Life Techonologies)	N/A	N/A	0.002%

Making the heterogeneous gels requires two crosslinking steps (Figure 9) while the homogeneous gels can be made in one single UV exposure (Figure 10). Both processes require the cleaning and preparation of glass coverslips. By controlling the affinity of the PAA gel to each coverslip, we can make the heterogeneous gels and control whether the gel will be attached to one coverslip or the other after polymerization. The protocols for functionalizing the coverslips are also included in Appendix 5: Experimental Methods.

Table 8 List of materials and equipment to fabricate PA gels.

Materials	Equipment
40% acrylamide solution (Biorad)	O_2 plasma cleaning device
2% Bis solution (Biorad)	254 nm UV light source – GelDoc
25x25 glass coverslips (VWR)	Razor blades
HEPES buffer (50 mM, 8.5 pH)	Glutaraldehyde container
0.5% glutaraldehyde	Ceramic boat for the coverslips
Dichlorodimethylsilane (DCDMS)	
(3-aminopropyl)-diethoxy-methylsilane (APTMS)	
Irgacure 2959 (Ciba)	

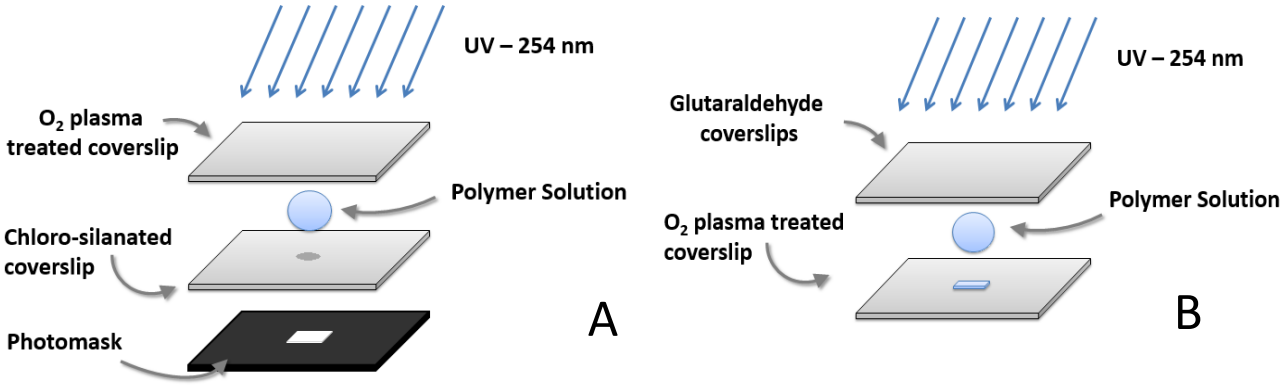

Figure 9 Preparation of Heterogeneous Gel

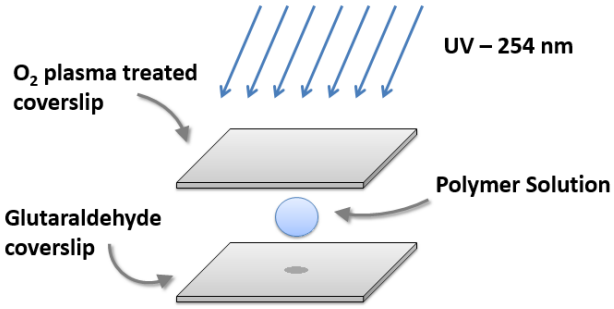

Figure 10 Preparation of Homogeneous Gel

Measuring Stiffness

The stiffness of the gels was measured using AFM. An operator took indentation measurements of the gels and using a custom MATLAB code (Appendix 8: MATLAB Code) provided by Professor Wen we were able to determine the elastic, loss, and storage moduli from the data. For the homogeneous gels, indentation curves were taken at 40 random points. For heterogeneous gels we performed three types of tests: (1) random indentation curves in the surrounding area and in the stiff island and (2) stiffness profiles created by taking indentation curves of points on a line starting at the center of the stiff island and stepping away in intervals of a particular distance and (3) stiffness profiles created by taking indentation curves of points across the stiff region of the gel. The data was used to determine the stiffness change from the hard region to the surrounding softer region.

Imaging Stiff Islands

The stiff islands were imaged using fluorescent and phase contrast microscopy. The fluorescent beads allowed the stiff regions to be easily located. These images were used to determine the shape of the stiff region and if there was any residue of the harder gel on the coverslip. Phase contrast microscopy was used to image the surface of the stiff regions. When the surrounding area swelled, it could crush the stiff region, causing the surface to wrinkle. Phase contrast microscopy was more convenient to see these ridges once the island had been located through fluorescence microscopy. Most of the images were taken at 10x magnification as either single shots or montages.

Cell Analysis

The PAA hydrogels were treated with sulfo-SANPAH in order to be functionalized with a collagen coating following standardized procedures from Prof. Wen's lab. The detailed protocol is found in Appendix 5: Experimental Methods. Preliminary tests of biocompatibility and cytotoxicity were conducted with NIH 3T3 cells. Cells were seeded onto the 25x25mm hydrogels of medium stiffness and then observed 48 hours after seeding. For the cell stiffness experiments, the coverslips with the heterogeneous gels were put into individual 60 mm petri dishes. The hydrogels were seeded with STO cells from a suspension containing 10^6 cells per mL. Half of the hydrogels were seeded with 100,000 cells while the other half with 200,000 cells. After seeding the cells, they were allowed to attach to the gel for 30 min in the incubator before the cell culture media was added. The cells on the gels were incubated for a minimum of 24 hours before taking the cell stiffness measurements with AFM. On average, the stiffness of five cells on each region of each heterogeneous gel was measured by taking five force-indentation curves.

Preliminary Data

Our preliminary data consisted of stiffness measurements of four gels: three were homogeneous controls (soft, medium, and hard), and the fourth was a heterogeneous gel. Force indentation curves of 24 points were taken on each gel, the data is summarized in Figure 11. The raw data is included in Appendix 6: Preliminary Data.

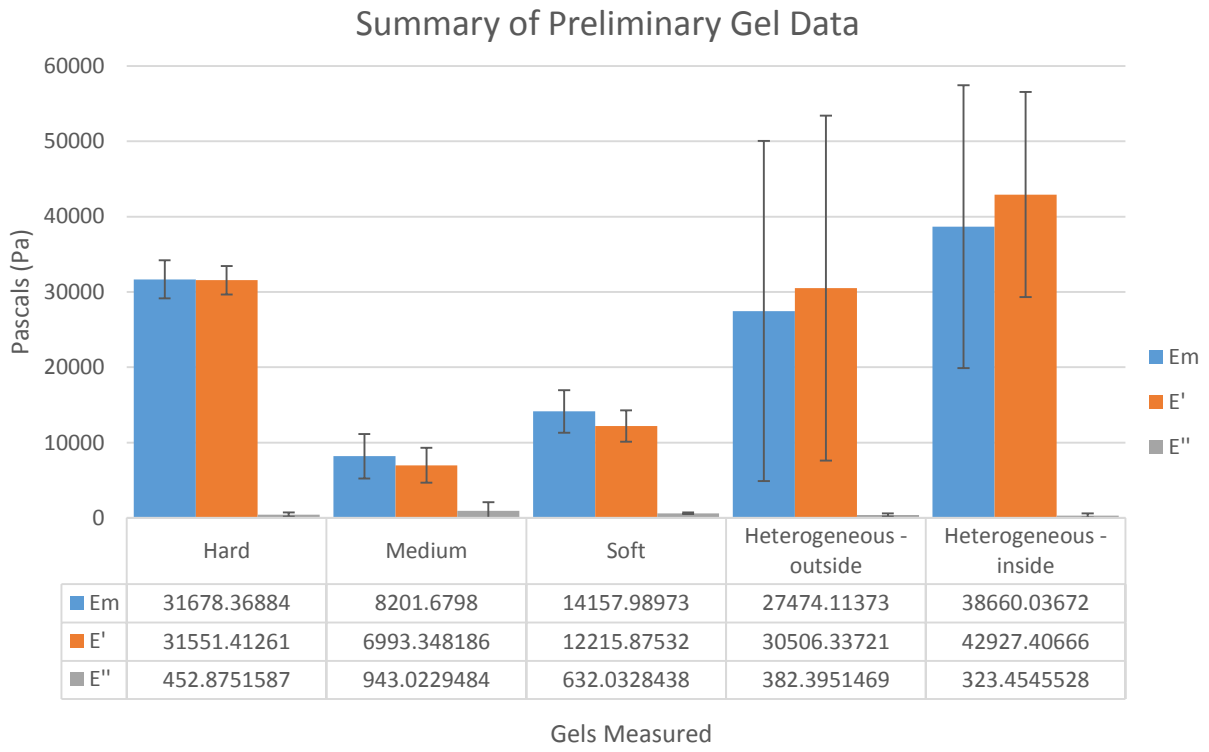

Figure 11 Summary of Preliminary Results

From Figure 11 we can see that the formulation for the Hard and Medium gels achieve distinctly different stiffness values, 31.7 (±2.5) kPa and 8.2 (±2.9) kPa respectively. The polymer solution intended to yield a softer gel resulted in a stiffness of 14.2 (±2.8) kPa – much higher than intended. Therefore, this formulation was discontinued for further gels. Finally, the results of the heterogeneous gel indicated a stiff and soft region. The stiff region is stiffer than the outside even though the values were consistently higher than the stiffness of the control gels. Additionally, there were many outliers in the data that resulted in high standard deviations. To address this, the gel formulations and the fabrication process were standardized for all the following experiments.

Preliminary biocompatibility and cytotoxicity tests with NIH 3T3 fibroblasts showed that the cells were incredible sensitive to the change in substrate stiffness. After 48 hours of being on the hydrogel, many cells had migrated to the bottom of the petri dish and those growing on the gels died. Figure 12

shows NIH 3T3 cells forming clumps when cultured on substrates softer than the standard tissue culture dish where they spread out and proliferate.

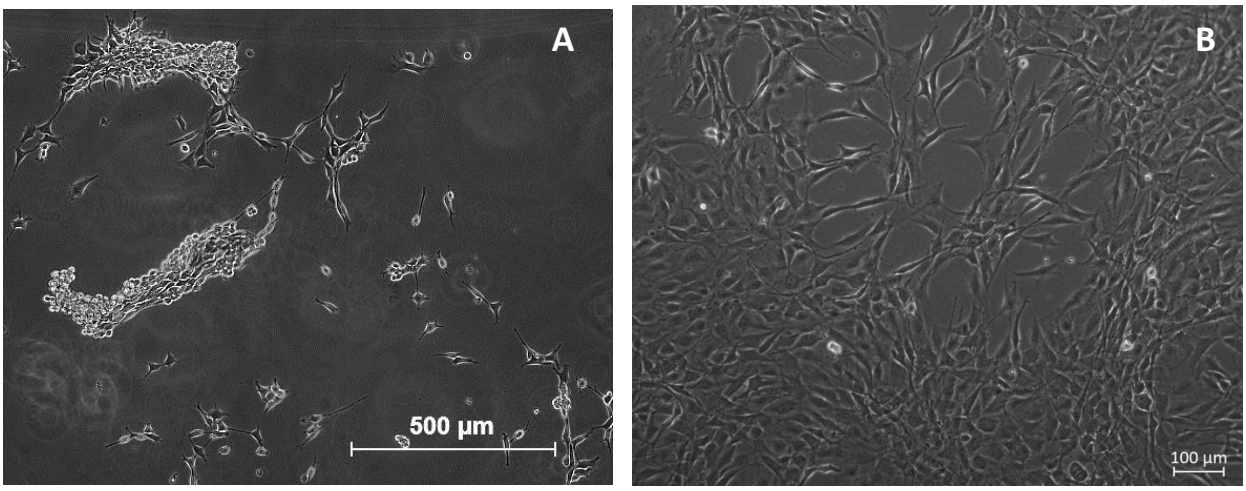

Figure 12 10x image of NIH 3T3 cells growing on (A) hydrogels with an elastic modulus of 30.4 kPa (±3.8) and (B) a regular tissue culture dish.

Optimization

After conducting the feasibility study and examining the preliminary data of the hydrogels, our team came to a few conclusions to modify and improve the hydrogel system's design. Alterations were made to the volumes of solution used, the size of the coverslips used, the order in which the coverslips are used for fabricating the heterogeneous gels, the UV light used to crosslink, the Irgacure stock solution, and BIS-Acrylamide ratios to prevent cloudiness in the gel. Additionally, the preliminary cell studies indicated that acclimatization of NIH 3T3 cells would be needed or a different cell line must be used.

The first alteration was made to the thickness of the gel. The specifications of our project state that the gel must have a thickness between 100-200µm, so our team calculated the exact volume of BIS-Acrylamide solution that would be necessary in order to obtain this thickness.

It was also decided that 25x25mm coverslips would need to be used as top and bottom slips to obtain the best possible hydrogels. Previously, a 25x25mm glutaraldehyde treated coverslip was used as

the bottom coverslip, and an 18x18mm oxygen plasma cleaned coverslip was used as the top coverslip. However, in order to successfully make hydrogels within the desired stiffness using two 25x25mm coverslips was a necessary change to the protocol.

Also, the order in which the coverslips were used when creating the heterogeneous hydrogels was changed in order to make the surface of the hydrogel as smooth as possible. Previously, two oxygen plasma treated slips were used to create the stiff island, and a normal coverslip and glutaraldehyde slip were used when making the surrounding medium gel. After discovering that the surface of the gel was often imperfect, our team decided that making the gel and using the underside for testing would provide the most ideal surface for measurements, as it would be the smoothest. Therefore, the coverslip order for the construction of the gel was changed to using a DCDMS treated slip and oxygen plasma cleaned slip to create the stiff island, and an oxygen plasma treated slip and a glutaraldehyde treated slip to create the surrounding medium gel. In this way it is possible to make a circular stiff island, and then create the surrounding gel in such a manner that the 'bottom' slip can be removed, leaving the bottom smoother section of the gel to be tested as the top of the gel binds with the glutaraldehyde slip.

Further modifications after analysis of preliminary hydrogel AFM testing results included choosing to polymerize the hydrogels in a UV box (GelDoc) rather than with two UV light strips. This modification was decided in order to decrease personal UV exposure while providing the hydrogel solution with a better chance of receiving constant polymerization with no variance in strength based on location. After switching to the GelDoc, the hydrogels polymerized much faster and more evenly than with previous methods.

Our team also quickly discovered that it was not possible to create a stock solution to make the hydrogel solutions, due to the insolubility of Irgacure. After attempting to make a stock solution, our team discovered that the amount of Irgacure necessary to dissolve into the DI water solution was not

viable. Therefore, a 5% dry weight percentage of Irgacure must be dissolved into each BIS-Acrylamide solution as it is made in order to add Irgacure to the solutions and achieve photo-initiation and overall polymerization.

Hydrogels that remained cloudy after polymerization were not viable for testing because of the transparency specification. In order to remedy the issue, our team altered the BIS in the BIS-Acrylamide solution, and ensured that the BIS percentage was below 0.1% as recommended by Professor Wen. After taking Prof. Wen's advice and altering the BIS-Acrylamide ratios accordingly, our team did not see any issues with opaque gels, and transparency was not an issue. Overall, each of these modifications was completed in order to optimize the process of making the hydrogels while achieving the best possible results from our experimentation. Our team believes that these changes will result in the production of much better hydrogels for testing and experimentation.

Finally, to conduct cell studies on the gels a cell line that could grow on the gels was needed. The preliminary data underscored the importance of substrate stiffness and how NIH 3T3 cells are conditioned to growing on tissue culture dishes. In order to have a healthy cell population, an attempt to acclimate the NIH 3T3 cells to the gels was taken but since it was unsuccessful, the team changed cell lines. The NIH 3T3 cells were replaced with STO cells per Prof. Ambady's recommendation. STO cells are also mouse fibroblasts but they grow faster than the NIH 3T3 cells and are more resilient.

Chapter 5: Design Verification & Results

Control Gels & AFM Control Gel Data

From this point onwards, by discarding the 'soft' hydrogel solution, the 'medium' solution will be referred to as the 'soft' hydrogel. Gels homogeneous in stiffness of the 'Hard' or 'Soft' stiffness were used as the controls. The Young's Modulus, Loss Modulus, and Storage Modulus of the gels were characterized through AFM indentation curves using a custom MATLAB code. For the gels of uniform stiffness, 40 randomly distributed points were measured. Figure 13 shows the Young's Modulus (Em), Loss Modulus (E'), and Storage Moduli (E'') of the soft and hard gels which are found in Table 9 and Table 10.

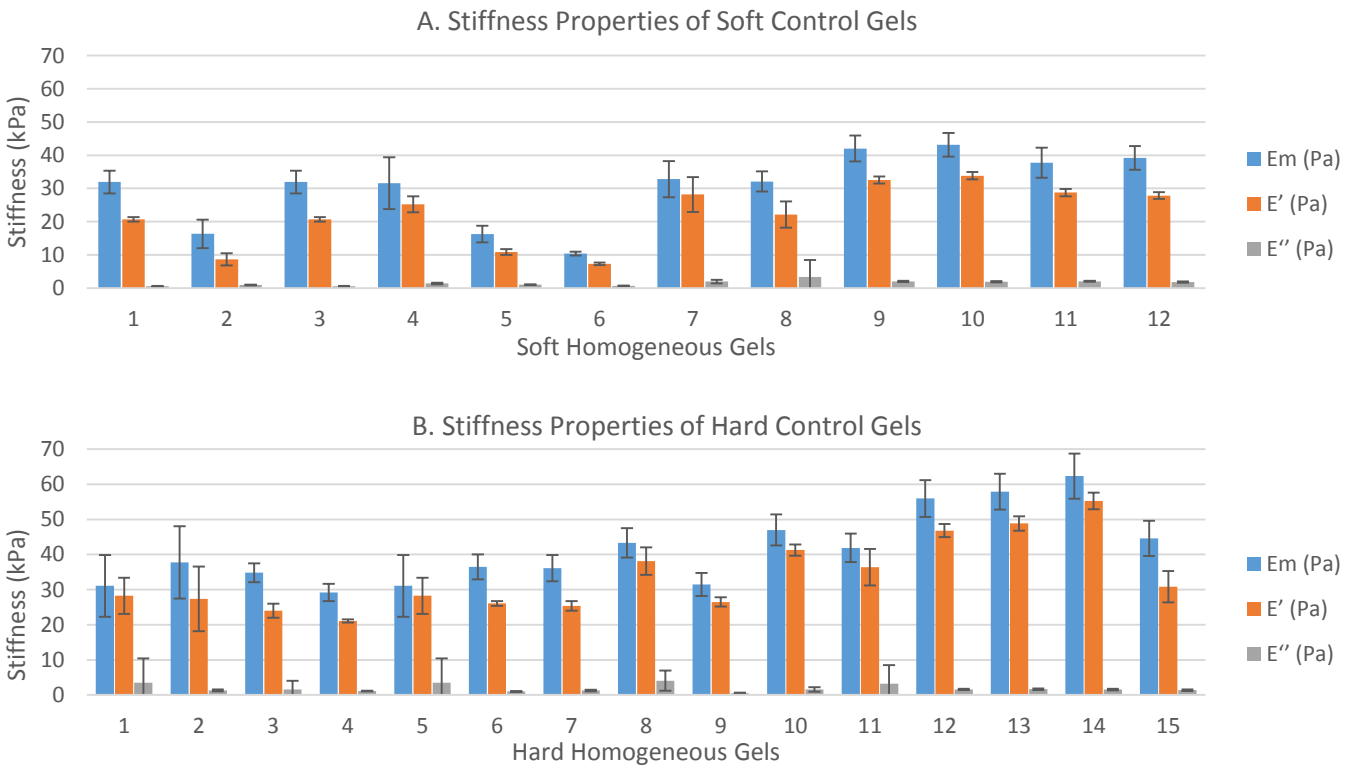

Figure 13 Average Elastic (Em), Storage (E'), and Loss (E'') Moduli of (A) Soft Control Gels and (B) Hard Control Gels

Table 9 Raw Data for Homogeneous Soft Gels

SOFT GELS	Em (Pa)		E' (Pa)		E'' (Pa)	
	Average	Standard Deviation	Average	Standard Deviation	Average	Standard Deviation
1/14/2014	31923	3419	20667	662	519	159
1 (1/28/14)	16319	4260	8666	1846	935	106
2/14/14	31923	3419	20667	662	519	159
2/18/14	31569	7782	25257	2409	1385	212
1 (3/1/14)	16266	2479	10865	861	1015	96
N (3/1/14)	10374	563	7336	380	690	66
A (3-11-14)	32791	5425	28197	5249	1948	521
B (3-11-14)	32106	3061	22131	3987	3341	5067
1 (4-3-14)	42027	3924	32537	1073	2035	199
2 (4-3-14)	43110	3563	33826	1080	1893	198
3 (4-3-14)	37726	4531	28751	1085	2008	136
4 (4-3-14)	39191	3561	27862	1031	1808	210
Average	**30444**	**3832**	**22230**	**1694**	**1508**	**594**

Table 10 Raw Data for Homogeneous Hard Gels

HARD GELS	Em (Pa)		E' (Pa)		E'' (Pa)	
	Average	Standard Deviation	Average	Standard Deviation	Average	Standard Deviation
1/14/2014	31082	8789	28251	5144	3460	6970
1 (1/28/14)	37777	10266	27376	9221	1306	261
Fl-1 (1/28/14)	34808	2693	24028	2023	1563	2447
Fl-2 (1/28/14)	29188	2497	21076	479	1113	110
Fl-3 (1/28/14)	36480	3548	26067	673	1001	164
Fl-4 (1/28/14)	36120	3741	25340	1354	1291	221
1 (3/1/14)	43342	4174	38135	3952	4087	2893
N (3/1/14)	31495	3306	26492	1295	456	173
A (3-11-14)	46981	4430	41293	1607	1597	626
B (3-11-14)	41907	4050	36421	5196	3191	5318
1 (4-3-14)	55960	5220	46798	1858	1591	190
2 (4-3-14)	57888	5117	48852	2077	1635	213
3 (4-3-14)	62336	6456	55301	2375	1546	242
4 (4-3-14)	44609	5009	30848	4473	1390	225
Average	**44382**	**4894**	**34020**	**2980**	**1802**	**1432**

Heterogeneous gels

There were different methods of measuring the heterogeneous hydrogels. First, 40 random points were taken inside the stiff island and 40 random points were taken outside the stiff island. The stiffness of four hydrogels can be seen in Figure 14.

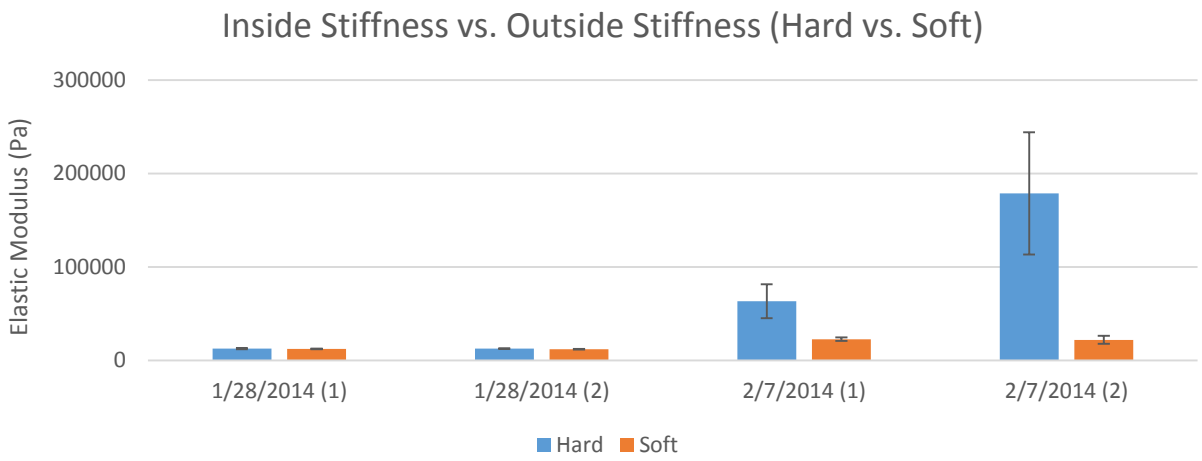

Figure 14 Heterogeneous Hydrogel Inside Stiffness vs Outside Stiffness

It would be beneficial to determine if the heterogeneous hydrogels had a distinct difference between the hard and soft elastic moduli. Therefore from this point onwards, heterogeneous gels were measured by the AFM operator taking stiffness profiles from the visualized center of the gel to the outside at 100µm increments. A 'Good' stiffness profile for a heterogeneous gel was determined by a sharp stiffness change which would indicate a sharp edge between the hard and soft region. The gel must also have a consistent high stiffness before the change and a consistent low stiffness after the change. A decent heterogeneous hydrogel showed characteristics of a boundary point between the hard and soft elastic moduli, however they did not have a consistent high stiffness before the boundary point and a consistent low stiffness after the boundary point. An unacceptable heterogeneous hydrogel showed no characteristics of a boundary point between the hard and soft elastic moduli. Examples of 'Good', 'Decent', and 'Unacceptable' heterogeneous hydrogels are seen in Figure 15, Figure 16, and Figure 17 respectively.

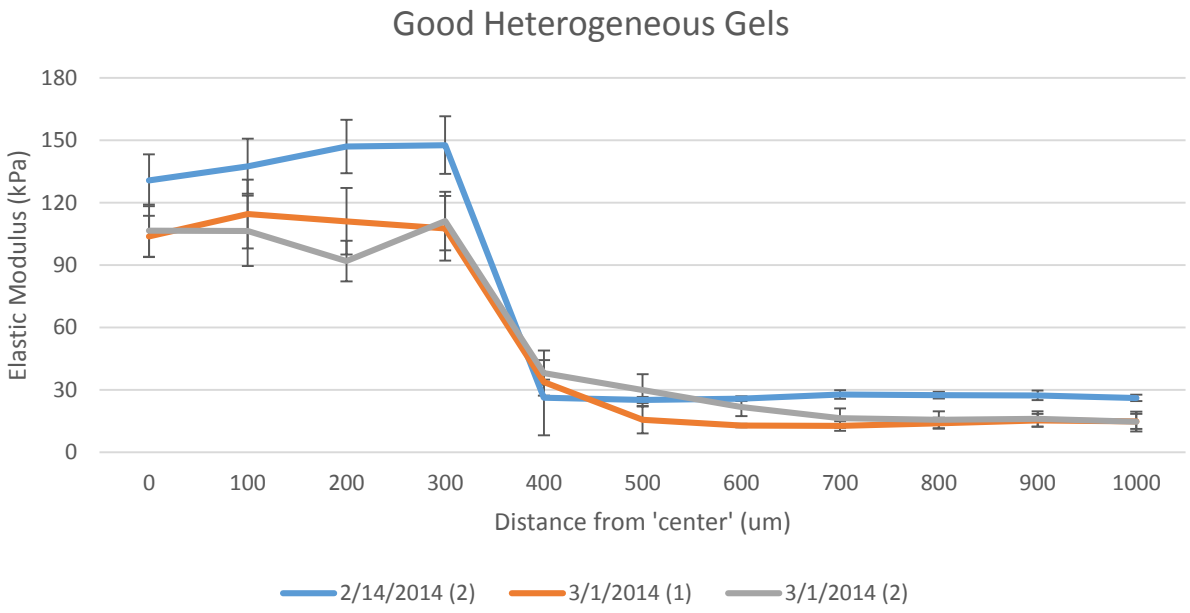

Figure 15 Stiffness Profiles of Good Heterogeneous Hydrogels

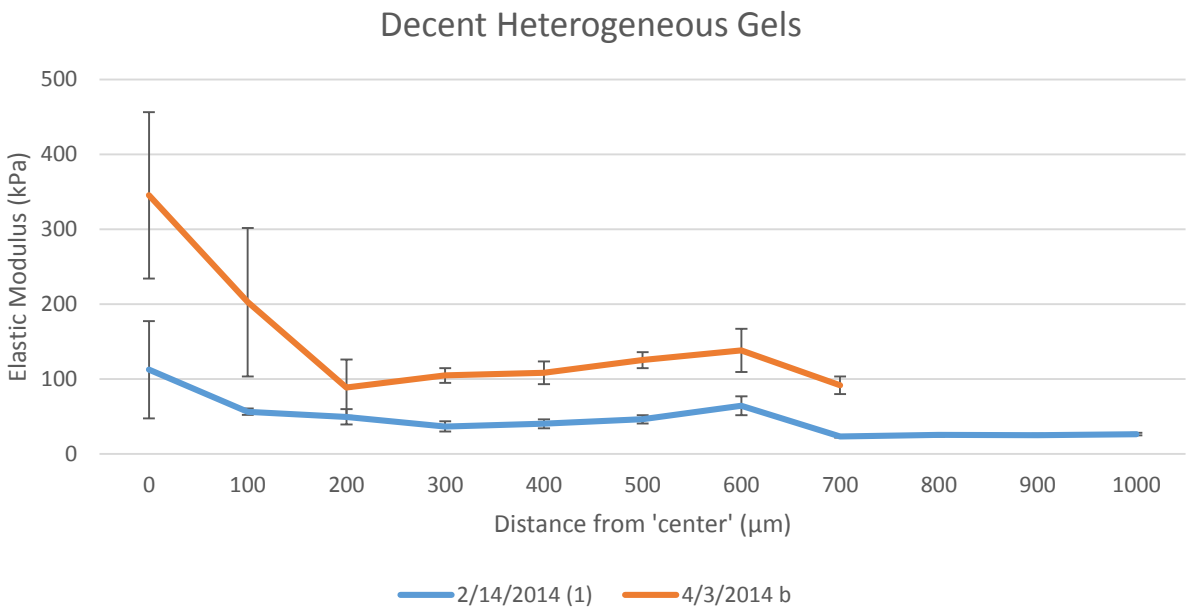

Figure 16 Stiffness Profiles of Decent Heterogeneous Hydrogels

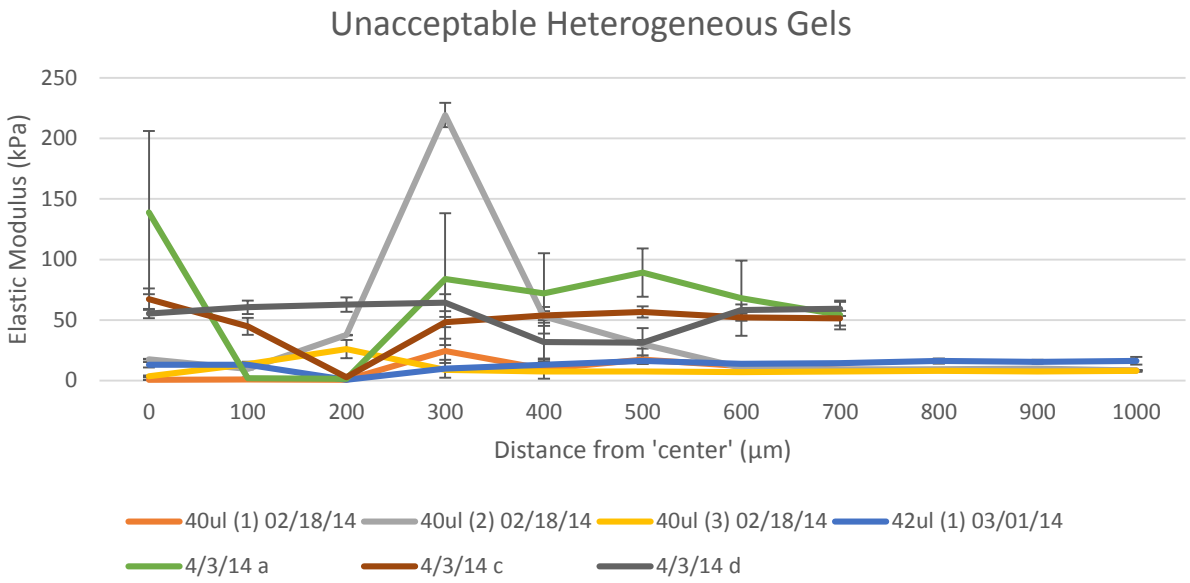

Figure 17 Stiffness Profiles of Unacceptable Heterogeneous Hydrogels

All heterogeneous hydrogels stiffness profiles can be found in Appendix 7: Heterogeneous Gels. To validate the radius of the stiff island, profiles were taken across the entire stiff island. However, the AFM was unable to reach across the entire stiff island as it was outside of the window of the microscope. This can be seen by the abrupt stop seen in Figure 18 in both profiles.

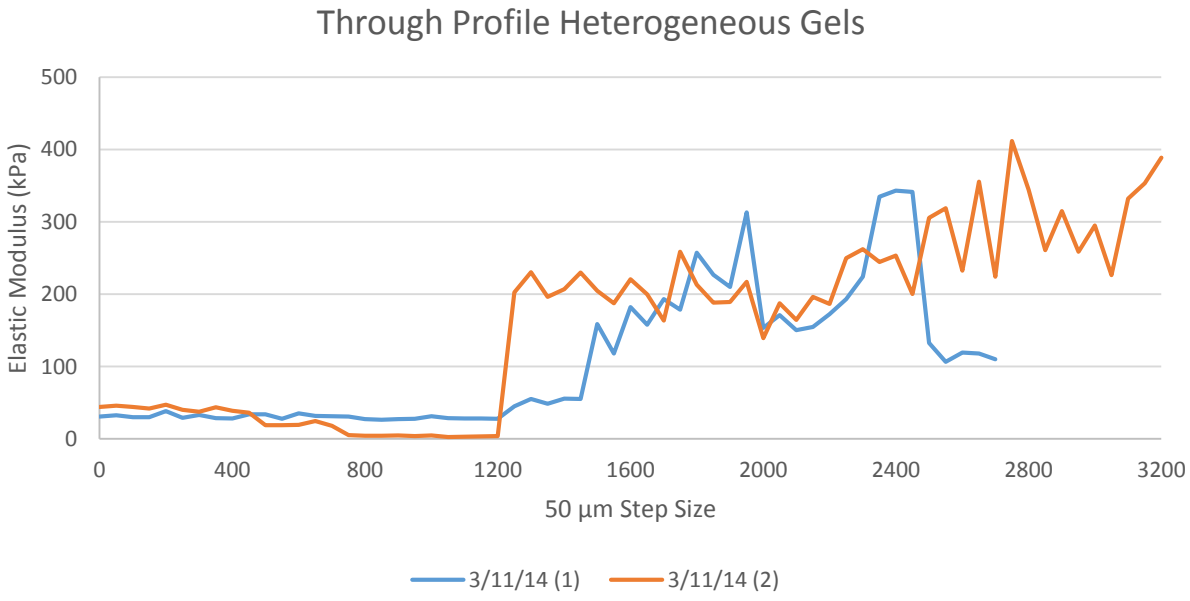

Figure 18 Through Profile of Heterogeneous Hydrogels

Stiff Region Shape

A photomask was created by laser-cutting 6 holes (diameter = 1 mm) on a UV-light resistant acrylic pane. The mask worked for making the small islands. Figure 19 shows that the fluorescent beads effectively mark the stiff regions. Most importantly, the stiff islands can be identified by their fluorescence in order to take the AFM measurements. The last row of two stiff islands had actually floated off the coverslip during their hydration period. These were picked up with forceps and put back on the coverslip to polymerize the surrounding gel as an experiment to see if it was feasible. It is not; the islands get torn by the forceps or are not placed flat on the glass.

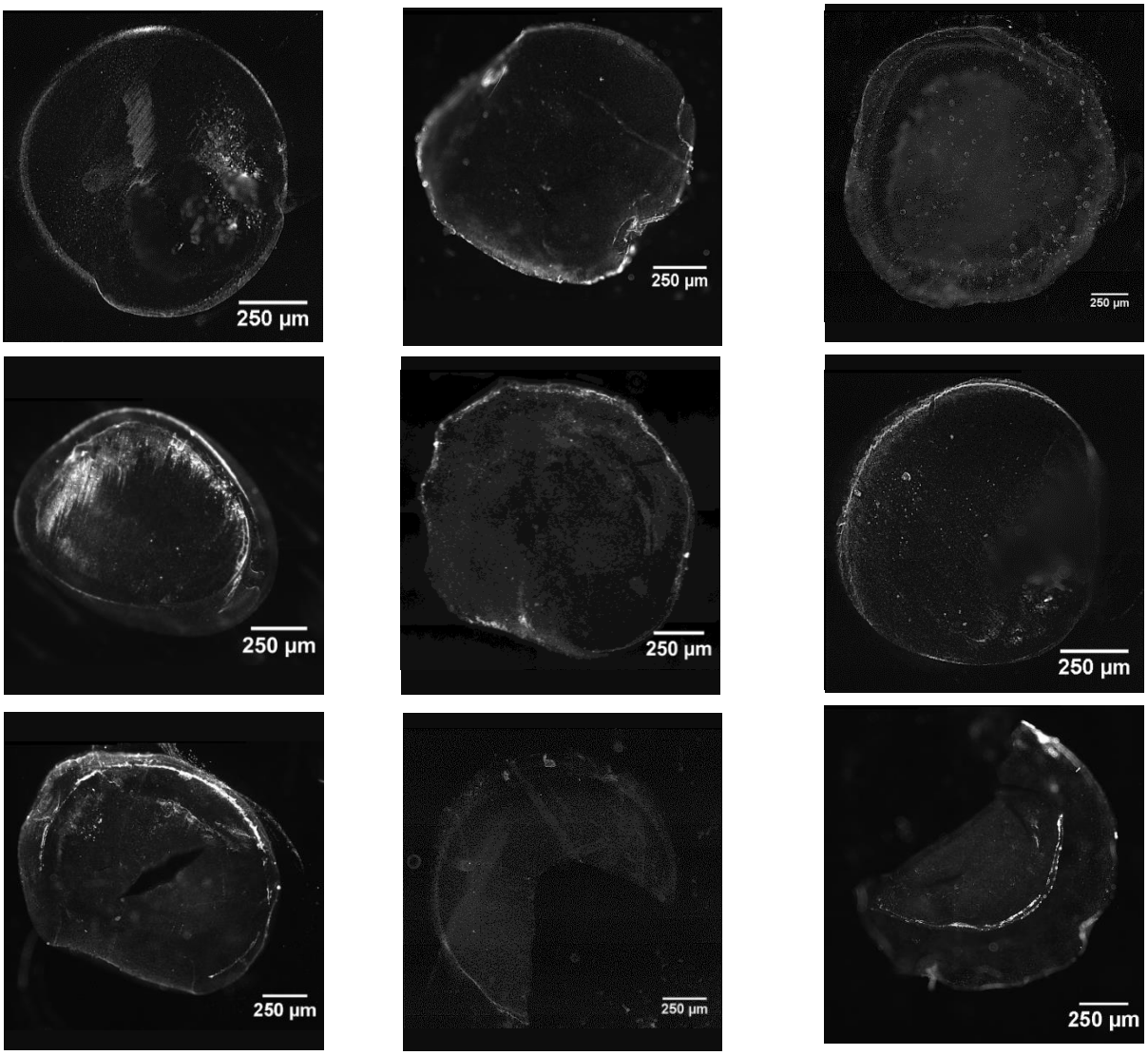

Figure 19 Fluorescent images of the stiff islands loaded with 0.2 µm green fluorescent microbeads

Background Fluorescence

Not all the fluorescent beads were rinsed off the coverslip after the stiff island had been made. Examples of fluorescence of residual beads can be seen in Figure 20. While this background fluorescence is inconvenient, it does not make it impossible to find the stiff regions. As long as the stiff region can be clearly identified, the fluorescence due to the residual beads is not a problem.

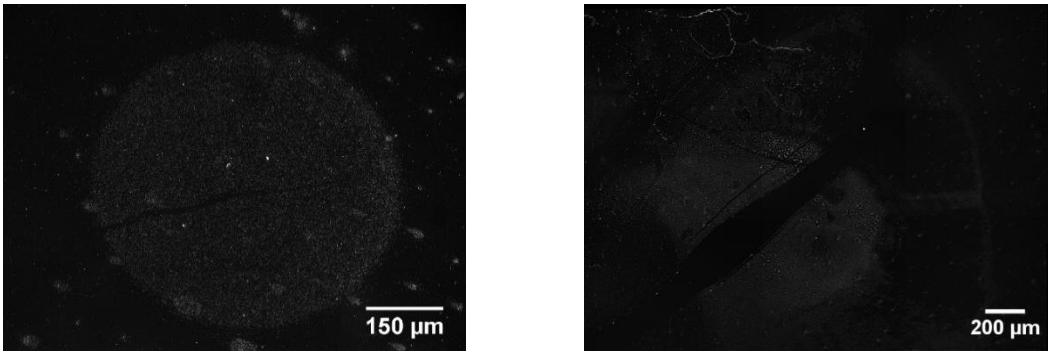

Figure 20 Representative images of background fluorescence due to the microbeads not being washed away properly

Surface Characteristics

Due to differences in swelling ratios between the hard and soft gels there was a difference in gel thickness in the heterogeneous gels. Measurements were not taken since the difference could be seen with the naked eye. Since our team could visually identify the stiff region as the thickest part, different volumes were used for the stiff island (30 µL instead of 62 µL) in order to match the thickness of the surrounding gel. This overcompensated for the difference in swelling ratios and was adjusted until the AFM operator indicated the step had been reduced considerably. The stiff islands were made with 43 µL of polymer solution from this point onwards. After polymerizing the surrounding region, the surface of the stiff region formed wrinkles. Figure 21 shows three wrinkled stiff islands. In some cases no wrinkles appeared at all. Figure 21B shows a stiff island that has become very wrinkled in comparison to Figure 21A and Figure 21C. All these images were taken with phase contrast microscopy. It is important to note that the wrinkles were not discernible with the naked eye.

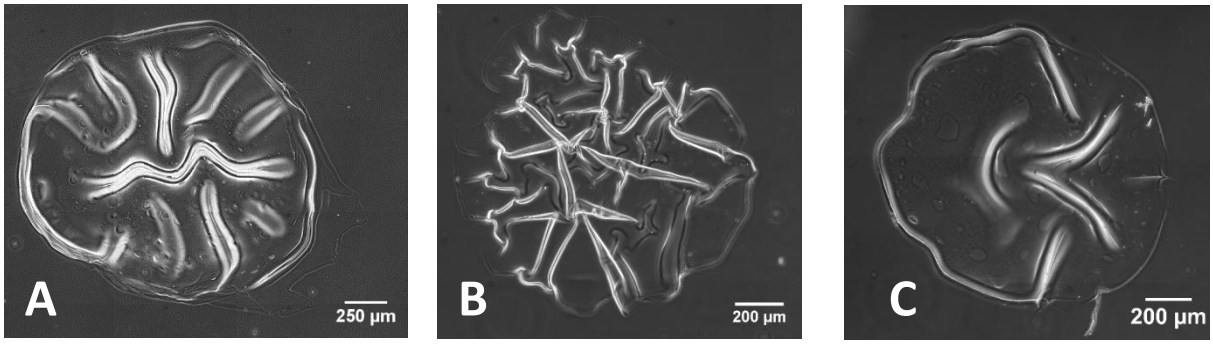

Figure 21 (A-C) Phase contrast of a wrinkled stiff island

Cell Analysis

The STO cells were imaged 30 min after seeding when the cell culture media was added to the 60 mm petri dish. Figure 22 shows STO cells growing on the hard, soft, and heterogeneous gels.

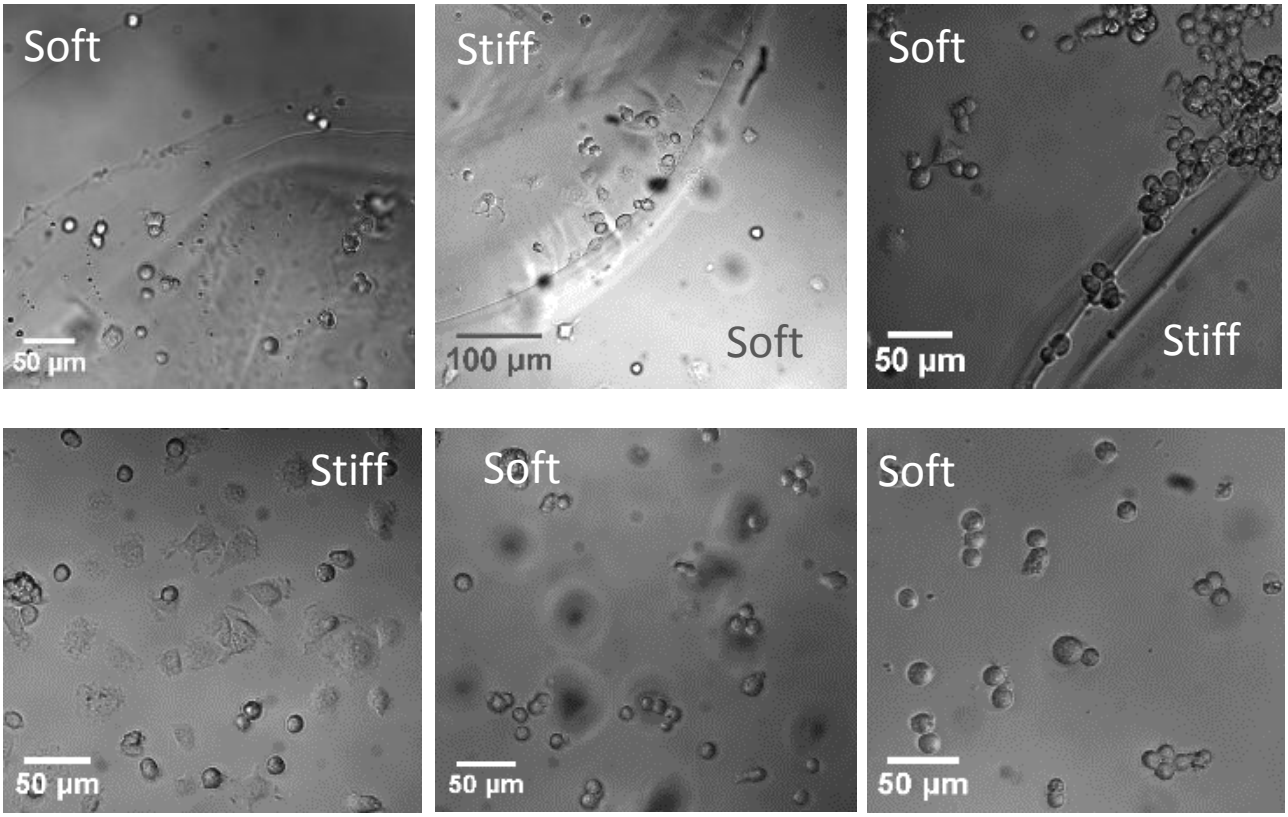

Figure 22 cells growing on heterogeneous (first row) and homogeneous hydrogels (second row).

Cell attachment on the gels was interesting – many cells clustered on the boundary region and attached to the hard regions faster than to the soft regions (Figure 22 first row). Figure 22 (second row)

shows cells at 30 min after seeding on the control hydrogels. The cells on Figure 22 (stiff gel on the second row) are much more spread out than those on Figure 22E and Figure 22F showing that the cells took longer to adhere.

The stiffness of ten STO cells was measured more than 24 hours after seeding for each of the three heterogeneous gels used in this study. Half of the cells were on the stiff region and the other half on the soft region. The results showed that the difference in elastic, storage, and loss moduli between cells growing of the stiff regions and those growing on the soft regions were not significantly different (Table 12).

Table 11 Cell stiffness data of STO cells

	Average on hard (n=15)	Standard Deviation (±)	Average on soft (n=15)	Standard Deviation (±)
Em (kPa)	3.4	1.5	2.8	1.3
E' (kPa)	2.7	0.7	1.7	0.7
E'' (kPa)	0.9	0.2	0.6	0.2

Chapter 6: Discussion

The control gels had an average stiffness of 30.44 (±3.83) kPa for the soft (n = 12), and 44.38 (±4.89) kPa for the hard (n = 15). The values reported in literature were 10.61 (no standard deviation reported) and 40.40 (±2.39) kPa for the soft and hard gels respectively (Tse & Engler, 2010). The authors also used AFM to characterize the elastic modulus of their gels – 50 indentations in 3 or more hydrogels. Our results for the soft gels are not consistent with the values reported in literature; our soft gels were almost three times stiffer than the values in literature. We believe that the main contributions to this error could be that the elastic modulus is calculated differently or that there are discrepancies in our process. While we also used AFM nano-indentation to calculate elasticity, the data analysis done by the custom MATLAB code provided by Professor Wen could yield different results. The main challenge in standardizing the gel fabrication process was coordinating the gel fabrication with the AFM operator who took the measurements. Therefore, the gels soaked in HEPES buffer for different time intervals before the elasticity was measured. We hypothesize that the elasticity of the gels is time dependent until they are fully hydrated. Due to time constraints we could not investigate this hypothesis fully. Our hard gels, on the other hand, are within experimental error of the values reported in literature.

The heterogeneous gels presented a similar case although there were other problems associated with the stiff region, such as stiff region shape, surface wrinkles, and thickness difference with the surrounding gel. We were able to produce heterogeneous gels with a sharp decrease in stiffness from the stiff region to the surrounding softer region (Figure 15). The stiffness gradient from one area to the next can be affected by the stiff region's shape – especially when the surface area of the bottom of the stiff region is larger than that on the top. The acrylic mask had 1 mm diameter holes laser cut into it. This should have produced a precise cut however the heat of the laser melted the acrylic and warped the shape of the holes. Despite this, many of the stiff islands had acceptable shapes (Figure 19). Finally, wrinkles appeared on the surface of the stiff regions (Figure 21). We believe this is caused by the

surrounding gel crushing it as it hydrates. The measures we took to address this were not sufficient: increasing the hydration time of the stiff region prior to gelling the surrounding gel did reduce the severity of the wrinkles; however it did not eliminate them entirely. Furthermore, with hydration periods longer than 24 hours, the stiff region was prone to lifting off the coverslip.

The STO cells seemed to adhere and spread out faster on the stiff substrate, they seemed to cluster on the edges of the stiff regions, and the cell stiffness was not significantly different when changing the substrate stiffness. Due to the small sample sizes we cannot draw any conclusions from these results. Experiments with larger sample sizes, more data points, and controlled variables would be necessary to investigate the cells' behavior. In the case of cell adhesion, the experiments would have to determine cell adhesion strength and cell spreading to the stiff and soft substrates at different time points. The clustering of cells at the boundary of the regions was definitely the most interesting cell behavior we observed. Our team would have controlled the AFM measurements so that cells on the boundary point between the hard and soft elastic moduli were measured. Additionally, we would have investigated cell migration to determine if the cells migrated towards the stiff regions. Further data on these cell responses to substrate stiffness could provide insight into tumor formation and metastasis. Before conduction more experiments however, the gel surface should be validated as perfectly smooth and even as this could greatly influence the cells' behavior.

Limitations

Limitations of the data found include the timeline and flexibility in which the AFM measurements were taken, inaccuracies in measuring mass or volumes for the polymer solutions, and wrinkles on the stiff regions' surface. Our team was not able to use the AFM, and an AFM operator had to do so. Therefore, our team had very little control over when the hydrogels were being measured and analyzed and this resulted in many complications.

Sometimes the AFM operator was unable to analyze all the gels due to scheduling conflicts or analyzed the gels days later. Therefore, not all the gels we made were measured. The AFM operator's lack of scheduling was another huge limitation. Despite many attempts to standardize the time when the stiffness measurements were taken, this remained a variable we could not control or plan for. The time dependence of the hydrogel's swelling was never fully understood because this would have been too time consuming for the AFM. Due to the hydrogel's swelling properties this could account for a significant amount of error in our data as some gels were not analyzed for weeks after fabrication. The AFM operator was also working on other projects, and sometimes measured our data according to other team's specifications rather than our own. This was out of our team's control, but often provided hard to read, variable, or inconsistent data due to the measurement style in which the data was obtained. Even if we could analyze the data, we could not compare it to our other data. This flaw could again be remedied through allowing the students to do their own testing and work with the AFM.

Limitations of the data could also include human error or laboratory equipment inaccuracy. For example, variations when measuring small masses or volumes to make batches of polymer solutions could cause inaccuracies. These problems could be minimized by producing large enough batches that the error per measurement is smaller as a percentage of the amount being measured.

Finally, the hydrogels that were produced had a relatively smooth surface, but some had small wrinkles within the gel's stiff island. This could have had an effect on the cell-substrate behavior in that region, and it is recommended that in the future, a protocol should be made to ensure the gel's surface is made completely smooth before cell seeding.

Our team observed that NIH 3T3 cells were not viable on soft control gels. In an attempt to continue using the NIH 3T3 cell line, our team performed a cell acclimation study where NIH 3T3 cells were seeded on soft gels for 10 days. Our team attempted to culture these cells so that they would

become accustom to the softer surroundings and therefore not be affected when seeded on the heterogeneous gels. However, this study was unsuccessful as the cells were not viable after 10 days. It was from that point on our team used STO cells as they do not adversely react to the softer surroundings. Although STO cell stiffness data was taken, it is difficult to determine if the data is statistically significant due to a small sample size. This is a result from the coordination between our team, the other teams that used the AFM, and the AFM operator. Our team had to make sure the AFM operator had time to measure the cells days in advance because if our team had seeded the cells too early, the cells would have been overly confluent and the data would be inadequate, but if our team had seeded the cells too late, none of the cells would have adhered to the surface of the hydrogel.

Furthermore, we were unable to test varying time points for cell stiffness because the cells are no longer in a sterile environment after they have been tested the first time. If our team were to continue the project, it would be interesting to observe cell stiffness over a period of time as well as other cell properties. On the other hand, we were unable to collect more data on cell stiffness purely due to time limitations. Experiments with larger sample sizes and controlled variables would be necessary to investigate cell adhesion, migration, and proliferation as functions of time and substrate stiffness. Additionally, our team would have observed how the cell's stiffness would transcend across the boundary and how far their interactions would travel. This data would have provided valuable insight into cell-cell and cell-substrate interactions. Also, although it was outside the scope of our project, investigating different cell lines interactions across the boundary of the stiff and soft elastic modulus would have been interesting.

Other Considerations

The purpose of our gel primarily serves to facilitate research in any cellular engineering field. If this were to be marketed as a research device factors such as economic impact, societal impact, political

and ethical ramifications, health and safety, manufacturability and repeatability would need to be taken into account.

Economic and Environmental Impact

In terms of economic and environmental influence, our method does not directly impact the economy or environment significantly. Our method uses relatively inexpensive raw materials but expensive equipment. The materials we use, namely the polymers, sulfo-SANPAH, collagen, glass coverslips and 60mm petri dishes are commercially available at the typical research prices. The greatest cost would be the Atomic Force Microscope ($260,670, Asylum Research MFP3D BIO) and the respective tips used to validate the gels. Although these costs are high for an individual laboratory, it is minimal in the long term cost of cancer research. As further investigation of cancer and healthy cell's response to heterogeneous elastic moduli is conducted, this novel heterogeneous hydrogel may be a stepping stone towards a treatment. This future for our system would have economic impacts. However, at this time, there are minimal economic impacts. All of these materials are classified under a Biosafety level 1, meaning they have a minimal potential hazard to laboratory personnel and the environment.

Societal Influence

Our team believes that in the future, there will be many tests of cells' response to surfaces that are heterogeneous in stiffness. Since substrate stiffness has been shown to play a key role in processes like cancer metastases, stiffening of blood vessels, and cell differentiation, we believe that the demand for a device like this to conduct research will increase. Research on this could lead to great societal advances. For example, using tumorigenic cells, cancer metastases could be better understood, could even help physicians predict cancer cell movement, and could maybe even lead to the development of therapeutics for its prevention. Unfortunately there are still limitations to using this device for such research.

Political Ramifications and Ethical Concerns

The political and ethical ramifications of the design are currently non-existent. The cells used in analysis are a mouse fibroblast line, and all materials are purchased for laboratory use. However, in the future should the design be perfected, stem cells could be introduced to the heterogeneous PAA hydrogels for analysis. Should this be the direction that the design takes, there will be political and ethical controversy about the use of stem cells in research. While stem cell harvesting and research is allowed in the United States, many political and religious groups believe that this should not be the case. Should the design be taken in this direction, however, it would receive no more critique than any other scientific research device which requires embryonic stem cells for experimentation.

Health and Safety Issue

In terms of health and safety of our design, the safety of the user was our primary objective. As mentioned before, all materials for this project are Biosafety level 1. This means the materials used are not known to consistently cause disease in healthy adult humans and have a minimal potential hazard to laboratory personnel and the environment. There have been neurotoxic and carcinogenic reports for acrylamide and bis-acrylamide and therefore these reagents are considered a potential occupational carcinogen by US agencies. These concerns stem mostly from the ingestion of acrylamide in foods; therefore it's not a concern for our hydrogel synthesis system. Our team still took precautions and by using personal protective equipment, such as nitrile gloves, apron, and goggles, any possible hazards were minimized.

Manufacturability

In the current market, the manufacturability of this hydrogel based system would be extremely poor. While the protocol to make the heterogeneous gels is reproducible, the testing equipment to validate the stiffness of the hydrogels is extremely costly. It is also very difficult to make many hydrogels at one time, and for now the process must be completed by hand since there is no automated system

capable of this task. Based on the amount of time and material it takes to make one hydrogel, and the fact that sometimes the hydrogels don't turn out useable for cell testing, our team would rate the overall manufacturability of the gels to be very poor. This can be investigated and changed, though, perhaps with an automated system to make and dispense the hydrogel solution onto coverslips. The human error could be eliminated, the process sped up and should there ever be a need for these hydrogels in bulk, an automated system would be a necessity.

Repeatability

While our process is repeatable, the process is not consistent enough. When the stiff regions are hydrated overnight as seen in Appendix 5: Experimental Methods, the gels have a tendency to lift off the coverslip. While this step is necessary to allow the gel to fully swell to decrease the surface wrinkles, it lowers the success rate to approximately 60%. This creates an unsustainable method for a long term project. For future work on this method, improving the success rate would be optimal so that it is sustainable for long term and short term projects.

Chapter 7: Final Design and Validation

In Table 12 the costs of the main components that were used to polymerize a single hydrogel are outlined. Other materials that were used in the hydrogel construction were one time purchases, used in minimal quantities, or readily available in the laboratory so that these costs were negligible. The final cost per gel was $.36, and therefore we were within our constraint of $1 per gel.

Table 12 Final Cost of a Single Heterogeneous Gel

Material	Bulk Cost ($)	Quantity per Gel	Cost per Gel ($)
40% acrylamide (Biorad) – 500 mL	48	0.6 µL	0.000576
2% bis-acrylamide (Biorad) – 500 mL	49	0.6 µL	0.000588
200 Glass Cover Slips, #1 thickness, 25x25mm	24.21	3	0.36
Total			**$ 0.36**

In our final design, the stiff region of the heterogeneous gels was crosslinked first and then the surrounding area was polymerized as illustrated in Figure 23. We laser cut 1 mm diameter holes on a UV-blocking acrylic pane (TAP Plastics, OP-3 Clear) to make the photomask. The stiff region was made by pipetting 43 µl of the degassed hard solution for the stiff region onto a coverslip treated with dichlorodimethylsilane (DCDMS), covered with a clean coverslip, set on the photomask and exposed to UV light (256 nm) for 10 minutes. The unpolymerized solution was rinsed off and the stiff gel was soaked overnight in HEPES buffer. Next the surrounding region was made; 64 µl of the degassed soft solution for the surrounding area was pipetted onto the slip with the stiff island, covered with an APTMS-glutaraldehyde treated slip, and exposed to UV-light for 8 min. The bottom slip was removed, and the hydrogel was left in HEPES buffer at 4^{o}C until use.

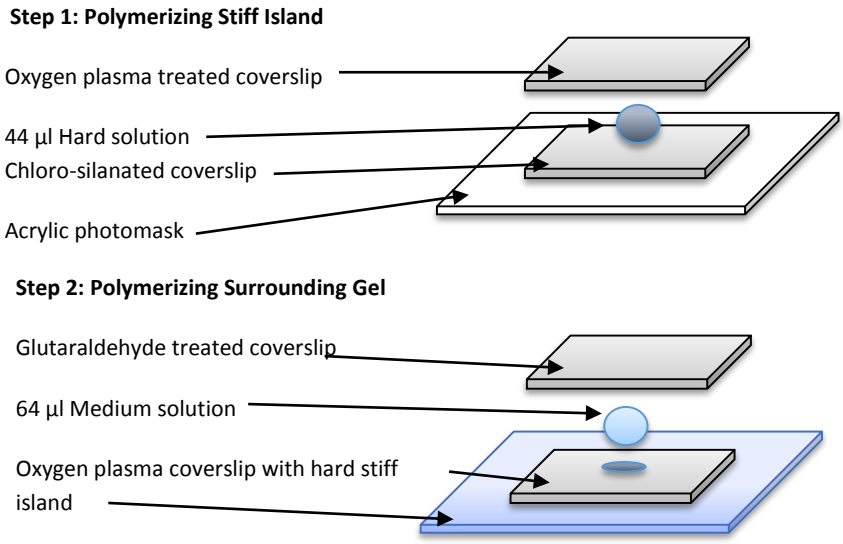

Figure 23 Heterogeneous Fabrication Method

To validate our heterogeneous hydrogels, the shape of the stiff island, surface uniformity, and stiffness was confirmed through various methods. First, the shape of the stiff island needed to be confirmed as a circular patch within the heterogeneous hydrogel. The island should be circular because that was the shape which the photomask allowed UV light to pass through, thereby creating the stiff region of the hydrogel. This was validated through fluorescence microscopy as the hard solution contained microbeads that would fluoresce under excitation. This way, the microbeads will locate and validate the stiff region of the heterogeneous gel. Next, the surface uniformity needed to be flat and smooth. By controlling the volumes used to create the stiff island and the surrounding region, the overall surface characteristic was uniform. This was further confirmed by observing the top of the hydrogel through phase contrast microscopy. By observing the changes in brightness, we were able to determine if the surface of the heterogeneous hydrogel was even between the stiff and soft regions. Lastly, to the heterogeneous stiffness needed to be confirmed. The stiff island's elastic modulus needed to be noticeably harder than the surrounding area. Furthermore, there shouldn't be a gradient change from the hard elastic modulus to the soft elastic modulus; rather it should be a distinct change in

stiffness creating a boundary between the two. This was validated by using AFM to measure a stiffness profile from the center of the stiff region to the surrounding region in 100µm increments. This would confirm the stiffness of the heterogeneous hydrogel as well as determining if there was a distinct boundary between the soft and hard elastic modulus.

For the cellular studies, the PAA hydrogels were coated with collagen as per the protocol found in Appendix 5: Experimental Methods. The coverslips with the heterogeneous gels were put into individual 60 mm petri dishes and half of the gels were seeded with 100,000 STO cells and the other half with 200,000 STO cells, both from a cell suspension containing 10^6 cells per mL. The cells were allowed to attach to the gel for 30 min in the incubator before adding the rest of the complete media. After incubation for at least 24 hours, the cell stiffness measurements were taken with AFM. On average, the stiffness of five cells on each region of each heterogeneous gel was measured by taking five force-indentation curves.

Chapter 8: Conclusions and Recommendations

In conclusion, the final design of the hydrogel *in vitro* system for cell stiffness testing was successful in meeting all of the 'heterogeneous gel' objectives set forth by our team. In meeting these objectives, the system designed by our team was also successful in fulfilling the goals established in the revised client statement. We were effective in creating a hydrogel construction process which was safe to the user. The protocol for creating a heterogeneous hydrogel allowed for reproducible gel creation, as well as the production of hydrogels which were sterile and biocompatible. Through the use of fluorescent microbeads, we were able to visually discern the stiff regions from the surrounding soft regions of the hydrogel, which allowed our results to be verified on a specific stiffness within the gel. The hydrogel system is portable, user friendly with specifically and well outlined experimental protocols, and extremely monetarily sustainable at a cost of only $0.36 per hydrogel. Finally, since the BIS and Acrylamide ratios used to create the different regions of stiffness within the gel are variable according to desired stiffness, the user is able to control the stiffness of the gel depending on the preferred application.

After making our hydrogels, both heterogeneous and homogeneous, we were able to validate their respective stiffness values and compare them to published stiffness values. We concluded that our stiffness values for the homogeneous gels were very close to published values, while the heterogeneous values were slightly different than published values. We believe that this difference could be a result of the increased UV exposure time of the heterogeneous gel, which would allow more time for the gel to photo-crosslink, and essentially become stiffer. Overall, though, our method succeeded in creating heterogeneous PAA hydrogels which can be used in future cell stiffness studies.

After creating the hydrogel in vitro system, we then set out to accomplish the second half of our revised client statement which focused on cell analysis. We came to the conclusion that the final

hydrogel system we created also successfully met the objectives which outlined the cell analysis goal of our project. The final hydrogel system was compatible with standard cell culture techniques, and allowed both cell-substrate and cell-cell investigation. The cell-substrate investigations were carried out using the AFM to test the cell stiffness reactions to the varying stiffness values within the heterogeneous substrate. Our team concluded that the cell stiffness was affected by the substrate stiffness which the cells chose to settle on. The cell-cell investigations were also successful as we observed the cell's behavior under phase contrast and fluorescence microscopy.

While our in vitro hydrogel system succeeded in fulfilling our objectives for both the heterogeneous gel and cell analysis portions of our project, there are also many future recommendations that should be completed in order to perfect our preliminary system.

For future project work, we recommend that ways to make the surface of the heterogeneous hydrogel perfectly smooth should be investigated. The difference in swelling ratios between the regions of different stiffness resulted in different thicknesses within the heterogeneous gel as well as wrinkles on the surface of the gel due to the inability of the stiff region to swell outwards because of the surrounding softer gel. Our team found ways to minimize these effects however the surface was still not entirely smooth or even when we began cell analysis. A smooth and even surface would allow us to attribute results to the change in stiffness with minimal interference from a change in surface height or surface roughness.

Furthermore, an automated system for hydrogel construction should be established due to the long length of time necessary to manually create each gel. With an automated system, the hydrogels produced would also all be identical. This would improve the accuracy of the measurements used in hydrogel fabrication, and would ultimately improve overall experimental ability. An automated system would also improve the success rate of gel production, as human error left the success rate of our

method of gel assembly at around 60%. A machine automated system would essentially create a better hydrogel system for future experimentation.

Improving the validation of the gels stiffness would also greatly improve the ability to obtain consistent results. As discussed in the limitations section, our team was unable to take our own AFM measurements. This kept us from performing further experiments that would have given us better insight into the data. It also kept us from standardizing tests, which would be imperative to achieve more consistent results. Therefore, it would be recommended that laboratory teams that work on this project in the future do so with access to an AFM.

Further cell testing on the heterogeneous hydrogels should also be conducted in order to examine problems more consistent with those found in the human body. More testing on the STO cell line would reveal whether or not the preliminary cell data that we got as a team was accurate. Conducting these STO cell behavior investigations over a longer period of time would also reveal whether or not the cells preferred the stiff region within the softer surrounding gel, and if they began forming a malignant tumor within the stiff region. Also, testing the behavior of other cell lines on the heterogeneous hydrogels could eventually lead to valuable results involving cell morphology, migration, proliferation, and adhesive behavior.

As far as the fabrication of the heterogeneous hydrogel, future work should be focused on investigating other stiffness values as well as different stiffness geometries within the gel. Within the time frame of the project our team was only able to look into the 30kPa and 40kPa stiffness values and circular stiff islands as the stiffness geometry. In future studies, though, the research team will have the freedom to examine multiple circles, squares, lines, or any other desired shape as the stiffness geometries. Future work may reveal that different stiffness geometries affect the cell behavior and stiffness in different ways. Similarly, future research can be focused on different stiffness values which

correlate to various elastic moduli found within the body. This research can also further investigate how different stiffness values besides those investigated in our project affect the cell stiffness and behavior on the heterogeneous hydrogel system.

References

Allyson Beuhler. 2002. US6391937 B1. USPTO.

Amshey Joseph. 2008. 1281070. EP Register.

Brandl, F., Sommer, F., Goepferich, A., (2007). Rational design of hydrogels for tissue engineering: Impact of physical factors on cell behavior. Biomaterials 28, 134-146.

Gallant, N. D., Michael, K. E., & Garcia, A. J. (2005). Cell Adhesion Strengthening : Contributions of Adhesive Area , Integrin Binding , and Focal Adhesion Assembly. *Molecular Biology of the Cell*, *16*(September), 4329–4340. doi:10.1091/mbc.E05

Goldstein, A. S. (2006). Cell Adhesion. In J. D. Bronzino (Ed.), *Tissue Engineering and Artificial Organs* (pp. 34–1–34–17). Taylor and Francis Group, LLC. doi:10.1201/9781420003871.ch34

Gulrez, S. K. H., Al-assaf, S., & Phillips, G. O. (2003). Hydrogels: Methods of Preparation, Characterisation and Applications. In P. A. Carpi (Ed.), *Progress in Molecular and Environmental Bioengineering - From Analysis and Modeling to Technology Applications*. InTech.

Hennink, W. E., & van Nostrum, C. F. (2012). Novel crosslinking methods to design hydrogels. *Advanced Drug Delivery Reviews*, *64*, 223–236. doi:10.1016/j.addr.2012.09.009

Khademhosseini, A., & Langer, R. (2007). Microengineered hydrogels for tissue engineering. *Biomaterials*, *28*(34), 5087–92. doi:10.1016/j.biomaterials.2007.07.021

Lee, K. L., & Mooney, D. J. (2001). Hydrogels for Tissue Engineering, Chemical Reviews, 101(7).

Mahaffy, R.E., Shih, C.K., MacKintosh, F.C., Kas, J., (2000). Scanning probe-based frequency-dependent microrheology of polymer gels and biological cells. Physical Review Letters 85, 4, 880-883

Markert, C.D., Guo, X., Skardal, A., Wang, Z., Bharadwaj, S., Zhang, Y., Bonin, K., Guthold, M., (2013). Characterizing the micro-scale elastic modulus of hydrogels for use in regenerative medicine. Journal of the Mechanical Behavior of Biomedical Materials 27, 115-127.

Omidian, H., & Park, K. (2010). Introduction to Hydrogels. In Biomedical Applications of Hydrogels Handbook, Chapter 1.

Popovic, S., Tamagawa, H., Taya, M., (2000). Mechanical Testing of Hydrogels and PAN gel fibers. Smart Structures and Materials 3987, 177-186.

Pramanick, A.K., Gupta, S., Mishra, T., Sinha, A., (2011). Topographical heterogeneity in transparent PVA hydrogels studied by AFM. Materials Science and Engineering C 32, 222-227.

Sazonova, O. V, Lee, K. L., Isenberg, B. C., Rich, C. B., Nugent, M. a, & Wong, J. Y. (2011). Cell-cell interactions mediate the response of vascular smooth muscle cells to substrate stiffness. *Biophysical Journal*, *101*(3), 622–30. doi:10.1016/j.bpj.2011.06.051

Swaminathan, V., Mythreye, K., O'Brien, T., et al. (2011). Mechanical Stiffness Grades Metastatic Potential in Patient Tumor Cells and in Cancer Cell Lines. Cancer Research, June.

Travis Johnson. 2001. 6686161. USPTO.

Tse, J. R., & Engler, A. J. (2010). Preparation of hydrogel substrates with tunable mechanical properties. *Current Protocols in Cel Biology*, *Chapter 10*(June), Unit 10.16. doi:10.1002/0471143030.cb1016s47

Wong, J.Y., Leach, J.B., Brown, X.Q., (2004). Balance of chemistry, topography, and mechanics at the cell-biomaterial interface: Issues and challenges for assessing the role of substrate mechanics on cell response. Surface Science 570, 119-133.

曹孟君. 1999. *CN1228447 A.* SIPO.

Appendices

Appendix 1: Means to Determine Cell Adhesion

Methods to calculate cell adhesion all use the same principle: free, spherical cells are first allowed to settle and adhere onto a substrate, and then a sudden, well-defined force is applied to the cells with the aim of removing them from the substrate. Probability distribution curves of the cell adhesion as a function of the applied force can then be calculated from the data. Despite that the most common tests to measure cell adhesion are based on the same concept, there are three distinct approaches. Micropipette aspiration, centrifugation of the seeded substrate, and submersing the seeded substrate in laminar flow chambers are the most common ways of measuring cell adhesion (Goldstein, 2006).

Micropipette Aspiration

This test measures cellular adhesion by applying a negative pressure on the cell surface. This essentially suctions the cell into the micropipette's tip, thus straining the membrane until all the tension is concentrated at the last point of contact. The greatest advantage of this method is the fact that the adhesive strength of individual cells can be measured. Micropipette aspiration is also extremely precise, meaning that the cells can be probed with forces in the 10^{-3} to 10^{2} pN range; such assays can actually deform the cell membrane, extract receptors anchored in lipids, but not fracture actin filaments. The disadvantage would be that such precise equipment is costly (Goldstein, 2006).

Centrifugation

Centrifugation is perhaps the easiest assay of the three described in this section as centrifuges are readily available across research laboratories. This assay consists of mounting the test sample onto a centrifuge and calculating the percent of cells that are still attached after being centrifuged. In order to increase the sensitivity of this assay, cells can be induced to phagocytose glass beads, thus increasing the difference of density between the cell medium and the actual cells (Gallant et al., 2005; Goldstein, 2006).

Laminar Flow Chambers

In this case, the tangential force applied onto the cells to remove them from the substrates is the hydrodynamic torque and drag. The setup of this equipment consists of two parallel plates and an induced laminar flow in between (Figure 24). Different geometries in the plates can measure adhesive strength at a range of shear stresses (Figure 24b) while the traditional parallel plates will take measurements at a constant shear stress (Figure 24a). Advantages of these assays are that through a single experiment, cellular attachment, detachment and rolling processes can be observed. Additionally, the tests can be conducted non-destructively and *in situ*. (Gallant et al., 2005).

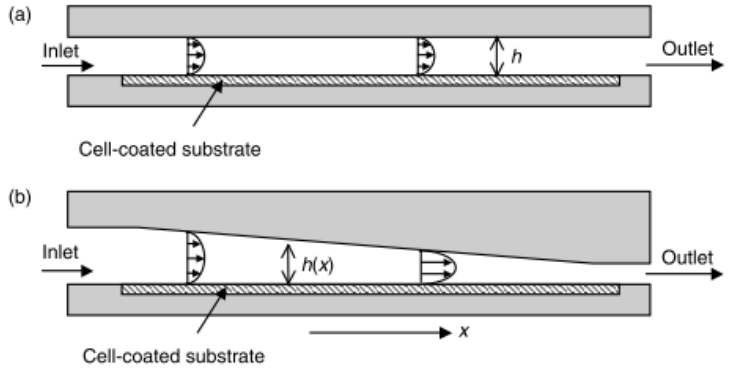

Figure 24 Experimental setup for Laminar Flow Chambers of different height: (a) height, h, is constant; (b) height varies with linear distance, denoted as h(x) (Gallant et al., 2005)

A popular variation of this set up consists of a motor rotating a disk (Figure 25). This setup is often preferred because it does not require a pressure gradient to induce fluid flow as the motor is doing the work. Similar to the laminar flow chamber illustrated in Figure 1b, the rotating disk also generates a shear stress dependent on distance. In this case it would be radial distance (r) as opposed to linear distance (x). A disadvantage of this assay is that the seeded test material needs to be mounted and secured to the device, an inconvenient procedure as the test material would need to be constantly removed to be imaged (Gallant et al., 2005).

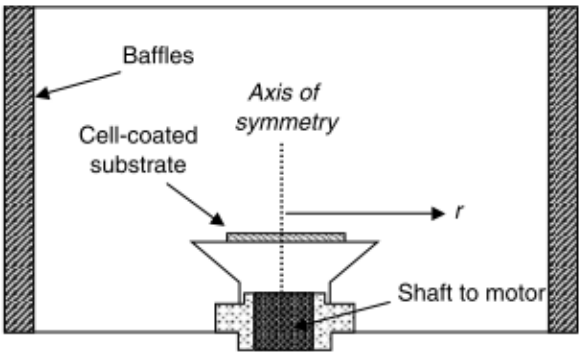

Figure 25 Rotating disk variation of a laminar flow chamber (Gallant et al., 2005)

Appendix 2: Hydrogels

Hydrogels are defined as polymeric networks which are able to absorb large amounts of water. (Hennink & van Nostrum, 2012) As a hydrogel forms a network, more or less crosslinks are present depending on the specific properties of the materials chosen to create the hydrogel, as well as the processing techniques used in order to synthesize the hydrogel (Omidian et al., 2010). Furthermore, these varying degrees of cross-linking directly correlate to the different behavior of the hydrogel. Some hydrogels with lower degrees of cross-linking show Newtonian behavior, while other hydrogels with different polymer chains introduced through cross-linking show viscoelastic, and even pure elastic behavior (Hennink & van Nostrum, 2012). Also, as different polymeric chains are introduced to the hydrogel, their physical, chemical, and mechanical properties differ allowing different polymers to be

chosen in hydrogels for different applications (Omidian et al., 2010). Due to their ability to be heavily modified based on want or need of function, hydrogels are currently being investigated for use in a large number of fields, from agriculture to household items, to medical device and biomedical research.

Classification of Hydrogels

Based on their degree and type of crosslinking hydrogels are often categorized into two different categories, permanent and reversible hydrogels. Permanent gels are chemically bonded, with covalently crosslinked networks (Gulrez, Al-assaf, & Phillips, 2003). Due to their covalently bonded networks, these hydrogels tend to be stronger than reversibly hydrogels. Reversibly hydrogels are physically bonded, and are often held together because the molecules are tangled within one another, or are bonded using ionic or hydrogen bonding (Gulrez et al., 2003). Physically bonded hydrogels often exhibit lower mechanical properties than chemical gels, and can easily be broken down through physical changes in environment or through the introduction of stress on the system. Overall, the type of hydrogel that is created and used depends solely on the need of the application, and whether the desired gel is strong or weak, reversible or permanent. Gels are also able to be further modified for function based on the polymers that make up the structural elements of the gel.

Polymers Used in Hydrogel Formation

When polymers are chosen for hydrogel formation, they are often specifically chosen based on what properties they can bring to the hydrogel and what is needed for any specific function. Polymers have a unique property in which their molecular weight can be regulated from low to high in order to control different properties (Omidian et al., 2010). This is useful in the creation of hydrogels because low weight and high weight versions of the same polymer can be used in different ways, rather than needing an entirely new polymer for a specific need. For example, high weight polymers provide an increased melting temperature, an increased stability, and superior mechanical properties to low weight polymers. However, low weight polymers are often used in circumstances where these properties would be superfluous to the overall function of the hydrogel (Omidian et al., 2010). Polymers can also be either natural or synthetic, and are often chosen again based on the need of the application. Most often the most important consideration in these decisions is the biocompatibility of the polymer. It is important that the body will accept the polymer and that the material can exist within the body without causing any damage. Typically, natural polymers are far more biocompatible than their synthetic counterparts, but they are not accepted as readily by the body (Lee and Mooney, 2001).

Natural Polymers

Natural polymers are often used in the formation of hydrogels due to their outstanding biocompatibility. They are often used for applications in biomedical and more specifically tissue engineering, such as scaffolds for cell seeding, wound healing, and even drug delivery. Two of the most used natural polymers are collagen and gelatin. Collagen is naturally found within the body, and therefore is easily accepted as a hydrogel and has very high biocompatibility. However, collagen on its own is not mechanically strong, and needs to be cross-linked in order to be effective in many circumstances (Lee and Mooney, 2001). Unfortunately, this often means that the use of collagen is expensive, and variable. For example, collagen is not always as easily duplicated as some synthetic polymers. The uses of collagen far outweigh its negatives, though, as it is used to reconstruct organs

such as the liver, skin, and small intestine as well as other tissue culture scaffolds (Lee and Mooney, 2001). Gelatin is derived from collagen, through breaking the helix structure of collagen into single strand molecules. In order to break the triple helix, either acidic treatment followed by thermal denaturation or alkaline treatment is used. Gelatin is often appealing to work with because as its name suggests it gels extremely easily, and as a collagen derivative is known to be highly biocompatible, it is however extremely weak (Lee and Mooney, 2001).

Fibrin is another polymer derived from the human body, as it is produced from blood. This, like collagen, is extremely beneficial because of the resulting high biocompatibility. Fibrin gels are formed through the use of thrombin, which induces an enzymatic polymerization. Fibrin is often used in wound healing as it is able to remodel itself once inside the body as a result of enzymatic activity in vivo (Lee and Mooney, 2001). The degradation rate of fibrin is also controllable through the use of apronitin which makes it extremely appealing in the world of tissue engineering. Fibrin has found a lot of use in engineered tissue seeded with skeletal and smooth muscle cells as well as chondrocytes. Again, the only conceivable drawback to the use of fibrin gels is the fact that they have a low mechanical strength.

Alginate and agarose, two more natural polymers, are derivatives of marine algae and as a result are both biocompatible. Alginate is able to form a gel in the presence of Ca^{2+}, Mg^{2+}, Ba^{2+}, and $Sr^{2+}$and is often used in drug delivery, wound healing, and dental work (Lee and Mooney, 2001). Unfortunately, alginate experiences extremely unpredictable degradation and therefore must always be cross-linked in order to control this as best as possible. Also, alginate has limited cellular interaction, and is often modified with lectin, a binding protein, to allow cell adhesion and proliferation upon the alginate matrix (Lee and Mooney, 2001). Agarose, on the other hand, is used In order to form thermally reversible gels. The physicality of the gels is controlled with varying agarose concentrations, which controls the pores in the structure. The porous structure of agarose allows above average cell migration and proliferation, which when bound to chitosan leads to neurite growth (Lee and Mooney, 2001). Chitosan is another natural polymer which introduces a charge into the hydrogels.

Synthetic Polymers

Unlike many naturally found polymers, synthetic polymers often need to be cross linked or modified in some way in order to become biocompatible, or degradable for use in the body. It is important that these synthetic polymers be investigated, however, because they have far superior mechanical properties to many naturally occurring polymers. Poly (HEMA) is one of the most researched of the synthetic polymers, and is used in a variety of procedures from making contact lenses to cartilage replacement to drug delivery. Poly (HEMA) must be cross linked in order to become hydrophilic, permeable, and degradable within the body. (Lee and Mooney, 2001) Once the poly (HEMA) is successfully created, it can be used in many tissue engineering applications. Polyethylene oxide and its copolymers have also been researched thoroughly, and is even approved by the FDA since it is low in toxicity and extremely high in biocompatibility. Polyethylene oxide (PEO) is extremely hydrophilic and can be synthesized and prepared using UV photopolymerization with acrylate termini at each end of the PEO molecule as well as hydroxyl acid. PEO can also be used as a building block in PEO-PPO-PEO tri-block copolymers known as Pluronics or Poloxamers. These polymers form micelles, which are thermally reversible hydrogels that undergo self-assembly in order to come together without any permanent

crosslinking. These polymers are then used primarily in drug delivery where their unique structure allows them to deliver drugs to the optimum location within the body. Pluronics are even being further researched as they may be able to aid in cancer drug delivery through targeting tumors and delivering drugs directly to the tumor site. The only drawback to the pluronic and poloxamers is their degradation, because they are not naturally biodegradable. To fix this issue, they have been synthesized with PLA and are being further tested to see if the addition of PLA will help with the problem (Lee and Mooney, 2001).

Polyvinyl alcohol (PVA) is another widely used synthetic polymer, which is highly hydrophilic. It is easily able to form hydrogels with chemical cross linking, and can also have a controlled hydrophilicity and solubility based on the chosen molecular weight of the polymer (Lee and Mooney, 2001). The gels are then formed using the freezing/thawing technique which creates stable gels that are elastic in nature. However, PVA is not degradable within the body, and therefore is often used as a scaffold for long periods of time. Toxicity is another issue that must be dealt with prior to PVA being implanted into the body, because of the chemicals used to cross link the polymer. Polyphosphazenes and polypeptides are the last two types of synthetic polymers that have been extensively studied for application in biomedical devices. Polyphosphazenes are degradable within the body, and therefore were immediately attractive for use in controlled drug delivery. Polyphosphazenes can be altered through changes to their side chain structure, rather than in the typical fashion of changing their polymer backbone, and is typically created through ring opening polymerization (Lee and Mooney, 2001). Due to their variability, polyphosphazenes can be used as the base to create multiple hydrogels, and are currently being looked into for their ability to react to a change in pH. Polypeptides, on the other hand, are currently being researched in order to create synthetic polymers which mimic natural polymers. Polypeptides vary based on the amino acid sequence they are synthesized with, and as a result have a large discrepancy in weight. Polypeptides have the ability to create artificial extracellular matrices within the body, but are currently not a viable option due to cost (Lee and Mooney, 2001).

Polymer Applications in Biomedical Field

As can be expected, many of these polymers, both natural and synthetic, have huge applications within the biomedical and pharmaceutical fields. In pharmaceutical fields, polymers are used in order to control drug delivery. They can be used in targeted drug delivery as well as controlled release drug delivery. Hydrogels are often used in these fields due to their high biocompatibility, which means that they are safe to place within the body and are sometimes even able to communicate with the cells around them (Omidian et al., 2010). Hydrogels in biomedical applications also must be non thrombogenic in order to allow them to come in contact with blood. In other medical applications, hydrogels are used in wound healing and personal care. Polyacrylic acid specifically is also being further investigated for uses parallel to their ability to be sensitive to salts, pH, and temperature (Omidian et al., 2010).

Appendix 3: Means of Fabricating Hydrogels

Hydrogels can be classified in two main groups, reversible and permanent. In order to create a hydrogel with a reversible bond they must undergo some form of physical crosslinking, while chemical crosslinking will form permanent bonds. While there are many various methods for physically and

chemically crosslinking polymers, there are only a few specific procedures in order to create microgels. Therefore, while there are many methods for chemically crosslinking polymers into hydrogels, they may not be able to create hydrogels that are on the micron scale. So, this section will focus on some physical crosslinking processes, but mainly on methods in which chemical crosslinking can be used in order to form hydrogels at the micron scale (also called microgels).

Physical Crosslinking

As research about the effects of the chemical agents used to permanently crosslink hydrogels has progressed, physical crosslinking has become a more advantageous option. While physical crosslinking only produces temporary bonds, it also maintains the integrity of the polymers used, and is safe for physiological use (Gulrez et al., 2003).

Heating/cooling a polymer solution

Hydrogels are formed using the heating/cooling method when heated solutions of gelatin and carrageenan are cooled. While the solution cools, junction zones form as the helices break and reform with the changes in temperature. Carrageenan, especially when heated, exists in an extremely random coiled formation which forms helical rods the more it cools (Gulrez et al., 2003). Block copolymerisation can also occur when a polymer solution is heated, such as polyethylene oxide-polypropylene oxide and polyethylene glycol-polylactic acid hydrogels which form in this way.

Hydrogen Bonding

Hydrogen bonding is also used as a form of physically bonding polymers into hydrogel networks. This is accomplished through lowering the pH of an aqueous solution of polymers which contain carboxyl groups (Gulrez et al., 2003). A specific example of this process involves forming a network of hydrogen bonds in carboxymethyl cellulose (CMC) through place it in a HCL solution. In this example, the sodium in the CMC would be replaced with the hydrogen, and hydrogen bonding would occur throughout the polymeric network because it is placed in the acid. Depending on the polymers involved, an insoluble network of hydrogen bonds is sometimes formed. This phenomenon occurs when xanthan and alginate are placed together (Gulrez et al., 2003).

Chemically Crosslinking Microgels

There is a huge variety of ways in which polymers can be chemically cross-linked in order to form hydrogels. Some of the most common include reaction of complementary groups, addition reactions, condensation reactions, radiation crosslinking, grafting, enzyme induced crosslinking, and surface crosslinking. All of these way in which chemical crosslinking can be induced are excellent for creating hydrogels, but not necessarily hydrogels at the micron scale. The scope of our project is focused on looking at hydrogels that are mere microns thick, and therefore it is important to focus on chemical crosslinking processes specific to these types of hydrogels, called microgels. Microgels are created in four main ways: emulsification, photolithography, micro fluid synthesis, and micro molding.

Emulsification

Of all four of the techniques used to produce microgels, emulsification is the most widely known. At the beginning of this process a multi-phase mixture is mixed and used to produce small

droplets of the desired hydrogel in aqueous form. The size of the drops is easily controlled based on inducing mechanical agitation, or differing of the viscosity in a phase of the mixing process (Khademhosseini & Langer, 2007). The droplets are then gelled in order to create microgels with a spherical shape. The way in which the droplets are gelled can vary, though the spherical shape of the gels cannot. Typically, natural polymers are used in this process, such as collagen, agarose, and alginate. This is useful if the gel is needed for a biomedical application, because cells can be seeded into the biocompatible microspheres (Khademhosseini & Langer, 2007).

Photolithography

While photolithography was originally developed for microelectronics applications, it has recently moved into the biomedical field for use in creating microgels. In this process, photocrosslinkable pre polymers are needed for everything to work correctly. The pre polymers can be natural or synthetic, and are exposed to light through a UV mask. Since the polymers being used are light sensitive, as the light reaches the polymer film through the mask a reaction takes place and the polymers become cross-linked as a result (Khademhosseini & Langer, 2007). The masks have both opaque and transparent regions, and can be useful in creating patterns of crosslinking on the polymer films. The most common photocrosslinkable polymer is polyethylene glycol (PEG), though natural polymers have been developed for use in this process as well. Since photolithography has the potential to change resolutions, it is possible to create hydrogel structures than range from microns to millimeters. Unlike emulsification, however, photolithography is only able to make two dimensional materials from photocrosslinkable polymers.

Microfluids

The process of designing microgels using the microfluids method is extremely unique because it offers the opportunity to design a desired hydrogel. In fact, using this method it is possible to control the features of the hydrogel (Khademhosseini & Langer, 2007). Using the method of microfluidic systems, viscous and surface tension forces are used to form particles that are homogenous in nature. These particles are then cross-linked in order to form microgels. By using different microfluidic channels in the design, these micro scale hydrogels can be created with different shapes. With this technique it is even possible to create microgels with stiffness gradients. This is achieved through using a special microfluidic device than contains two inlets of varying stiffness, so the resulting microgel has a stiffness gradient. This design is particularly useful in tissue engineering research where a stiffness gradient may be useful in creating a scaffold for implantation.

Micromolding

Micromolding, similar to microfluids, is a process in which there is control over the features of the hydrogels being created. Currently, premade silicon wafers are used with precursor polymers to mold the polymers which are then gelled. In this manner, polymers can be gelled into a variety of shapes and sizes (Khademhosseini & Langer, 2007). Polydimethylsiloxane (PDMS) is the main polymer used in micromolding right now, though other polymers have the potential to create microgels in this way as long as they have the crosslinking agents to be considered a precursor polymers in this process. By creating micromolds which deliver the necessary crosslinking agents to any polymer, there are vast possibilities opening up using this method. Finally, micromolding is further novel in idea because it is

able to produce 3D hydrogels. This is achieved by forming macromers around a bed of polymeric beads. The gel is then formed, and the beads dissolve, leaving just the gel in whatever shape was desired (Khademhosseini & Langer, 2007).

Appendix 4: Means of measuring stiffness of hydrogels

An important aspect of hydrogels is its substrate properties for cell culture. Cell function and morphology is regulated by chemical, physical, and topographical factors. The adhesiveness of cells and surrounding substrate stiffness has been recognized as interdependent factors that influence cell function and behavior (Brandl et al., 2007). Determining the local mechanical properties of a hydrogel substrate is vital to understanding the mechanisms of cell motion and cytoskeletal changes (Mahaffy et al., 2000). Therefore, it is imperative to conduct mechanical tests to determine properties such as elastic modulus and viscoelastic behavior.

Atomic Force Microscopy

Atomic force microscopy (AFM) can be used for imaging the topography of surfaces as well as the elastic modulus of the given material. AFM determines the mechanical properties of the substrate by compressing an AFM tip on the substrate and the consequential loading force is calculated from the deflection and cantilever (Figure 26) (Brandl et al., 2007). The elastic modulus is calculated from the data collected. AFM is particularly favorable because it utilizes a noncontact (NC) mode of the AFM to study topography. This NC AFM has a short probe-sample interaction with respect to time and area so it produces minimal to no surface deformation (Pramanick et al., 2012). Another advantage AFM has is its ability to detect varying elastic modulus at the micro-scale. Local variations of mechanical properties would be determined and analyzed. Furthermore, AFM can be used in liquid or semi-solid environments, which is favorable as hydrogels often swell and expand when soaked in water. Finally, when a spherical bead is used as the tip of the probe, the geometry measurement is simple, making the data analysis feasible (Markert et al., 2013).

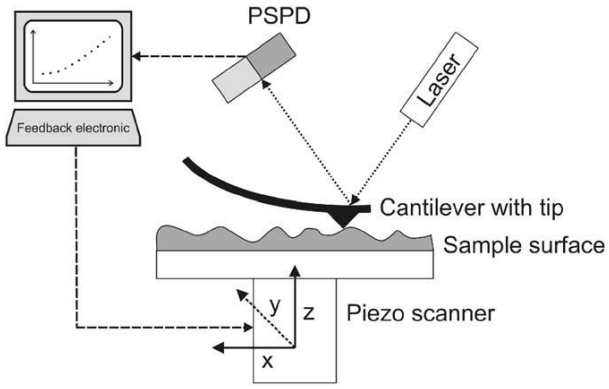

Figure 26 Diagram of AFM instrumentation

There are a few drawbacks from using AFM. First, AFM is slow and tedious to set up and perform measurements. Secondly, it takes training or a trained expert to use the microscope and collect measurements. Also, although AFM is able to determine the elasticity of substrates accurately, it does not determine shear storage modulus and shear loss modulus very well due to drag forces on the cantilever and probe shear storage modulus and shear loss modulus (Markert et al., 2013).

Tensile Tests, Compressive Tests, and Dynamic Mechanical Analysis

A common method to measure the mechanical properties of hydrogels is through tensile and compressive tests. For uniaxial tensile tests, the substrate will be loaded between two clamps and stretched at a constant rate (Brandl et al., 2007). A software such as LABVIEW, will be programed to acquire data and determine the elastic modulus of the substrate. Sometimes the surface of the hydrogel will be randomly sprinkled with small graphite particles and recorded with a CCD camera to monitor displacement. The deformation of the hydrogel under the applied load creates a stress-strain curve to determine elastic modulus (Popovic et al., 2000). Similarly, for uniaxial compressive test, the substrate is confined between two smooth impermeable plates and compressed at a constant rate. The experiment will determine the compressive modulus of the given material. Both elastic modulus and compressive modulus is a measure of the stiffness of the material (Brandl et al., 2007). Another test to determine the viscoelastic behavior of the substrate is through dynamic mechanical analysis (DMA) or rheological tests. A shear load is placed on the sample and shear storage modulus and shear loss modulus will be determined of the given substrate.

While these tests are relatively simple and inexpensive, tensile and compressive tests on hydrogels are limited by the size of the substrate. As our hydrogel will be the on micron level, it is infeasible to conduct tensile or compressive tests on the micron level accurately. Another aspect to consider with tensile tests, compressive tests, and DMA tests is the effect on the substrate tested. Often times, these tests will affect the structural integrity or even destroy the substrate (Brandl et al., 2007). In addition, tensile tests, compressive tests, and DMA tests measure the bulk elastic modulus of the substrate. Bulk techniques are not sensitive to local variations in mechanical properties that may be present (Wong et al. 2004). Therefore, when determining the mechanical properties of hydrogels, it is favorable to use a non-invasive and non-destructive method with high spatial resolution.

Magnetic Resonance Elastography

Magnetic Resonance Elastography (MRE) can be used to characterize elastic properties and mechanical properties of gels. MRE uses shear waves generated within the sample using an electromechanical actuator coupled to the surface of the object. Then, a magnetic resonance imaging (MRI) system measures the displacement patterns from the shear waves in the gel. The measured waves can then be reconstructed as viscoelastic parameters throughout the entire material (Figure 27) (Brandl et al., 2007). MRE is favorable because it is non-invasive and non-destructive and detects subtle mechanical changes. A drawback of MRE is the access availability our team has to this system.

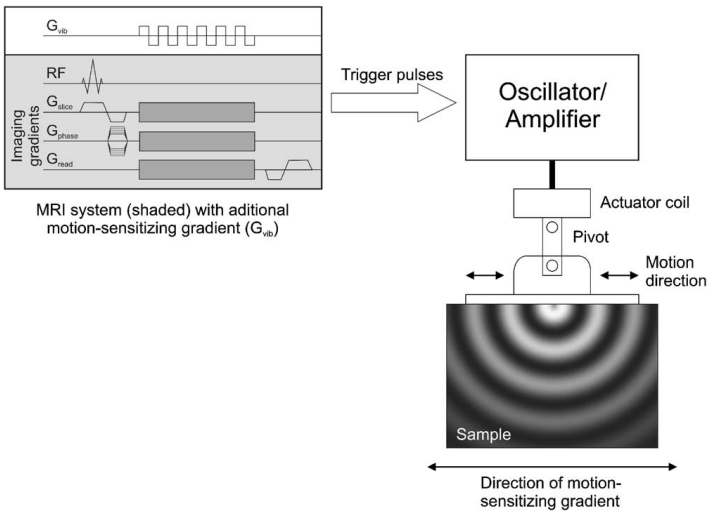

Figure 27 Diagram of MRE system.

Appendix 5: Experimental Methods

A. Clean Coverslips

Materials

- 25x25 glass coverslips
- 100 ml alcohol
- Deionized (DI) water
- O_2 plasma cleaner

Protocol

1. Place the ceramic holder with the slips in beaker full of alcohol and sonicate for 5 min and then blow dry the coverslips. *About 12 slips fit in the holder.*
2. Treat the coverslips with O_2 plasma for 1 min. Place the whole ceramic holder with the slips inside, make sure to turn on all the valves before using it and to turn them all off when done.

B. Glutaraldehyde/Aminosilanated Treated Coverslips

Materials

- 25x25 clean glass coverslips
- 1 ml (3-Aminopropyl)triethoxysilane (APTMS)
- 100 ml alcohol
- Deionized (DI) water
- 0.5% Glutaraldehyde solution (GA) (*Dilute 50% GA 100x in DI water to get 0.5%)*

Protocol

1. Submerge clean coverslips in 1% APTMS
   a. Dilute 1 ml of APTMS in 100 ml of alcohol.
   b. Place the ceramic holder with the coverslips in the APTMS-alcohol solution for 5-6 min and stir with a magnetic stirring bar.
   c. Rinse the coverslips with DI water and vacuum excess solution.
2. Submerge the coverslips in the plastic holder in 0.5 % glutaraldehyde (GA) solution.

a. Refrigerate and soak the coverslips in GA for at least 2 hours.
b. Dry the glass using vacuum aspiration.

Note: coverslips can be stored indefinitely in GA and the GA can be reused up to 5 times. Alternatively, the APTMS treated coverslips can be stored in petri dishes no more than one week.

C. Chloro-silane Treated Coverslips

Materials

- Distilled H_2O
- Dichlorodimethylsilane (DCDMS)
- Kimwipes
- 25 × 25 mm glass coverslips

Protocol

1. Pipette 100 µl of DCDMS onto each slide in the fume hood. Ensure that the solution coats the entire surface of the slides.
2. Allow to react for 5 min. Remove excess DCDMS with a Kimwipe.
3. Rinse 1 min under distilled H2O.

Note: Excess DCDMS can be transferred to the other coverslip during photocrosslinking. This can prevent the gel from attaching to the other coverslip and so all excess DCMS must be removed.

D. Photocrosslinking Homogeneous Gels – Irgacure 2959

Materials

- 40% Acrylamide
- 2% Bis-acrylamide
- 50 mM HEPES buffer (8.5 pH)
- Irgacure 2959

Protocol

1. Mix 40% Acrylamide and 2% Bis-acrylamide to desired concentration in 50 mM HEPES buffer.

Notes: Acrylamide and Bis-acrylamide are very toxic, always add the buffer first, HEPES fixes the pH, and the AA:Bis solution can be stored up to 2 weeks when refrigerated.

2. Add Irgacure 2959 to a concentration of 0.5% (w/v).
3. Degas solution under a strong vacuum for 60 min to speed up polymerization.

Note: it is better to degas a larger volume at a time to minimize evaporation.

4. Pipet 64 µl of solution onto treated coverslips. *Volume determines gel thickness.*
5. Turn on UV light for the desired exposure time – 8 min.
6. Remove top coverslip with a razorblade and set in a 60 mm petri dish.
7. Rinse twice with HEPES and refrigerate.

E. Photocrosslinking Gels Heterogeneous in Stiffness – Irgacure 2959

Materials

- 1 chlorosilanated coverslip (25x25mm)
- 1 aminosilanated/glutaraldehyde coverslip (25x25mm)
- 1 clean coverslip (25x25mm)
- Gel solutions – stiff region should be loaded with fluorescent beads

Method

1. Place the acrylic mask onto the holder and center the chlorosilanated coverslip with one of the openings in the mask. Pipette 44 µl onto the chlorosilanated coverslip (25x25mm), and cover with a clean coverslip (25x25mm). Photocrosslink in the GelDoc for 10 min.

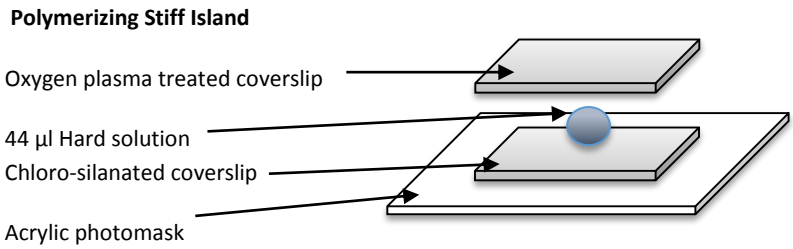

2. Remove the chlorosilanated coverslip (bottom). Rinse with DI water and suction dry carefully from the corners.

3. Hydrate the gel overnight in HEPES buffer at 4°C.

4. Place the glass pane onto the holder and the coverslip with the stiff island on top. Pipette 64µl onto the coverslip with the previously made gel, and cover with a glutaraldehyded coverslip (25x25mm).

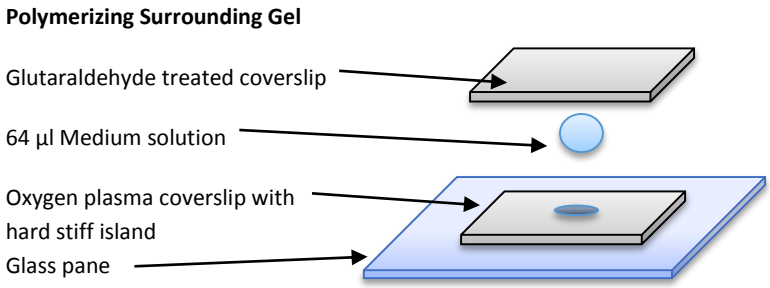

5. Photocrosslink in the GelDoc for 8 min.

6. Remove the bottom coverslip and soak in a dish with HEPES.

F. Protocol for Coating PA Gels with Collagen

Materials

- Sulfo-SANPAH
- DMSO

- 50 mM HEPES buffer (8.5 pH)
- Aluminum foil
- 0.1 mM acetic acid
- PBS
- Collagen Type I

Method

1. Warm up sulfo-SANPAH, making sure moisture does not affect the container
2. Pipette 4-5uL of DMSO in 2mL container
3. Dissolve 0.5 mg/mL (estimate small spoon amount) of sulfo-SANPAH into container
4. Pipette 500uL of HEPES into container and wrap the container in foil (do not expose to sunlight)
5.
    a. Remove as much liquid as possible from the surface of hydrogel with vacuum
    b. Pipette 250uL of solution to completely cover gel
    c. Expose to UV light for 8 minutes
6. Repeat #5.
7. Pipette 250uL of 0.1mM Acetic Acid and 2.5uL of collagen type I into container creating a 0.1mg/mL solution
8. Vortex solution
9. Rinse solution off gel with HEPES 2-3 times
10. Pipette 250mL of solution to completely cover gel
11. Cover and wait 2 hours
12. Rinse with PBS or HEPES

Appendix 6: Preliminary Data

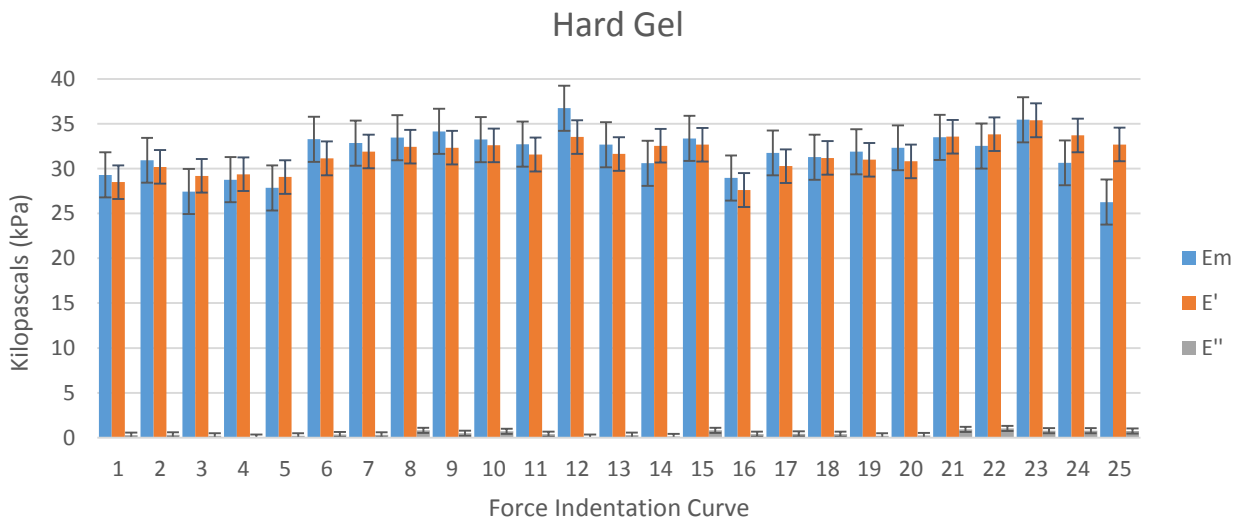

Figure 28 Preliminary data for hard homogeneous gel

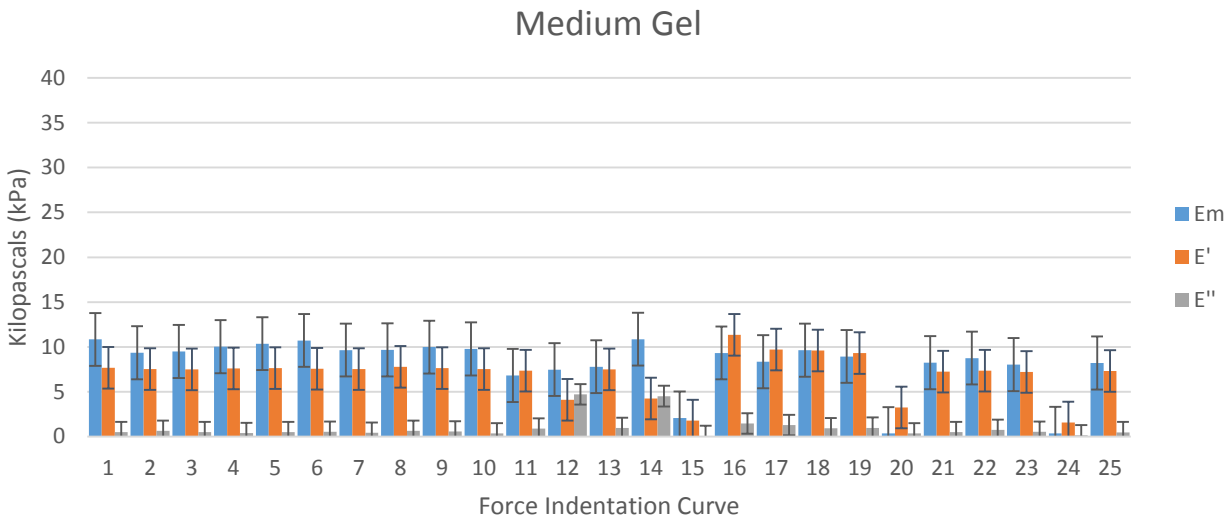

Figure 29 Preliminary data for medium homogeneous gel

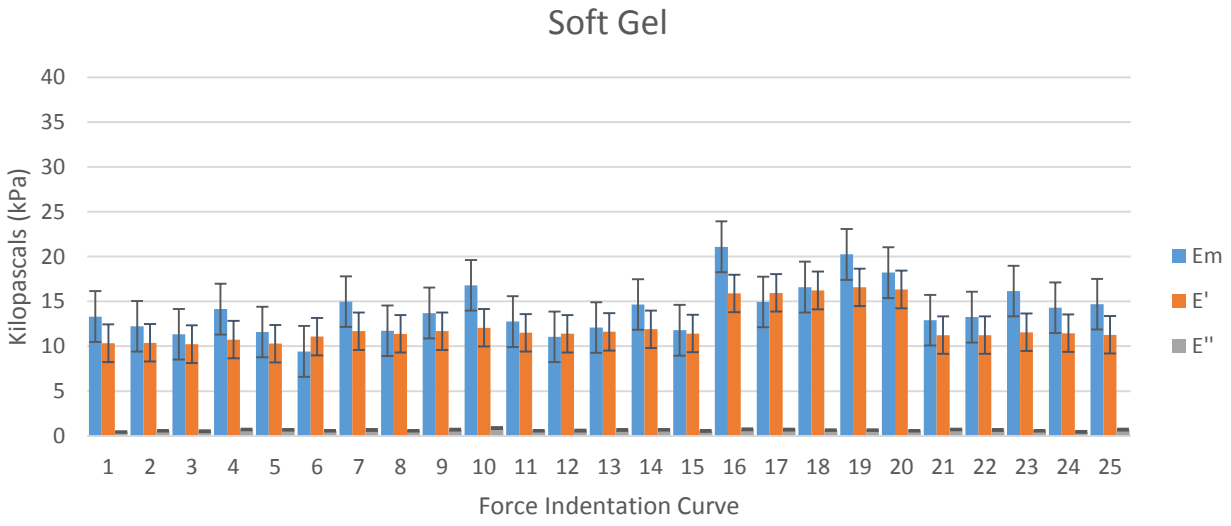

Figure 30 Preliminary data for soft gel

Table 13 Preliminary data for 'Hard', 'Medium', and 'Soft' gels

Hard (n=25)			Medium (n=25)			Soft (n=25)		
Em	**E'**	**E''**	**Em**	**E'**	**E''**	**Em**	**E'**	**E''**
29308.02	28489.56	277.6803	10840.42	7673.088	505.0008	13309.53	10332.68	432.2374
30931.55	30194.43	308.1452	9343.729	7515.466	631.2039	12235.63	10388.2	567.1481
27447.73	29196.17	201.8592	9495.934	7501.328	509.7979	11339.31	10232.18	517.4257
28766.85	29371.1	74.63784	10028.65	7586.967	391.9525	14138.2	10740.54	716.5582
27853.61	29059.07	190.4697	10358.43	7638.947	487.4368	11584.53	10290.22	675.4764
33273.82	31146.31	346.0703	10722.03	7550.26	527.7547	9419.831	11076.07	570.9742
32851.03	31909.76	311.2746	9648.14	7527.367	433.5847	14983.79	11674.73	668.7381

33451.39	32441.3	826.569	9665.051	7765.195	628.6537	11736.74	11375.67	569.9152
34161.69	32340.58	485.8375	9977.918	7629.544	577.6918	13702.73	11683.62	708.1478
33244.23	32600.91	694.7324	9779.206	7520.057	357.3245	16789.12	12053.05	882.1195
32724.19	31569.91	391.4351	6815.426	7360.81	877.9545	12751.44	11509.25	584.4779
36740.72	33530	63.74839	7466.527	4094.833	4707.403	11043.36	11393.39	591.7913
32673.45	31635.72	276.856	7796.306	7491.052	964.2993	12091.88	11607.28	659.3217
30601.77	32547.03	123.3856	10857.33	4251.395	4511.058	14645.55	11898.85	683.9163
33371.06	32668.02	821.4932	2063.231	1777.293	72.74315	11787.47	11412.02	550.3118
28952.88	27618.39	389.8133	9326.817	11355.54	1459.747	21088.92	15892.29	738.7945
31751.77	30280.95	420.5746	8345.937	9712.799	1275.121	14949.97	15955.43	703.8833
31278.24	31187.99	382.9565	9631.228	9590.95	921.7517	16598.86	16226.83	649.2361
31882.83	30998.61	221.5029	8929.391	9297.089	979.5171	20243.34	16572.4	640.985
32322.54	30815.16	252.2017	338.2345	3250.506	354.6776	18205.47	16333.58	576.8391
33485.22	33562.21	914.7367	8244.466	7248.721	508.5238	12903.65	11236.76	718.0867
32521.25	33832.17	1018.107	8756.046	7364.514	750.7178	13250.34	11237.09	666.162
35446.98	35389.12	791.6995	8033.07	7222.437	534.1194	16163.38	11553.4	579.4098
30644.05	33708	787.6702	372.058	1578.982	131.9337	14290.41	11447.8	443.3334
26272.37	32692.85	748.4222	8206.415	7328.565	475.6053	14696.29	11273.56	705.5319

Table 14 Preliminary data on heterogeneous gel

Surrounding (n=25)			Stiff Region (n=25)		
Em	E'	E''	Em	E'	E''
47894.01	48699.47	373.2246	59385.53	52469.08	186.9549
54223.22	50699.96	265.3275	48655.04	50214.2	99.61852
63402.06	54151.1	60.15725	56332.96	53595.68	406.0886
59495.45	52520.97	335.4952	42008.73	49150.17	354.3967
62649.49	52954.36	100.5812	60620.08	54782.81	160.2301
26255.45	40886.1	140.1809	46507.25	47874.7	367.111
29117.76	42247.37	459.0174	43285.56	47813.12	34.82256
42947.33	47218.16	63.29112	26788.17	41615.48	179.4204
26936.15	42239.45	178.3458	39784.84	45830.91	152.4138
46253.57	48250.5	214.1527	50346.21	49300.16	44.50602
31049.93	47349.27	1000.739	52984.44	52805.05	226.4087
37104.33	48629	533.7136	37104.33	48250.47	278.3421
33041.28	47925	283.146	63114.56	56439.23	640.1159
39438.15	50274.25	590.5215	60290.3	56240.12	411.243
54988.48	55210.5	620.4956	42338.51	50394.01	21.32031
2469.112	3238.174	344.7703	33874.19	42906.23	166.7199
3729.036	3233.939	392.5209	42761.3	46569.64	38.93397
2841.17	3184.137	398.5837	51014.22	49521.35	17.97301
3306.242	3216.754	304.9984	24847.55	41248.65	126.6982
2765.067	3152.366	309.7995	48866.43	49359.82	302.1062
4430.872	3665.587	591.9596	5631.605	16033.91	711.3783
3762.859	3490.137	565.1087	7762.482	17267.96	877.0314
3424.625	3399.675	427.7116	7644.1	17513.47	743.0285
2553.671	3437.945	559.1676	8667.26	18484.09	799.4068
2773.523	3384.244	446.8689	5885.281	17504.86	740.095

Table 15 Summary of preliminary data on homogenous gels.

	Hard			Medium			Soft		
	Em	E’	E’’	Em	E’	E’’	Em	E’	E’’
Average	31678.37	31551.41	452.8752	8201.68	6993.348	943.0229	14157.99	12215.88	632.0328
Standard Deviation	2509.331	1878.467	284.2115	2949.965	2321.24	1148.43	2826.038	2091.288	97.87181

Table 16 Summary of preliminary data on heterogeneous gel.

	Surrounding Gel			Stiff Region		
	Em	E'	E''	Em	E'	E''
Average	27474.11	30506.34	382.3951	38660.04	42927.41	323.4546
Standard Deviation	22557.76	22877	211.9806	18766.77	13616.84	273.7098

Appendix 7: Heterogeneous Gels

The following Appendix contains all heterogeneous gel profiles.

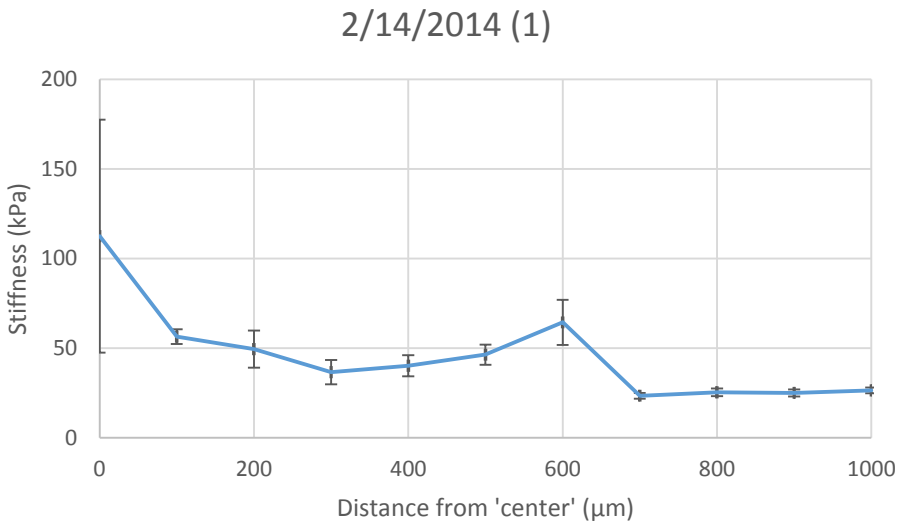

Figure 31 2/14/14 (1) Heterogeneous Hydrogel

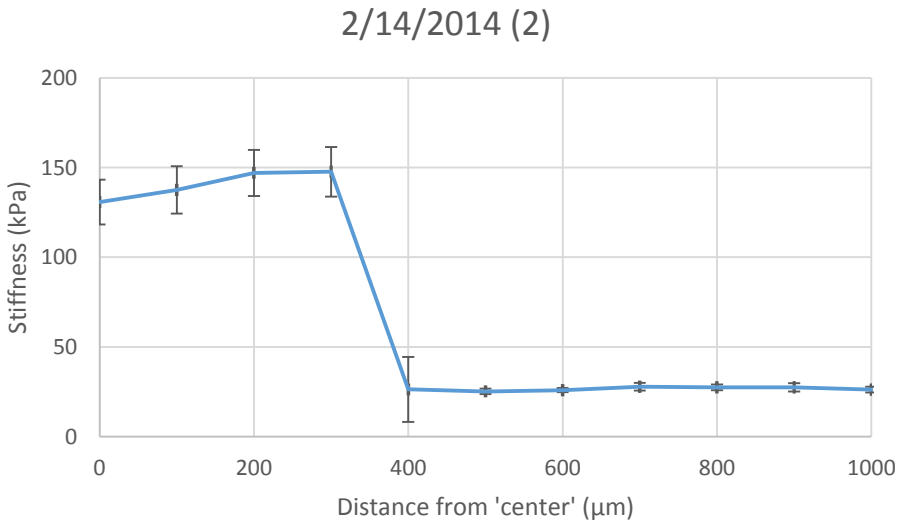

Figure 32 2/14/14 (2) Heterogeneous Hydrogel

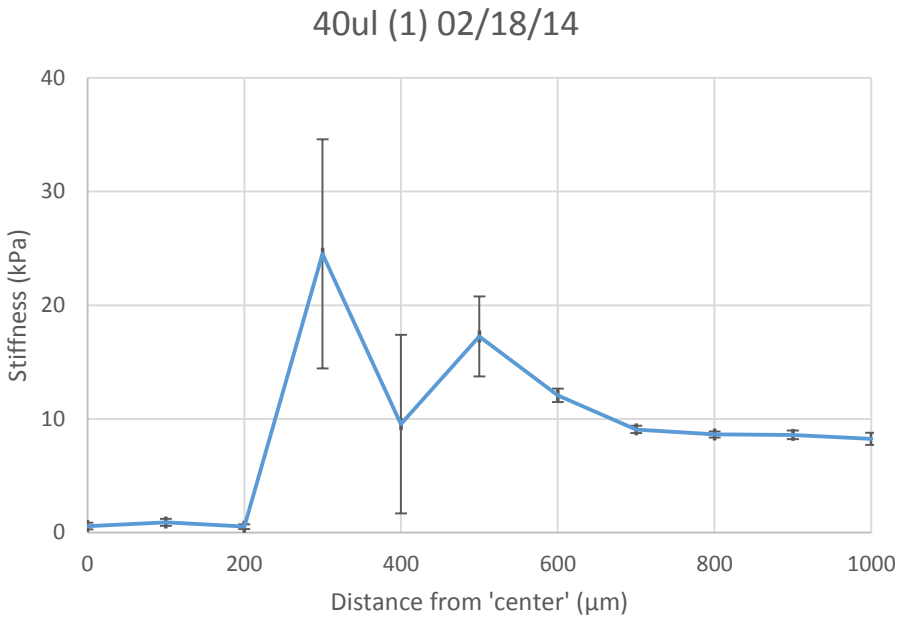

Figure 33 2/18/14 (1) Heterogeneous Hydrogel

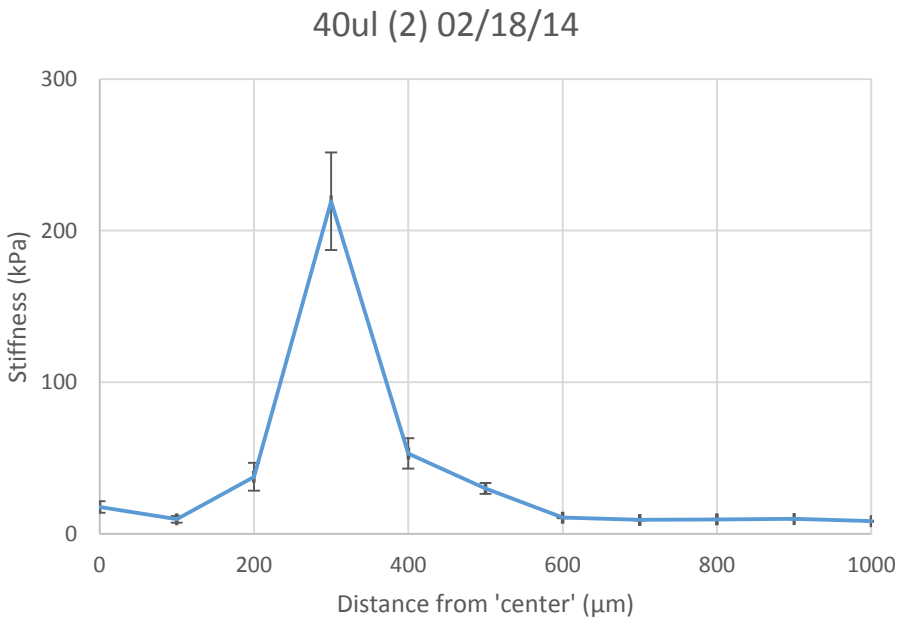

Figure 34 2/18/14 (2) Heterogeneous Hydrogel

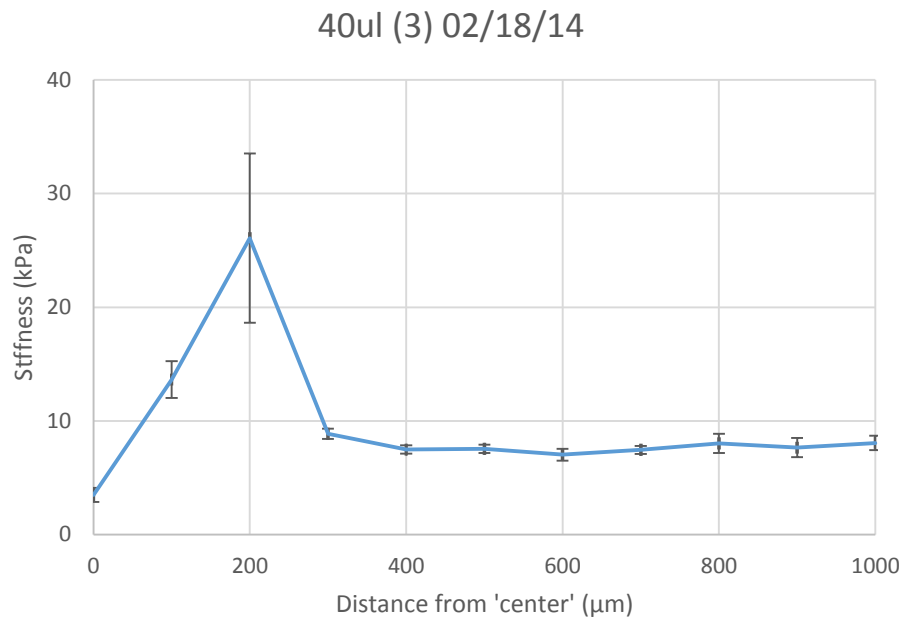

Figure 35 2/18/14 (3) Heterogeneous Hydrogel

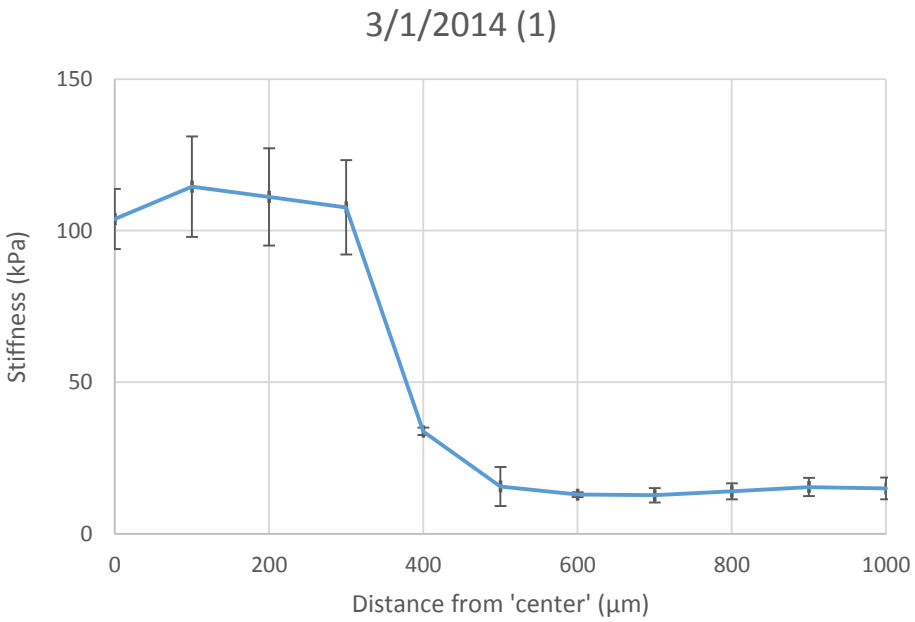

Figure 36 3/1/14 (1) Heterogeneous Hydrogel

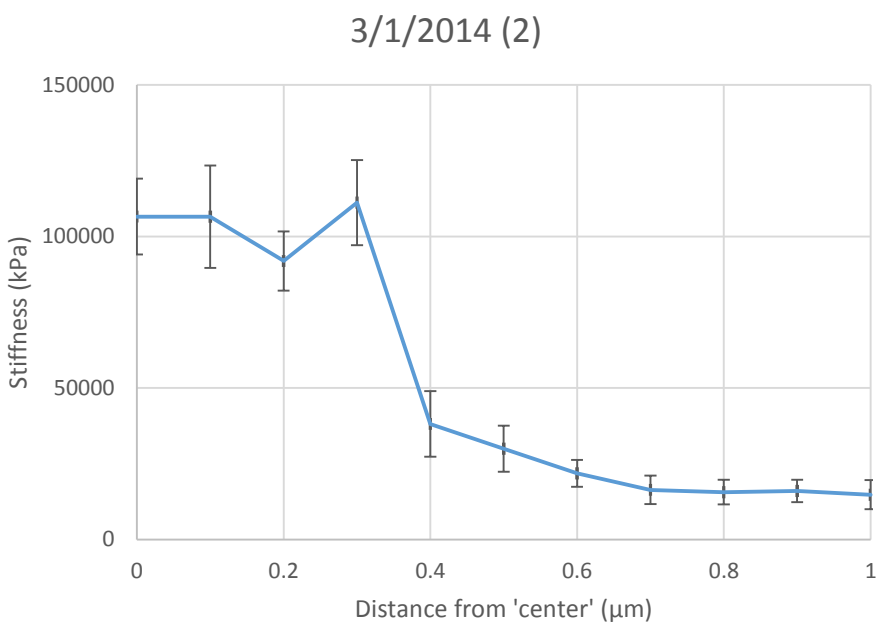

Figure 37 3/1/14 (2) Heterogeneous Hydrogel

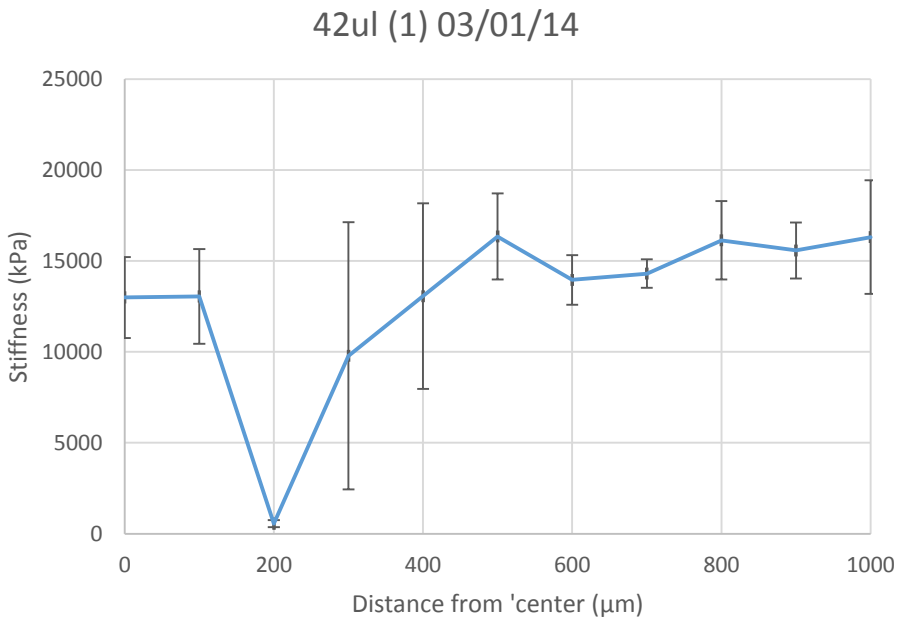

Figure 38 3/1/14 (3) Heterogeneous Hydrogel

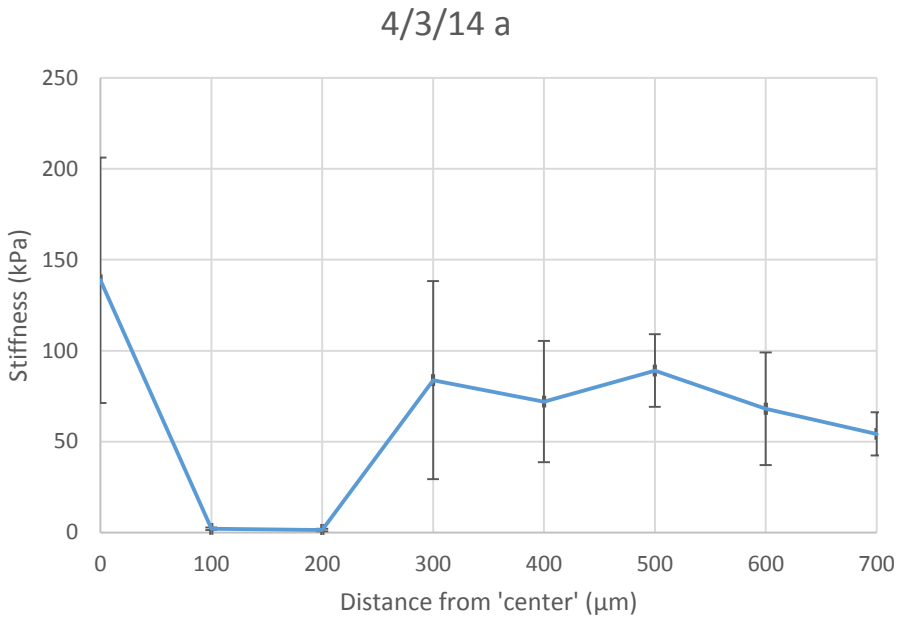

Figure 39 4/3/14 (1) Heterogeneous Hydrogel

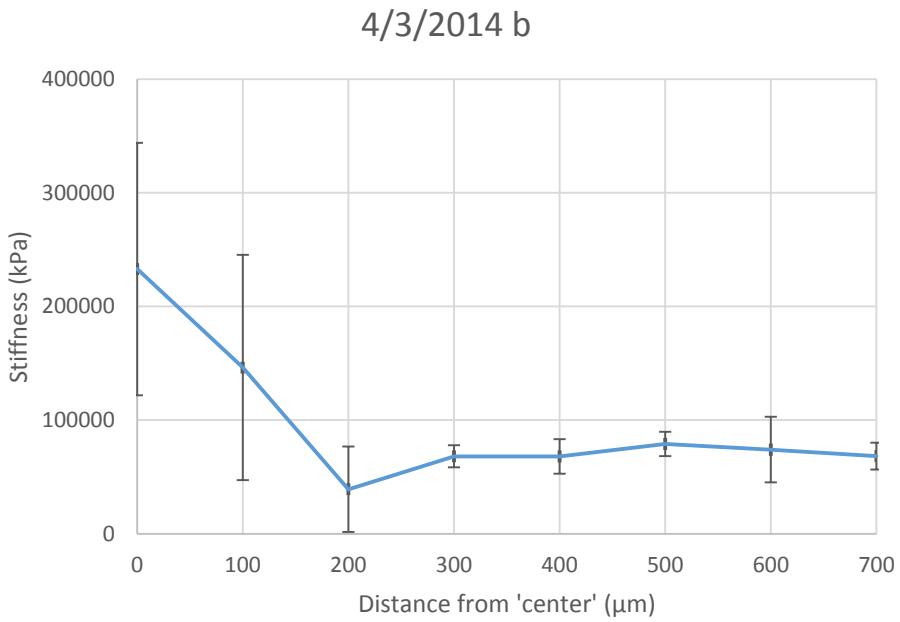

Figure 40 4/3/14 (2) Heterogeneous Hydrogel

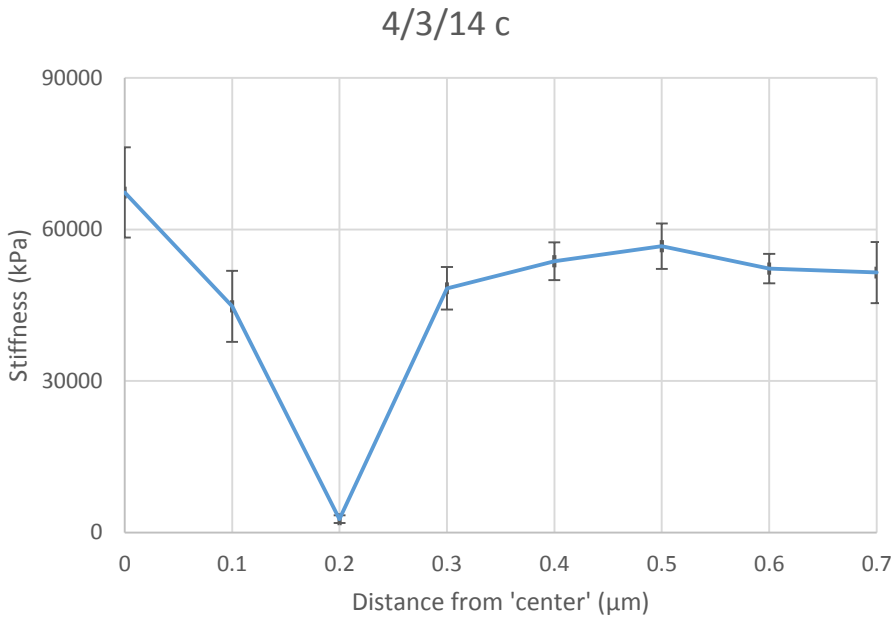

Figure 41 4/3/14 (3) Heterogeneous Hydrogel

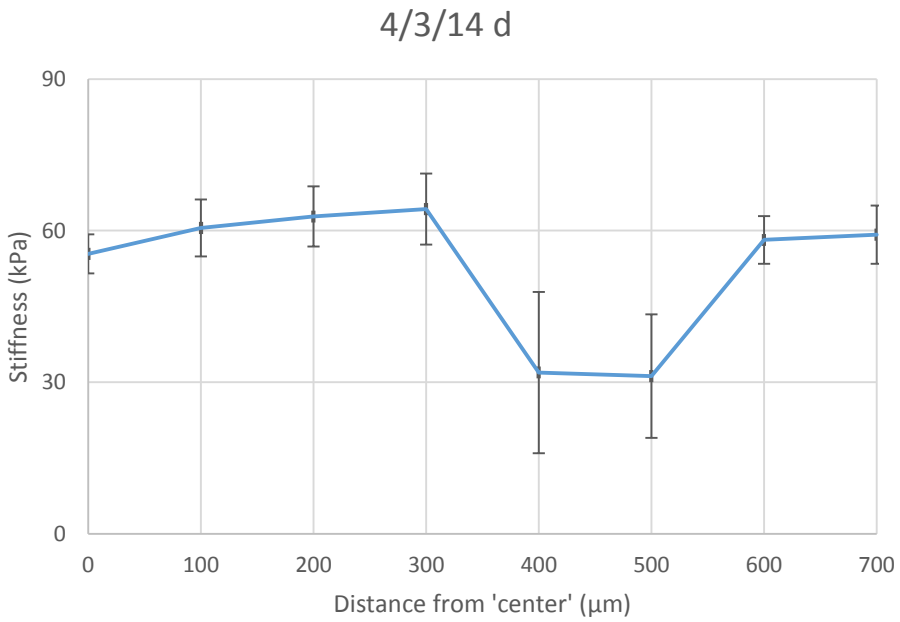

Figure 42 4/3/14 (4) Heterogeneous Hydrogel

Appendix 8: MATLAB Code

The following MATLAB code was provided by Gawain Thomas and was used to measure hydrogel stiffness and cell stiffness.

```
clear all;
close all;

mainfold = '3.1.14.A/Hetero-41uL-1/200um/'
posl = [0:9];
m_size = 24;
tip.type = 'Cone';
tip.geom = 35;
tip.k =  0.06;
k = tip.k;
msize=24;
maxind=250;
samplerate = 2000;
freqguess = 20*pi;
numchan = 3;
manual_contact = 1;
    n = 1;
for posn=1:length(posl)
    filn=[mainfold,'Image',num2str(posl(posn),'%4.4d'),'.ibw'];
    disp(['Processing  ',filn]);

    %Read Force Curve
     clear fc;
     fc=ReadIBW([filn]);


     %Split Channels
     rawZ = fc(1:round(length(fc)/numchan)-1);
     d = fc(round(length(fc)/numchan)+1:round(2*length(fc)/numchan));
     z =
fc(round(2*length(fc)/numchan)+1:round(3*length(fc)/numchan));

     %Split approach and retraction curves

     if(find(z == NaN))
         z = rawZ;
     end
     [zmax, id] = max(z);
     dwell = find(abs(z-zmax) < 30e-9);
     dwell_start = dwell(1);
     dwell_end = dwell(end);
     if dwell_end > length(d)
        dwell_end = length(d);
     end
     z_app = z(1:dwell_start-1);
```

```
      z_ret = z(dwell_end+1:end);
      d_app = d(1:dwell_start-1);
      d_ret = d(dwell_end+1:end);
      z_dwell = z(dwell_start:dwell_end);
      d_dwell = d(dwell_start:dwell_end);
      ap(posn,1).z=z_app;
      ap(posn,1).d=d_app;
      rt(posn,1).z=z_ret;
      rt(posn,1).d=d_ret;
      dwl(posn,1).z = z_dwell;
      dwl(posn,1).d = d_dwell;



      if length(d_app)>0
         r = contactpoint3(d_app,z_app,tip,maxind);
         q = r(1,:);
         d0 = d_app(q);
         z0 = z_app(q);
         ind0(posn,1) = (z_app(end) - z0) - (d_app(end)-d0);

         %check that there is at least enough indentation
         if(abs(z_app(end)-z_app(1)) > maxind * 1e-9)
             %fit using the Hertz Model
             [Em(posn,1) ctp(posn,1)
err(posn,1)]=afmcntp(z_app,d_app,tip,[q(1) maxind],1);
             %Mark the points with bad fits and ask for manual point
             if (err(posn,1).rel > 0.05 || manual_contact == 1)
                 idsbad(posn,1) = 1;
                 cat = wavread('cat10.wav');
                 cat = [cat; cat; cat];
                 catplayer = audioplayer(cat, 22050);
                 play(catplayer);
                 q = manualContactPoint(z_app,d_app, tip, maxind)
                 d0 = d_app(q);
                 z0 = z_app(q);
                 ind0(posn,1) = (z_app(end) - z0) - (d_app(end)-d0);
                 if(abs(z_app(end)-z_app(1)) > maxind * 1e-9)
                     %do the fitting again with corrected contact point
                     [Em(posn,1) ctp(posn,1)
err(posn,1)]=afmcntp(z_app,d_app,tip,[q(1) maxind],1);
                 else
                     idsbad(posn,1) = 0;
                 end

                 end
           end



%do the dwell stuff
%filter out the exponential stress-relaxation
```

```
d_dwell = dwell_filter(d_dwell,d0,samplerate);

z_dwell = z_dwell(1:length(d_dwell));
ind_dwell = (z_dwell - z0) - (d_dwell - d0);
d_dwell = d_dwell';
F_dwell = (d_dwell - d0)*tip.k;
ind_dwell = ind_dwell(1:length(F_dwell));
ind_slope = polyfit((1:length(ind_dwell))',smooth(ind_dwell,200),1);
ind_dwell = ind_dwell - polyval(ind_slope,(1:length(ind_dwell))');
ind_dwell1 = real(ind_dwell);
F_dwell1 = real(F_dwell);

%fit F_dwell and d_dwell to a sine curve
[x1 x2 resnorm1 resnorm2 tdata F_dwell1 ind_dwell1] =
sinefit(F_dwell1, ind_dwell1, samplerate,freqguess);
sinerr(posn,1).z = resnorm1;
sinerr(posn,1).d = resnorm2;

%calculate & normalize phase offset
ind_offset = x1(3);
F_offset = x2(3);
zcos = cos(ind_offset);
dcos = cos(F_offset);
ind_offset = acos(zcos);
F_offset = acos(dcos);
offset1 = (F_offset - ind_offset);
offset_cos = cos(offset1);
offset(posn,1) = acos(offset_cos);

%get amplitudes
amp_ind(posn,1) = abs(x1(1));
amp_F(posn,1) = abs(x2(1));

%calculate the modulus
Estar(posn,1) = (amp_F(posn,1) / amp_ind(posn,1)) / (ind0(posn,1) *
4/pi * tan(tip.geom*pi/180) / 0.75);
%uncomment if spherical tip:
%Estar(posn,1) = 0.75 * amp_F(posn,1) / (amp_ind(posn,1) * 2 *
(tip.geom/2/1e9 * ind0(posn,1))^0.5);


%calculae E' and E''
Eprime(posn,1) = Estar(posn, 1) * cos(offset(posn,1));
Edoubleprime(posn,1) = Estar(posn, 1) * sin(offset(posn,1));



%if it's a bad fit, ask for inputs
if sinerr(posn, 1).d > 0.60
    cat = wavread('cat10.wav');
    cat = [cat; cat];
    catplayer = audioplayer(cat, 22050);
```

```
    play(catplayer);
    [x,y, z] = ginput(2);
    if z == 29
    elseif z == 110
        %if skip using N key, change everything to NaN
        amp_ind(posn,1) = NaN;
        amp_F(posn,1) = NaN;
        Estar = NaN;
        Eprime(posn,1) = NaN;
        Edoubleprime(posn,1) = NaN;
        mu(posn,1) = NaN;
        Edp(posn,1) = NaN;
        ind0(posn,1) = NaN;
        Em(posn,1) = NaN;
        ctp(posn,1) = NaN;
        sinerr(posn,1).d = NaN;
        sinerr(posn,1).z = NaN;
        offset(posn,1) = NaN;
        amp_ind(posn,1) = NaN;
        amp_F(posn,1) = NaN;
        time(posn,1) = NaN;
    else
        %if not skipped, redo all the fitting
        amp_guess = (y(2)-y(1))/2
        freq_guess = 2*pi/(abs(x(2)-x(1))*2)
        parms2(1) = abs(amp_guess);
        parms2(2) = freq_guess;
        parms2(3) = 0;
        parms2(4) = 0;
        LB2 = [0.8*parms2(1) 0.8*freq_guess, -pi, -0.1];
        UB2 = [1.2*parms2(1) 1.2*freq_guess, pi, 0.1];
        [x2 resnorm2] =
lsqcurvefit(@sinefunction,parms2,tdata,F_dwell1(1:length(tdata))',LB2,
UB2);
        sinerr(posn,1).d = resnorm2;
        F_offset = x2(3);
        dcos = cos(F_offset);
        F_offset = acos(dcos);
        offset1 = (F_offset - ind_offset);
        offset_cos = cos(offset1);
        offset(posn,1) = acos(offset_cos);
        amp_F(posn,1) = abs(x2(1)) / 1e9;
        Estar = (amp_F(posn,1) / amp_ind(posn,1)) / (ind0(posn,1) *
4/pi * tan(tip.geom*pi/180) / 0.75);
        Eprime(posn,1) = Estar * cos(offset(posn,1));
        Edoubleprime(posn,1) = Estar * sin(offset(posn,1));

        subplot(2,1,2)
        plot(tdata, F_dwell1(1:length(tdata)))
        ylabel('Force');
        hold on; plot(tdata, sinefunction(x2, tdata),'r')
        hold off;
```

```
        title(['Eprime = ',num2str(Eprime(posn,1))]);

    end

    end
else
amp_ind(posn,1) = NaN;
amp_F(posn,1) = NaN;
Estar = NaN;
Eprime(posn,1) = NaN;
Edoubleprime(posn,1) = NaN;
ind0(posn,1) = NaN;
htmap(posn,1) = NaN;
height(posn,1) = NaN;
Em(posn,1) = NaN;
ctp(posn,1) = NaN;
sinerr(posn,1).d = NaN;
sinerr(posn,1).z = NaN;
offset(posn,1) = NaN;
amp_ind(posn,1) = NaN;
amp_F(posn,1) = NaN;
height_tp(posn,1) = NaN;
time(posn,1) = NaN;
end
end

Eall = [Em, Eprime, Edoubleprime];

%save everything
save([mainfold 'data.mat'] , 'Estar', 'ind0',  'Em', 'ctp', 'sinerr',
'err', 'offset', 'Eprime', 'Edoubleprime',
'ap','rt','dwl','tip','maxind');
```

Appendix 9: Cell stiffness Data

Table 17 Elastic modulus of STO cells growing on soft PAA hydrogels

ELASTIC MODULUS		Curve 1 (Pa)	Curve 2 (Pa)	Curve 3 (Pa)	Average (Pa)	Standard Deviation (± Pa)
Soft A	**Cell 1**	24427.76	28234.41	16267.65	22976.6	6113.937
	Cell 2	4416.555	3596.338	3617.369	3876.754	467.5998
	Cell 3	1519.505	4847.695	2450.137	2939.112	1717.13
	Cell 4	7481.855	7739.487	5846.678	7022.673	1026.556
	Cell 5	2344.981	5652.139	4532.227	4176.449	1682.04
Soft B	**Cell 1**	8969.813	431.1399	8097.018	5832.657	4698.163
	Cell 2	19653.67	6025.443	6225.24	10634.78	7811.223
	Cell 3	2497.457	5541.725	10888.91	6309.365	4248.068
	Cell 4	5941.318	2402.816	1819.2	3387.778	2230.6
	Cell 5	12029.86	2728.8	2691.996	5816.884	5380.623
Soft C	**Cell 1**	3017.979	5983.381	17603.13	8868.162	7708.639
	Cell 2	389.0775	1151.459	1051.561	864.0324	414.3447
	Cell 3	9400.953	14132.98	2465.91	8666.613	5868.096
	Cell 4	1167.232	8396.713	3322.932	4295.626	3711.596
	Cell 5	-604.647	3133.651	630.9365	1053.313	1904.605
Soft D	**Cell 1**	1051.561	3470.151	2076.833	2199.515	1213.953
	Cell 2	4942.336	1088.365	3743.556	3258.086	1972.317
	Cell 3	741.3503	5026.46	2239.824	2669.212	2174.586
	Cell 4	2781.378	2891.792	672.9989	2115.39	1250.366
	Cell 5	504.7492	2734.058	3159.94	2132.916	1426.022

Table 18 Storage modulus of STO cells growing on soft PAA hydrogels

STORAGE MODULUS		Curve 1 (Pa)	Curve 2 (Pa)	Curve 3 (Pa)	Average (Pa)	Standard Deviation (± Pa)
Soft A	**Cell 1**	35866.78	23167.11	25433.83	28155.91	6773.303
	Cell 2	480.4285	488.1809	1641.832	870.1471	668.3099
	Cell 3	1887.683	1640.361	4349.844	2625.963	1498.038
	Cell 4	7539.328	5401.018	6442.04	6460.795	1069.278
	Cell 5	3762.929	2256.965	2074.421	2698.105	926.6704
Soft B	**Cell 1**	10120.4	7736.471	13411.05	10422.64	2849.338
	Cell 2	12550.98	6164.411	9173.199	9296.196	3195.059
	Cell 3	2015.27	3161.439	5325.016	3500.575	1680.733
	Cell 4	2422.827	2312.885	2597.017	2444.243	143.2715
	Cell 5	9592.209	4705.502	4605.929	6301.213	2850.521

Soft C	**Cell 1**	4331.525	7286.993	12552.37	8056.962	4164.156
	Cell 2	1358.012	2054.516	1106.776	1506.435	490.9939
	Cell 3	8466.764	16277.92	7776.79	10840.49	4721.571
	Cell 4	3014.493	6439.187	1709.291	3720.991	2442.813
	Cell 5	3950.923	4135.688	1810.987	3299.199	1292.136
Soft D	**Cell 1**	680.6934	1082.121	2230.144	1330.986	804.145
	Cell 2	2799.47	1019.405	2035.925	1951.6	893.0234
	Cell 3	2700.926	3635.524	2216.878	2851.109	721.1485
	Cell 4	2882.056	2704.26	1823.303	2469.873	566.9591
	Cell 5	1497.985	1489.65	1375.955	1454.53	68.17561

Table 19 Loss modulus of STO cells growing on soft PAA hydrogels

LOSS MODULUS		**Curve 1 (Pa)**	**Curve 2 (Pa)**	**Curve 3 (Pa)**	**Average (Pa)**	**Standard Deviation (± Pa)**
Soft A	**Cell 1**	3938.244	3088.868	2848.702	3291.938	572.454
	Cell 2	369.6528	961.8101	227.0725	519.5118	389.6192
	Cell 3	411.6953	1871.242	1039.832	1107.59	732.1289
	Cell 4	1562.907	1213.364	1004.544	1260.272	282.1213
	Cell 5	848.4261	374.8694	678.3729	633.8894	239.8918
Soft B	**Cell 1**	1524.733	836.0198	1785.123	1381.959	490.3953
	Cell 2	2870.734	1994.662	2393.398	2419.598	438.6234
	Cell 3	644.8162	835.2823	1220.24	900.1129	293.139
	Cell 4	952.6205	730.9922	813.5297	832.3808	112.0103
	Cell 5	2236.873	1543.833	1507.247	1762.651	411.0957
Soft C	**Cell 1**	1600.192	2994.073	4010.346	2868.204	1209.997
	Cell 2	621.606	832.5545	1216.931	890.3638	301.8432
	Cell 3	1579.379	1895.158	1778.066	1750.868	159.6369
	Cell 4	768.8427	1207.622	759.6773	912.0474	256.0163
	Cell 5	1297.463	1141.918	468.1316	969.1712	440.8277
Soft D	**Cell 1**	379.1797	479.7528	952.3403	603.7576	306.0411
	Cell 2	1042.356	1054.942	640.0719	912.4564	235.9759
	Cell 3	1019.37	1172.996	976.5362	1056.301	103.3058
	Cell 4	883.4018	938.2554	708.4638	843.3737	120.0114
	Cell 5	708.2567	716.9946	501.3375	642.1962	122.0655

Table 20 Elastic Modulus of STO cells growing on Heterogeneous gel 1

		Curve 1 (Pa)	Curve 2 (Pa)	Curve 3 (Pa)	Average (Pa)	Standard Deviation (± Pa)
Hard	Cell 1	2718.285	1777.138	3659.431	2718.285	941.1469
	Cell 2	6961.332	4579.547	4684.703	5408.528	1345.796
	Cell 3	1898.067	3659.431	3196.745	2918.081	913.149
	Cell 4	6782.567	6141.115	12240.17	8387.95	3351.5
	Cell 5	4563.774	4847.695	3070.557	4160.675	954.6836
Soft	Cell 1	1172.49	715.0613	1004.241	963.9307	231.3633
	Cell 2	2187.246	820.2174	594.1318	1200.532	861.9645
	Cell 3	799.1862	168.2497	2061.059	1009.498	963.7714
	Cell 4	967.4359	2176.731	914.8579	1353.008	713.8489
	Cell 5	3775.103	1240.842	1840.231	2285.392	1324.48

Table 21 Elastic modulus of STO cells growing on Heterogeneous gel 2

		Curve 1 (Pa)	Curve 2 (Pa)	Curve 3 (Pa)	Average (Pa)	Standard Deviation (± Pa)
Hard	Cell 1	683.5145	2807.667	2891.792	2127.658	1251.372
	Cell 2	1482.701	431.1399	1845.489	1253.11	734.595
	Cell 3	3943.353	5909.772	2670.964	4174.696	1631.75
	Cell 4	1345.998	1067.334	7613.3	3342.211	3701.495
	Cell 5	7077.004	5783.584	8233.721	7031.436	1225.704
Soft	Cell 1	1735.075	3522.729	4689.961	3315.922	1488.259
	Cell 2	5047.492	4821.406	5878.225	5249.041	556.4916
	Cell 3	6751.02	13191.83	6772.051	8904.967	3712.547
	Cell 4	683.5145	7639.589	1340.74	3221.281	3840.452
	Cell 5	3407.057	1940.13	3417.573	2921.586	849.9827

Table 22 Elastic modulus of STO cells growing on Heterogeneous gel 3

		Curve 1 (Pa)	Curve 2 (Pa)	Curve 3 (Pa)	Average (Pa)	Standard Deviation (± Pa)
Hard	Cell 1	2218.793	173.5075	1125.17	1172.49	1023.464
	Cell 2	1072.592	1819.2	5473.374	2788.389	2355.04
	Cell 3	925.3735	820.2174	641.4521	795.681	143.5422
	Cell 4	1603.63	3491.182	1177.748	2090.853	1231.273
	Cell 5	1850.747	1114.654	5263.062	2742.821	2213.406
Soft	Cell 1	1777.138	3659.431	2113.637	2516.735	1003.805

	Cell 2	2902.308	2776.12	1650.95	2443.126	688.9395
	Cell 3	6456.583	2439.621	3291.385	4062.53	2116.6
	Cell 4	504.7492	1267.131	2691.996	1487.958	1110.219
	Cell 5	1183.006	504.7492	473.2023	720.3191	401.0088

Table 23 Storage Modulus of STO cells growing on Heterogeneous gel 1

		Curve 1 (Pa)	**Curve 2 (Pa)**	**Curve 3 (Pa)**	**Average (Pa)**	**Standard Deviation (± Pa)**
Hard	**Cell 1**	4186.63	2216.918	1912.757	2772.101	1234.422
	Cell 2	3029.269	2490.364	2427.569	2649.067	330.7577
	Cell 3	4229.051	3991.734	2238.551	3486.446	1087.203
	Cell 4	4214.138	4978.042	5935.747	5042.642	862.6204
	Cell 5	2502.201	2192.461	1434.307	2042.99	549.4139
Soft	**Cell 1**	1740.948	1080.402	841.7069	1221.019	465.8201
	Cell 2	615.2318	1001.216	608.1849	741.5442	224.9098
	Cell 3	3458.759	1844.879	5265.427	3523.022	1711.179
	Cell 4	1342.662	1354.936	1439.692	1379.096	52.8345
	Cell 5	986.2673	896.926	2056.167	1313.12	645.0462

Table 24 Storage modulus of STO cells growing on Heterogeneous gel 2

		Curve 1 (Pa)	**Curve 2 (Pa)**	**Curve 3 (Pa)**	**Average (Pa)**	**Standard Deviation (± Pa)**
Hard	**Cell 1**	1169.803	1675.119	1652.509	1499.144	285.4411
	Cell 2	440.9955	481.6493	531.455	484.7	45.30681
	Cell 3	1488.919	2337.16	1059.597	1628.559	650.1275
	Cell 4	395.7163	1214.944	2033.674	1214.778	818.9787
	Cell 5	3107.019	890.5857	1863.938	1953.848	1110.949
Soft	**Cell 1**	2568.527	2324.308	1885.214	2259.35	346.257
	Cell 2	2341.385	3174.091	3082.704	2866.06	456.6738
	Cell 3	4418.277	6337.529	3089.719	4615.175	1632.833
	Cell 4	1423.842	4283.905	2234.641	2647.462	1474.044
	Cell 5	2935.077	1727.247	3107.995	2590.106	752.2435

Table 25 Storage modulus of STO cells growing on Heterogeneous gel 3

		Curve 1 (Pa)	Curve 2 (Pa)	Curve 3 (Pa)	Average (Pa)	Standard Deviation (± Pa)
Hard	Cell 1	1097.019	169.6287	1120.376	795.6746	542.2974
	Cell 2	639.5994	914.6927	1524.578	1026.29	452.9209
	Cell 3	323.2874	374.4894	1319.979	672.5854	561.2438
	Cell 4	1051.609	996.7104	2415.66	1487.993	803.852
	Cell 5	1418.58	648.6466	990.475	1019.234	385.7714
Soft	Cell 1	1639.072	2073.985	1556.338	1756.465	278.0741
	Cell 2	1055.119	2344.734	2073.262	1824.371	679.8799
	Cell 3	6315.033	3242.826	3643.921	4400.593	1670.039
	Cell 4	2638.685	926.2275	3320.003	2294.972	1233.347
	Cell 5	1796.078	1071.557	1405.725	1424.453	362.6232

Table 26 Loss Modulus of STO cells growing on Heterogeneous gel 1

		Curve 1 (Pa)	Curve 2 (Pa)	Curve 3 (Pa)	Average (Pa)	Standard Deviation (± Pa)
Hard	Cell 1	1356.92	832.0137	818.4797	1002.471	307.0361
	Cell 2	1086.19	1066.859	584.7283	912.5923	284.103
	Cell 3	332.4452	870.242	746.2131	649.6334	281.6062
	Cell 4	1447.93	2748.12	2018.404	2071.485	651.7178
	Cell 5	857.9382	913.9948	1791.697	1187.877	523.6746
Soft	Cell 1	757.4465	456.7828	569.6168	594.6154	151.8827
	Cell 2	418.7252	530.0574	393.0316	447.2714	72.83667
	Cell 3	1193.978	683.7259	1557.803	1145.169	439.078
	Cell 4	409.7482	335.2696	352.9427	365.9868	38.915
	Cell 5	432.3536	485.0258	531.9797	483.1197	49.84036

Table 27 Loss modulus of STO cells growing on Heterogeneous gel 2

		Curve 1 (Pa)	Curve 2 (Pa)	Curve 3 (Pa)	Average (Pa)	Standard Deviation (± Pa)
Hard	Cell 1	550.2999	670.6595	794.1138	671.6911	121.9102
	Cell 2	200.8818	253.8236	266.32	240.3418	34.73988
	Cell 3	606.9139	691.2382	300.5475	532.8999	205.5927

	Cell 4	219.0144	526.3527	680.5263	475.2978	234.9537
	Cell 5	865.6469	241.9922	707.6628	605.1006	324.2307
Soft	**Cell 1**	514.9102	472.6016	337.8655	441.7925	92.45598
	Cell 2	383.3802	443.3236	438.1088	421.6042	33.20548
	Cell 3	720.9166	620.4317	450.884	597.4108	136.4803
	Cell 4	538.2569	1614.462	920.1973	1024.305	545.6034
	Cell 5	938.8414	598.6205	537.2558	691.5725	216.328

Table 28 Loss modulus of STO cells growing on Heterogeneous gel 3

		Curve 1 (Pa)	**Curve 2 (Pa)**	**Curve 3 (Pa)**	**Average (Pa)**	**Standard Deviation (± Pa)**
Hard	**Cell 1**	578.4695	82.95302	522.8633	394.762	271.462
	Cell 2	456.7378	493.3829	504.2423	484.7877	24.89133
	Cell 3	150.9713	191.2752	537.4524	293.233	212.4581
	Cell 4	547.2962	363.0635	1516.106	808.8221	619.4141
	Cell 5	506.8314	253.9682	490.5085	417.1027	141.5142
Soft	**Cell 1**	842.0015	773.8424	713.9045	776.5828	64.09248
	Cell 2	484.3658	532.9751	490.3302	502.557	26.51109
	Cell 3	1722.601	1067.217	1100.901	1296.907	369.0468
	Cell 4	459.055	94.53185	88.03904	213.8753	212.3567
	Cell 5	854.7797	198.5912	1007.622	686.9976	429.8207